THE HETEROGENEOUS DECOMPOSITION OF HYDRAZINE

by

Courtnay Frederick Sayer

Thesis submitted in fulfilment of the requirements of the degree of Doctor of Philosophy at the University of Leicester

April 1974

UMI Number: U419322

All rights reserved

INFORMATION TO ALL USERS
The quality of this reproduction is dependent upon the quality of the copy submitted.

In the unlikely event that the author did not send a complete manuscript
and there are missing pages, these will be noted. Also, if material had to be removed,
a note will indicate the deletion.

UMI U419322
Published by ProQuest LLC 2015. Copyright in the Dissertation held by the Author.
Microform Edition © ProQuest LLC.
All rights reserved. This work is protected against
unauthorized copying under Title 17, United States Code.

ProQuest LLC
789 East Eisenhower Parkway
P.O. Box 1346
Ann Arbor, MI 48106-1346

THE HETEROGENEOUS DECOMPOSITION OF HYDRAZINE

by

Courtnay Frederick Sayer

Thesis submitted in fulfilment of the requirements of the degree of Doctor of Philosophy at the University of Leicester

April 1974

THESIS
460263
21·8 74

X75-339045-X

LIST OF CONTENTS

C H A P T E R O N E

INTRODUCTION

1.1 General background

The use of rockets may be traced back to the "fire arrows" used by the Chinese against the Monguls in the thirteenth century. Over the next seven centuries rockets were used for a variety of military purposes culminating in the V2 rockets used by Germany in the Second World War. In the last three decades the rocket has also been used for the exploration of space, an application for which no other form of propulsion can be used. On 4 October 1957 the Russians launched Sputnik I, the first satellite to be put into an orbit round the earth, and this was followed by the launching of the American satellite Vanguard I. Since then the Russians and Americans have launched several hundred satellites and spacecraft. Most of these have been destined for an orbit round the earth but some have been launched into deep space towards the moon and other planets. The highlights of the last sixteen years have been the manned spaceflights which began in 1961 when Yuri Gagarin became the first man to complete one orbit of the earth in his spacecraft Vostok I. The climax of the manned spaceflight programmes was reached in 1969 when Neil Armstrong became the first man to step on the surface of the moon.

All these satellites and spacecraft were launched from the surface of the earth using large rocket engines to accelerate the launch vehicle to the required velocity to put the spacecraft into orbit round the earth. After the launch of the spacecraft firings of smaller rocket engines are then required for such purposes as to acquire the correct orbit for a telecommunications satellite or to accelerate a spacecraft out of earth orbit and into the correct flightpath through space to the moon. But before this secondary propulsion system may be used very small rocket engines, known as the attitude control thrusters, must be used to orientate the spacecraft in the correct attitude to ensure that the firing of the secondary propulsion has the desired effect.

In the vacuum of space the only way in which an acceleration may be applied to a spacecraft is to expel a mass to provide an equal and opposite reaction on the basis of Newton's Laws of Motion. In the rocket engine the propellants react producing energy in the form of heat and the resulting hot gases are expanded through a nozzle to provide a thrust. It is this thrust which is the source of rocket propulsion. The thrust arises from the conversion of the enthalpy of the combustion process to kinetic energy. Although the system appears relatively simple complications arise from the number of reactions which may occur and the variation of these reactions under the different conditions of temperature and pressure found in the rocket chamber and nozzle. To allow a numerical evaluation of the specific impulse, the basic chemical comparison parameter for propellants, it is necessary to make various assumptions, the most important of which are:-

(1) Thermodynamic equilibrium is reached in the combustion chamber following adiabatic combustion.

(2) Combustion products are assumed to behave as ideal gases.

(3) The flow velocity in the chamber is negligible compared to the gas velocity at the nozzle exit.

(4) The flow through the nozzle is isentropic.

On the basis of these assumptions the following expression[1] may be derived for I_s , the specific impulse, in terms of γ , the ratio of the heat capacities, C_p/C_v , and the ratio of the exhaust pressure P_e and the chamber pressure P_c :-

$$I_s = \sqrt{\frac{2R}{g} \frac{\gamma}{\gamma-1} \frac{T_c}{M} \left[1 - \left(\frac{P_e}{P_c} \right)^{\frac{\gamma-1}{\gamma}} \right]} \qquad (1)$$

The other variables which determine the specific impulse are the chamber temperature T_c and the molecular weight of the product gas M . The ratio P_e/P_c is determined by the design of the rocket engine and although the I_s

may be increased by increasing the chamber pressure there are practical difficulties which limit the upper pressure range. Therefore maximising the chamber temperature and minimising the product gas molecular weight are the practical means by which the I_s may be increased.

Chemical rockets may be categorised by the nature of the propellant as being solid, liquid or hybrid systems. Solid propellant motors are normally used to provide the large thrusts required from a launch system and for a variety of reasons are seldom considered for satellite attitude control purposes. Hybrid liquid-solid rockets have little practical use at the present time. Liquid propellant rocket engines are used for a very wide range of applications as the thrust range covered extends from the very high levels required for launch vehicles down to the very low thrust levels required for attitude control systems. The large liquid propellant rocket engines are always bipropellant systems and use a fuel such as kerosene or liquid hydrogen and an oxidiser such as liquid oxygen. Smaller liquid propellant engines such as those used as secondary propulsion systems are also bipropellant but because of the difficulties of storing cryogenic propellants different fuel and oxidant combination are used, such as unsymmetrical dimethyl hydrazine and dinitrogen tetroxide. For attitude control systems the choice lies between a bipropellant system, using a hypergolic fuel and oxidant combination, and a monopropellant using either thermal or catalytic modes of decomposition. The heat evolved by the decomposition reaction providing the energy in the same way as the heat of combustion in the case of the bipropellant system.

Any compound which can be made to decompose exothermically may, in theory, be considered for use as a monopropellant. In practice, however, the choice of candidate monopropellants is limited due to difficulties in obtaining smooth decomposition in the chamber and in the storage characteristics of the compound. The specific impulse of a monopropellant is lower than a

bipropellant system but the loss of performance has to be set against the gain in simplicity and also reliability of the monopropellant system. For attitude control purposes reliability is a prime requirement as the satellite may have a lifetime in excess of five years and require hundreds of thousands of firings of the thrusters, and so monopropellants have been used extensively for attitude control purposes. However, even the best monopropellant system is a compromise and it may be expected that in the future electric propulsion techniques, in which electrical power is used to impart kinetic energy to a working fluid, will offer improvements over the present state of the art.

Both hydrogen peroxide and hydrazine are compounds which can be made to decompose exothermically and may therefore be considered as potential monopropellants. Up until 1965 hydrogen peroxide was used in preference to hydrazine despite the fact that hydrazine offered better performance and storage stability. But whereas hydrogen peroxide could be decomposed rapidly and smoothly on a rough plated silver catalyst at ambient temperature no such catalyst was available at that time for the decomposition of hydrazine. The only available hydrazine catalysts consisted of mixtures of iron, nickel and cobalt on a support but these catalysts required heating to a few hundred degrees by external means to give a reasonable rate of decomposition of hydrazine as the activity was very low at ambient temperature. In 1965 the Shell Development Company USA produced a new hydrazine decomposition catalyst, designated the Shell 405, which consisted of 33% iridium on an alumina support. This catalyst was extremely active at ambient temperature with respect to the decomposition of hydrazine and under practical conditions would provide rapid complete decomposition of liquid hydrazine injected into a thruster of reasonable dimensions to give acceptable starting characteristics at ambient temperature. Since 1965 hydrazine has been preferred to hydrogen peroxide for use as a monopropellant and hydrazine/Shell 405 thruster systems have been developed to meet the requirements for satellite attitude control systems.

A typical monopropellant hydrazine thruster system is shown in fig. 1.1. The system consists of the main hydrazine tank, this is normally used to supply propellant to all the hydrazine thrusters, which is pressurised using an inert gas such as nitrogen. From the tank the fuel lines lead to the filters, valves and the thrusters. Because of the requirement for a high reliability of the control system thruster assemblies are normally doubled up to provide a redundancy factor and valves fail shut to prevent propellant venting in the case of valve failure. In operation the on command signal opens the valve and, when the dead volume between the valve and the injector of the thruster has been filled, liquid hydrazine is injected into the catalyst bed. Some of the liquid hydrazine is decomposed to form nitrogen and ammonia in accordance with the reaction:-

$$3N_2H_4 \rightarrow N_2 + 4NH_3 - 335.4 \text{ kJ} \qquad (2)$$

The heat evolved by this exothermic reaction raises the temperature of the thruster to the point at which the liquid hydrazine is vapourised and further reaction then occurs in the gas phase. Ultimately the thermal decomposition of hydrazine may play a significant part in the reaction at temperatures in excess of 500-700^{o}C. The hot gases are forced through the catalyst bed and under the high temperature conditions the ammonia formed by reaction (2) is unstable, decomposing in accordance with the reaction:-

$$4NH_3 \rightarrow 2N_2 + 6H_2 + 184.0 \text{ kJ} \qquad (3)$$

If the thruster could be operated in such a manner that only reaction (2) occurred and no ammonia was decomposed, then the maximum temperature of the thruster gas space would be approximately 1400^{o}C and the specific impulse would be 2578 Ns/kg. In practice when the catalyst bed is sufficiently long to just decompose all the hydrazine then in addition approximately 30-40% of

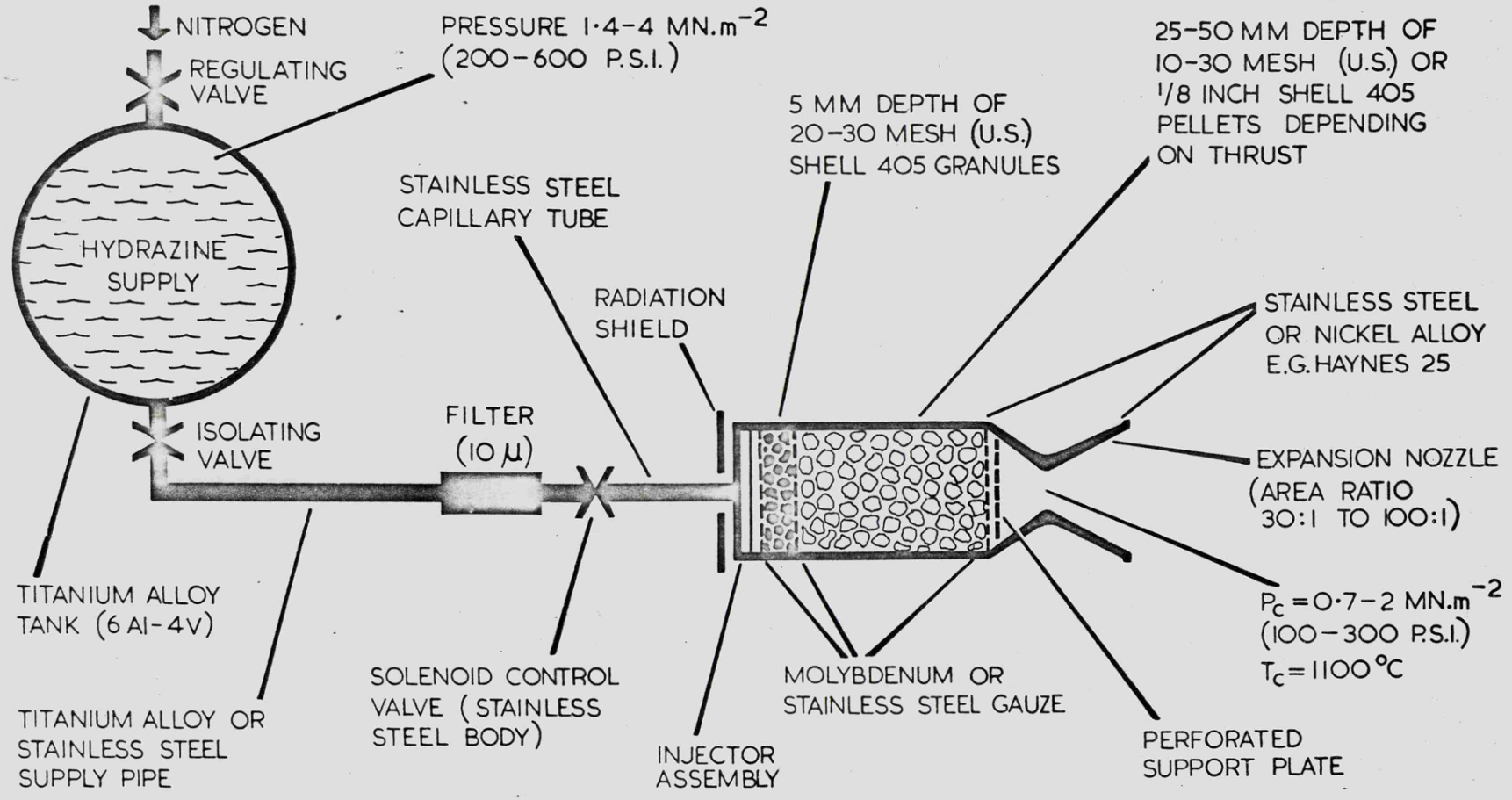

HYDRAZINE PROPULSION SYSTEM

the ammonia is also decomposed resulting in a decrease in gas space temperature to about 1000°C and a corresponding drop in specific impulse to 2450 Ns/kg. Decomposition of all the ammonia results in a further decrease in gas space temperature to 600°C and the specific impulse is reduced to 2078 Ns/kg. Fig. 1.2 shows the effect of the percentage of ammonia decomposed on the specific impulse and the gas space temperature. The overall decomposition reaction may be represented as:-

$$3N_2H_4 \rightarrow 4(1-x)\ NH_3 + 6x\ H_2 + (2x+1)\ N_2 - [335.4 - (184.0\ x)]\ kJ \qquad (4)$$

where x is the fraction of ammonia decomposed.

The critical factor in the development of a suitable hydrazine decomposition catalyst has been the activity of the catalyst with respect to the decomposition of liquid hydrazine at ambient temperature. The importance of this characteristic may be illustrated by considering the chemical factors affecting the performance of a monopropellant attitude control thruster which may be used to provide pulses of only 100 milliseconds duration or may be used for long duration firings. The ideal thrust-time relationship for such a thruster corresponds to a square wave shape, but for short duration pulses the time required for the chamber pressure, and hence the thrust, to rise to its limiting value and then decay to zero occupy a significant part of the pulse duration. Two of the parameters which contribute to the rise time of the chamber pressure are the induction period and the rate of decomposition of hydrazine on the catalyst. The higher the rate of decomposition of hydrazine the shorter is the time required for the full chamber pressure to be developed. If the thruster is packed with a catalyst of very low activity the rate of decomposition and of heat evolution will also be low. The heat evolved will not be sufficient to raise the temperature of the thruster, therefore the hydrazine will pass through the catalyst bed largely unchanged. At a threshold level of catalytic activity the decomposition of hydrazine

will generate sufficient heat to rapidly raise the temperature of the thruster and, by using a sufficiently long catalyst bed, no hydrazine will be observed in the gaseous products. With catalysts of greater activity the bed length may be reduced without effecting the extent of the reaction and the starting characteristics of the thruster will be improved.

Forbes and Huxtable[2] have evaluated some catalysts with respect to the decomposition of liquid hydrazine at ambient temperature. They found the Shell 405 to be the most active catalyst and the next on their list, but of much lower activity, was a ruthenium catalyst based on an alumina support. Other catalyst samples which were tested included Raney cobalt, silver alloy, molybdenum oxide, molybdenum and molybdenum plus 2% iridium. These workers also studied the induction period of the hydrazine/Shell 405 catalyst system but did not report any results.

Greer[3] studied the starting characteristics of monopropellant hydrazine thrusters which were packed with Shell 405 catalyst. He measured the ignition delay, defined as the time interval from the initiation of propellant flow to a chamber pressure of 1% of the design value, and observed that it decreased with increasing temperature. At $2^{o}C$ the observed ignition delay was about 120 milliseconds decreasing to about 20 milliseconds at $35^{o}C$.

At the present time it appears that only supported iridium catalysts have the high catalytic activity with respect to the decomposition of liquid hydrazine necessary for efficient thruster operation. A research programme was initiated at the Rocket Propulsion Establishment, Westcott to study the kinetics and mechanism of the decomposition of liquid hydrazine on supported metal catalysts. A total of five catalysts were studied and these consisted of iridium, rhodium, ruthenium, palladium and platinum supported on alumina. The aim of the programme was to either develop an alternative to a supported iridium catalyst for use as a hydrazine decomposition catalyst or to explain the unique characteristic of this catalyst if no alternative could be found.

1.2 The heterogeneous decomposition of liquid hydrazine

The first study of the heterogeneous decomposition of hydrazine was concerned not with free hydrazine but with an aqueous solution of hydrazine sulphate. Tanatar[4] observed that on active platinum the hydrazine sulphate solution evolved nitrogen gas and he postulated that the overall reaction could be represented as:-

$$3N_2H_5^+ + H^+ \rightarrow N_2 + 4NH_4^+ \qquad (5)$$

Tanatar[5] then went on to prepare solutions of free hydrazine by treating the solutions of hydrazine sulphate with barium hydroxide and filtering off the precipitated barium sulphate. The decomposition of the resulting hydrazine solution on the active platinum resulted in the evolution of gas which was analysed by burning the hydrogen with oxygen and measuring the change in volume at the various stages of the analysis. Tanatar found that the gas consisted of approximately equal quantities of nitrogen and hydrogen and on this basis he postulated the following reaction to account for the decomposition of free hydrazine on active platinum:-

$$2N_2H_4 \rightarrow N_2 + H_2 + 2NH_3 \qquad (6)$$

He then studied the catalytic decomposition of free hydrazine on active platinum but with sodium hydroxide dissolved in the solution and he observed that the proportion of hydrogen in the evolved gas was increased. The composition of the evolved gas approached the proportions required for the reaction:-

$$3N_2H_4 \rightarrow 2N_2 + 3H_2 + 2NH_3 \qquad (7)$$

Tanatar also observed that adding an equimolar quantity of sodium hydroxide to an aqueous solution of hydrazine sulphate resulted in the appearance of hydrogen in the evolved gas but only to the extent of approximately 10%.

Increasing the quantity of sodium hydroxide in the hydrazine sulphate solution resulted in an increase in the proportion of hydrogen found in the evolved gas, but only when a large excess of sodium hydroxide was added did the hydrogen content approach the 60% content required for reaction (7). Tanatar only analysed the evolved gas for nitrogen and hydrogen, under the conditions used to collect the evolved gas any ammonia present was dissolved in the water used as the confining liquid.

The work of Tanatar was subsequently confirmed by Purgotti and Zanichelli[6] who studied the decomposition of aqueous solutions of hydrazine sulphate on platinum black catalyst. The rate of reaction was found to be proportional to the weight of catalyst used and to the concentration of hydrazine in solution. It was also observed that the rates of decomposition of various hydrazine salts on the platinum black catalyst were effected by the nature of the anion of the salt. The one significant difference between the work of Tanatar and that of Purgotti and Zanichelli was that the latter observed a loss of activity of the platinum black catalyst with respect to the decomposition of hydrazine after boiling in water for 4 hours. The platinum black so treated would still bring about the decomposition of hydrogen peroxide and hydroxylamine but even after such reactions had been carried out the catalyst was still inert towards hydrazine. The authors considered from their evidence that the decomposition of hydrazine was initiated by small amounts of oxygen occluded by the platinum black.

A third study of the decomposition of hydrazine solutions on a platinum black catalyst was carried out by Gutbier and Neundlinger[7]. They observed that the only constituent of the evolved permanent gas was nitrogen and no hydrogen could be detected. Therefore the only reaction was:-

$$3N_2H_4 \rightarrow N_2 + 4NH_3 \qquad (2)$$

They tried to determine the kinetics of the system but could only show that

the kinetics were complicated and they experienced difficulty in obtaining reproducible results. Even when samples of the catalyst were prepared under identical conditions the results of the kinetic experiments were not reproducible.

Gutbier and Neundlinger went on to study the effect of alkali in the hydrazine solution on the decomposition reaction. Decomposing a hydrazine solution containing an equimolar quantity of barium hydroxide on the platinum black catalyst resulted in the evolution of equal parts of hydrogen and nitrogen. Under these conditions the decomposition reaction may be represented as:-

$$2N_2H_4 \longrightarrow N_2 + H_2 + 2NH_3 \qquad (6)$$

When sodium hydroxide was used in place of barium hydroxide it was found necessary to use two equivalents of alkali to bring about the same result. Increasing the concentration of alkali resulted in an increase in the proportion of hydrogen observed in the evolved permanent gas until at high alkali concentrations the composition of the permanent gas approaches that required for the reaction:-

$$N_2H_4 \longrightarrow N_2 + 2H_2 \qquad (8)$$

These workers postulated a mechanism for the decomposition of hydrazine in which the initial step was the breakdown of hydrazine to form nitrogen and hydrogen. The hydrogen then reduced further hydrazine molecules to form ammonia. In the presence of the hydroxyl ions the dissociation of the hydrazine molecule was hindered thus inhibiting the reducing power of the hydrogen molecule which was then liberated as gas.

In recent years the possible use of hydrazine in fuel cells has attracted a great deal of interest and this has resulted in some studies of the heterogeneous decomposition of liquid hydrazine. In the fuel cells the catalytic

decomposition of hydrazine is an unwanted side reaction and so the emphasis has been on studying the system with a view to its elimination. Vitvitskaya and Grabouskaya[8] have studied the decomposition of alkaline solutions of hydrazine on platinised carbon and found, under their experimental conditions, that the evolved permanent gas consisted of hydrogen and nitrogen, in molar quantities corresponding to reaction (8). It was inferred that the mechanism consisted of the adsorption of the hydrazine molecule followed by progressive dehydration to leave the nitrogen molecule and adsorped hydrogen atoms. The latter combined to be desorbed as hydrogen molecules and the nitrogen molecule was also desorbed. It was also postulated that the nitrogen molecule was formed without rupture of the original nitrogen-nitrogen bond of the hydrazine molecule.

All the early work on the heterogeneous decomposition of hydrazine solutions was carried out using dilute aqueous solutions, but as the interest in the use of hydrazine as a propellant increased it became desirable to study the decomposition of highly concentrated solutions of hydrazine. Audrieth and Jolly[9] studied the decomposition of concentrated solutions of hydrazine on a range of catalysts in an attempt to find one of high activity. On platinum, iron, aluminium and copper catalysts the rate of decomposition was very low but there was rapid decomposition on cobalt and nickel catalysts. As it was easier to prepare samples of Raney nickel having reproducible characteristics they then proceeded to study the decomposition of aqueous hydrazine solutions on this catalyst in some detail. The products of the reaction were nitrogen, hydrogen and ammonia but the proportions did not correspond to any single reaction previously postulated to account for the decomposition of hydrazine. The results of the analysis of the products were not sufficiently accurate to enable them to separate the individual reactions occurring on the catalyst in a quantitative manner. They suggested that the major reaction appeared to involve the dehydrogenation of hydrazine, the

process being initiated by either hydrogen adsorbed on the catalyst surface or the adsorption of a hydrazine molecule followed by fission of either the nitrogen-nitrogen or the nitrogen-hydrogen bonds. Either process, is was assumed, would lead to the formation of various radical intermediates. The kinetics of the decomposition reaction were studied over the hydrazine concentration range of 0.5 to 30.0 mole dm^{-3} and the rate of reaction was observed to be a maximum for 8 ± 2 mole dm^{-3} hydrazine solution. From the results of the variation of the rate of decomposition with respect to temperature the activation energy of the reaction was calculated to be 71.6 kJ $mole^{-1}$. However as the individual reactions could not be separated the activation energy relates only to the overall decomposition reaction which appears to consist of two, or more, competing reactions and the calculated activation energy is therefore only an apparent value.

The decomposition of dilute solutions of hydrazine on Raney nickel catalysts was also studied by Irrera[10] who found that the composition of the evolved gas approached that required for the reaction:-

$$3N_2H_4 \rightarrow 2N_2 + 3H_2 + 2NH_3 \qquad (7)$$

Kuhn[11] also studied the decomposition of hydrazine solutions on Raney nickel but found the main reaction to be:-

$$N_2H_4 \rightarrow N_2 + 2H_2$$

The development of the Shell 405 hydrazine decomposition catalyst and the subsequent use of hydrazine monopropellant systems for space applications has stimulated more research into the decomposition of liquid hydrazine. Santacesaria, Guiffre and Gelosa[12] studied the decomposition of liquid hydrazine on molybdate and heteromolybdate catalysts (see also the section on vapour phase decomposition) and also the Shell 405 catalyst. The experiments using the latter catalyst were carried out by suspending a stainless steel

mesh cage containing one catalyst pellet in the hydrazine solution which was agitated by means of a magnetic stirrer. The course of the reaction was followed by measuring the volume of permanent gas evolved with respect to time using a gas burette. The analysis of the evolved gas showed that only nitrogen and ammonia were evolved except for experiments using anhydrous hydrazine for which about 10% hydrogen was produced. Therefore the decomposition of hydrazine on the Shell 405 catalyst followed reaction (2) with side reactions occurring with anhydrous hydrazine to produce a small amount of hydrogen. The variation of the rate of decomposition of hydrazine with respect to temperature was studied for a range of hydrazine concentrations. The apparent activation energy increased from 21 to 42 kJ $mole^{-1}$ with increasing hydrazine concentration up to 16 mole dm^{-3}. Above 16 mole dm^{-3} hydrazine solution the activation energy was found to be almost constant except for anhydrous hydrazine when the calculated activation energy was 48 kJ $mole^{-1}$. The authors suggested that the rise in activation energy with respect to hydrazine concentration was the result of a change in kinetics from diffusion control at low concentrations to chemical control at high concentrations. The further increase in activation energy for anhydrous hydrazine was suggested to result from the violent nature of the reaction leading to a considerable thermal gradient between the catalyst surface and the bulk liquid. The suggestion that the rise in activation energy results from a change in kinetics seems to be incorrect as it is unlikely that diffusion control for a slow reaction would give way to chemical control as the speed of reaction increased as a result of increasing the reactant concentration.

Santacesaria, Guiffre and Gelosa then went on to study the decomposition of liquid hydrazine on reduced bismuth molybdate and reduced MoO_3. In both cases analysis of the products showed that only nitrogen and ammonia were produced and therefore the decomposition followed reaction (2). Water was found to have little effect on the rate of reaction and the overall kinetics

appeared to be first order. The activation energy of the reaction on both catalysts was about 42 kJ $mole^{-1}$.

So far as is known this constitutes the available information on the catalytic decomposition of liquid hydrazine. Some aspects of the vapour phase decomposition are also of relevance to the subject and so this is dealt with in the following section.

1.3 The vapour phase decomposition of hydrazine

1.3.1 The homogeneous vapour phase decomposition

The vapour phase decomposition of hydrazine has been the subject of much wider interest than that of the liquid phase but most of the vapour phase work has been devoted to the homogeneous decomposition. A variety of techniques have been used including:-

1) Flash photolysis (refs. 13,14)
2) Ignition limits (refs. 15,16)
3) Laminar flames (refs. 17-28)
4) Shock tubes (refs. 29-35)
5) Isothermal bombs (ref. 36)
6) Flow reactors (refs. 37-41)

In general terms the results using these techniques show that the thermal decomposition of hydrazine obeys first order kinetics at high pressures changing to second order kinetics at low pressures. The overall reaction may be considered to approximate to:-

$$2N_2H_4 \longrightarrow N_2 + H_2 + 2NH_3 \qquad (6)$$

and the activation energy is of the order of 250 kJ $mole^{-1}$. The mechanism is rather complex but it appears that the first step is the breaking of the nitrogen-nitrogen bond:-

$$N_2H_4 + X \longrightarrow 2NH_2 + X \qquad (9)$$

followed by propagating steps such as:-

$$N_2H_4 + NH_2 \rightarrow NH_3 + N_2H_3 \quad (10)$$

$$N_2H_3 + X \rightarrow N_2 + H_2 + H + X \quad (11)$$

$$N_2H_4 + H \rightarrow H_2 + N_2H_3 \quad (12)$$

and the terminating steps are those such as:-

$$NH_2 + N_2H_3 \rightarrow NH_3 + N_2 + H_2 \quad (13)$$

$$N_2H_3 + H \rightarrow N_2 + 2H_2 \quad (14)$$

$$2NH_2 \rightarrow N_2H_4 \quad (15)$$

$$N_2H_3 + N_2H_3 \rightarrow 2NH_3 + N_2 \quad (16)$$

In view of the high temperature reached in the catalyst bed of a monopropellant hydrazine thruster the homogeneous decomposition of hydrazine may be expected to occur but to what extent is not clear.

1.3.2 The heterogeneous vapour phase decomposition of hydrazine

The early studies of the heterogeneous decomposition of hydrazine were carried out using silica as the catalyst. Elgin and Taylor[42] were studying the photodecomposition of hydrazine when they observed the heterogeneous decomposition of hydrazine on silica at 250-300°C. They found the products of the reaction to be ammonia and nitrogen and the decomposition was represented by the reaction (2).

Askey[43] also studied the decomposition of hydrazine on silica and confirmed that reaction (2) occurred but also observed the production of small amounts of hydrogen. Kinetically the reaction was first order with respect to hydrazine concentration. Askey then studied the decomposition of hydrazine on platinum wires and in this case he observed that hydrogen was formed as a

major product. The decomposition under these conditions was represented by reaction (6), again the reaction was first order with respect to hydrazine concentration. The effect of the products of the reaction was to inhibit the reaction, adsorbed hydrogen strongly inhibited the reaction while adsorbed ammonia only weakly inhibited the reaction. On tungsten wires the overall decomposition reaction and the kinetics were the same as for the decomposition of hydrazine on platinum wires but the effect of adsorbed hydrogen was to bring about an increase in catalytic activity.

Both the heterogeneous and homogeneous decomposition of hydrazine were studied by Szwarc[37] using a silica apparatus. He was able to separate the two modes of decomposition by using toluene as a radical scavenger, this reacts with NH_2 radicals formed by the homogeneous fission of the nitrogen-nitrogen bond and forms dibenzyle. Szwarc observed that the gaseous products were not formed in the stoichiometric quantities required for just one reaction. He postulated that both reactions (2) and (6) were occurring and calculated activation energies of about 40 kJ $mole^{-1}$ for reaction (2) and about 80 kJ $mole^{-1}$ for reaction (6). Szwarc envisaged the mechanisms for the two reactions as follows:-

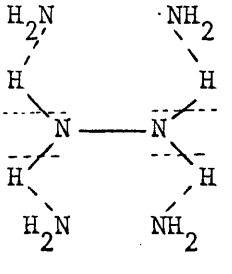

and

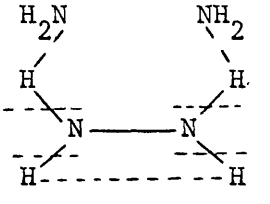

Birse and Melville[44] had previously studied the heterogeneous decomposition of hydrazine on silica and from their data Szwarc had calculated an activation energy of approximately 75 kJ $mole^{-1}$. Their study had been carried out using para-hydrogen as a radical sensor. The conversion of para-hydrogen to ortho-hydrogen is very sensitive to the presence of radicals. However no

ortho-hydrogen was formed and so it was concluded that no radicals were formed as intermediates in the reaction.

Hanratty, Pattinson, Clegg and Lemmon[38] also observed reaction (2) to be the main reaction for the heterogeneous decomposition of hydrazine on silica. At increasing temperatures the proportion of hydrogen observed in the products increased as reaction (6) became more important. They calculated the activation energy of reaction (2) to be 38.9 kJ $mole^{-1}$.

The decomposition of hydrazine on pyrex glass was studied over the temperature range 270° to 325°C by Kant and McMahon[45] who used ^{15}N as a tracer to study the formation of the nitrogen molecule. The isotope distribution of the nitrogen gas was the same as that of the original hydrazine solution and therefore no nitrogen-nitrogen bond fission had occurred in the formation of the nitrogen molecule. This result was consistent with the reaction mechanism envisaged by Szwarc.

The studies of the heterogeneous decomposition of hydrazine on silica have shown the existence of the two reactions (2) and (6). The activation energy of reaction (6) is greater than that of reaction (2) and therefore reaction (6) is favoured at high temperatures. No nitrogen-nitrogen bond fission occurred in the formation of the nitrogen molecule and no radicals could be detected. These results are consistent with Szwarc's postulated mechanism which envisaged the formation of activated complexes on the surface and then these break down to yield the products.

The heterogeneous decomposition of hydrazine has also been studied on various metals. Mention has already been made of the work by Askey[43] on the decomposition of hydrazine on tungsten and platinum. Mass spectrometric techniques were used by Willhoft and Robertson[46] to study the decomposition of hydrazine vapour on platinum wires at low pressures. A flow system was used in which hydrazine at 2×10^{-5} torr was passed over a heated platinum wire and the product gases pumped away as soon as they were formed. Their

results indicated that a reactive intermediate was being formed and they postulated that this intermediate was diimide.

The decomposition of hydrazine adsorbed on different crystal planes of copper was studied by Rienacker and Volter[47]. Over the temperature range 200-250°C the main products were observed to be nitrogen and ammonia and the activation energy was calculated to be 98 kJ $mole^{-1}$. Although the activation energy was calculated to be the same for both the (100) and (111) planes the rate of decomposition of hydrazine on the (100) plane was observed to be twice that on the (111) plane.

Volter and Kuhn[48] observed that the decomposition of hydrazine on a nickel/magnesium oxide catalyst produced only nitrogen and ammonia. The activation energy was calculated to be 58.5 kJ $mole^{-1}$. These authors went on to study the effect of doping the catalyst with singly or triply charged cations and found that the activation energy was effected by doping. The addition of Ga^{3+} resulted in a decrease in activation energy to approximately 50 kJ $mole^{-1}$ while the addition of Li^{+} resulted in an increase to 67 kJ $mole^{-1}$.

A micro catalytic pulse technique was used by Schulz-Ekloff and Jiru[49] to study the decomposition of hydrazine on an iron catalyst. Only nitrogen and ammonia were observed as major products and hence the decomposition followed reaction (2). Hydrogen was not produced in any appreciable quantity until the decomposition of ammonia contributed to the overall decomposition at temperatures in excess of 450°C.

A more extensive study of the decomposition of hydrazine on metals was carried out by Volter and Lietz[50] who used chromium, manganese, iron, tungsten, rhenium and osmium as catalysts. Analysis of the products showed that nitrogen, hydrogen and ammonia were produced but not in the stoichiometric quantities corresponding to one reaction. For all the metals the ratio of ammonia to total of nitrogen and hydrogen produced was approximately 2:1. The authors suggested that this could only be explained on the basis of the

simultaneous occurrence of reactions (2) and (6). The apparent activation energies calculated for the decomposition of hydrazine on the metals were:-

chromium	-	86.5 kJ $mole^{-1}$
manganese	-	61.2 "
iron	-	57.0 "
tungsten	-	60.0 "
rhenium	-	57.2 "
osmium	-	53.0 "

The authors postulated a mechanism in which there were three main steps, the initial one being the adsorption of hydrazine in the form of NH_2 radicals. These radicals further dissociate to form adsorbed nitrogen and hydrogen which are then desorbed as molecules. Some of the adsorbed NH_2 radicals may be hydrogenated to ammonia while the hydrogen atoms adsorbed on the surface may also react directly with hydrazine molecules.

Ken-Ichi Aika, Tomohisa Ohhata and Atsumu Ozaki[51] studied the decomposition and hydrogenolysis of hydrazine on various metals. Using helium as a carrier gas they observed the decomposition of hydrazine on the metals at 200°C to follow reaction (2) and no hydrogen was detected in the products. The data was presented in the form of a selectivity factor S , which was calculated from:-

$$S = 100 \times [NH_3] / (2[N_2] + [NH_3]) \qquad (17)$$

For reaction (2) the value of S is 66.7 but in practice values of 68 to 72 were observed which suggested that hydrogen deficient species, such as N_2H_2 or NH, were irreversibly adsorbed on the metal surface. Changing the carrier gas to hydrogen resulted in an increase in S showing that some hydrogenolysis of hydrazine occurred under these conditions. Some values of S for both carrier gases are given in Table 1.1.

TABLE 1.1

Variation of the value of S for hydrogen and helium gas carriers for the decomposition of hydrazine on various metals

Catalyst	Helium carrier gas		Hydrogen carrier gas	
	°C	S	°C	S
Platinum)	201	69.8	182	87.9
)				
)	240	68.2	240	87.7
Iridium	133	71.9	203	85.0
	213	71.2	258	87.1
Ruthenium	177	68.9	175	82.4
	227	68.8	219	85.1
Iron (Al, K)	247	69.1	233	81.9
Nickel	233	72.6	267	79.4
Iron	245	67.3	210	77.4
Tungsten	195	68.0	160	72.2
	275	68.8	200	74.2

The decomposition of hydrazine on tungsten films has been studied by Cosser and Tompkins[52] and the decomposition on molybdenum films has been studied by Contaminard and Tompkins[53]. In the opinion of the present author these two pieces of work are the most informative of all the studies of the heterogeneous decomposition of hydrazine. The authors have postulated a dual-plane theory to explain their observations and much of the previous work on the heterogeneous decomposition of hydrazine appears to be consistent with such a theory. For both studies hydrazine was adsorbed on the metal film to give a monolayer coverage and the products of the decomposition reaction were observed under isothermal and programmed temperature increase conditions.

The products were found to consist of hydrogen, nitrogen and ammonia; the ratio of nitrogen to ammonia was found to be constant at approximately 1:4 while the ratio of hydrogen to other products varied according to the experimental conditions. It was postulated that there were two reactions occurring, one reaction occurred to produce nitrogen and ammonia, the 1:4 ratio shows that this was reaction (2), while a second reaction yielded hydrogen as the only gaseous product. In addition to studying the decomposition of hydrazine on clean metal films some experiments were also carried out using metal films which had been treated with the products of the reaction and also carbon monoxide. The results indicated that the molecular adsorption of hydrazine occurred on the (110) plane and other planes were active for the dissociative chemisorption of hydrazine.

Mechanisms were postulated to account for the observations and on those planes which were active for the dissociative chemisorption of hydrazine the initial step was suggested to be the formation of NH_2 radicals on the surface. These further dissociate to form adsorbed NH radicals and N and H atoms. The latter were mobile under the experimental conditions and combined to be desorbed as hydrogen molecules. The nitrogen atoms however were strongly adsorbed due to the formation of strong nitrogen to metal multiple bond and under the experimental conditions remained adsorbed on the surface. From the measurements of the quantities of hydrazine adsorbed on the tungsten films Cosser and Tompkins calculated that each chemisorbed hydrazine molecule occupied four sites, and after complete decomposition the planes are saturated by adsorbed nitrogen atoms each of which occupies two sites.

On those planes which were not active for the dissociate chemisorption of hydrazine, namely the (110) plane, hydrazine was associatively adsorbed to form an activated complex which then decomposed to yield nitrogen and ammonia in accordance with reaction (2). On the (110) plane of tungsten Cosser and Tompkins calculated that each site was covered by one hydrazine molecule. It

was suggested that the hydrazine molecules were chemisorbed molecularly by bonding via one of the hydrogen atoms. However the lattice constants for the (110) plane were such that for the adsorption of one hydrazine molecule per tungsten atom lateral interaction between hydrazine molecules would be necessary, possibly in the form of hydrogen bonding.

Cosser and Tompkins also considered the application of the dual plane theory to the decomposition of hydrazine on other surfaces. They suggested that any metal capable of the dissociative chemisorption of nitrogen will also be capable of dissociatively chemisorbing hydrazine. In addition any metal which is able to dissociatively chemisorb hydrogen may be expected to dissociatively chemisorb hydrazine as the nitrogen-nitrogen bond of hydrazine is weaker than the hydrogen-hydrogen bond. For some metals both types of plane may be present in which case both dissociative and associative adsorption, and their consequent reactions, will occur. For other metals only one type of plane may be present and only one of the modes of adsorption and reaction will be observed. When experiments are carried out using more hydrazine than required for monolayer coverage there is the possibility of reaction between adsorbed species and gaseous reactant such that even when only active planes are present nitrogen and/or ammonia may be observed as a gaseous product.

A pulse chromatographic technique was used by Santacesaria and Guiffre[54] to study the decomposition of hydrazine on a number of reduced molybdate catalysts. The analysis of the product gases showed that on all the reduced molybdate and heteromolybdate catalysts used the only products were nitrogen and ammonia. The activation energies for the reactions were in the range 37 to 53 kJ $mole^{-1}$. The authors concluded that their experimental results were consistent with the decomposition mechanisms postulated by Szwarc.

The decomposition of hydrazine on the Shell 405 catalyst has been studied by Kesten, Rockenfeller and Sangiovanni[55] at the research laboratories

of the United Aircraft Corporation, USA. This work was part of a NASA contract study dealing with the vacuum start characteristics of hydrazine thrusters. Because the decomposition of hydrazine on the Shell 405 catalyst is a rapid reaction it was found necessary to use a flow reactor to study the kinetics of the reaction. The initial stage of the study was devoted to establishing the range of experimental conditions under which the reaction was chemically controlled. At low flow velocities the rate constant for the reaction was found to vary with respect to flow velocity showing that the reaction was mass transfer controlled under these conditions. Increasing the flow velocity to between 1000 and 7000 cm sec^{-1} resulted in a rate constant which was independent of flow velocity indicating that under these conditions the reaction was chemically controlled. Having established the range of usable experimental conditions they then studied the effect of hydrazine concentration on the rate of reaction. This was carried out using only one flow velocity and varying the hydrazine concentration by varying the temperature of the hydrazine saturator bath. When the results were plotted in the form of log rate of decomposition with respect to log hydrazine concentration the result was a straight line plot with a slope of 1.0 showing that the reaction was first order with respect to hydrazine concentration. Before studying the effect of temperature on the rate of decomposition the authors studied the effect of flow velocity on the rate constant over the desired temperature range to establish the region in which the reaction was chemically controlled. These tests showed that a temperature range of 50°C to 200°C could be used and the activation energy was calculated to be 36.17 ± 9.3 kJ $mole^{-1}$ from the variation of the rate of decomposition with respect to temperature over this range. Analysis of the products of the decomposition reaction showed that the overall stoichiometry was:-

$$3N_2H_4 \rightarrow 3.8\ NH_3 + 1.1\ N_2 + 0.3\ H_2 \qquad (18)$$

The reaction stoichiometry was observed to be distinctly temperature sensitive, the proportion of ammonia decreasing, while those of hydrogen and nitrogen increased, with increasing temperature. The change of stoichiometry may result from either ammonia decomposition or the effect of a second contributory reaction.

The decomposition of hydrazine on a supported iridium catalyst has also been studied by Pannetier and Contour[56]. Hydrazine was adsorbed on the surface of the catalyst and the products of the reaction was studied by infrared spectroscopy following programmed thermodesorption of the products. At temperatures up to 27°C only nitrogen and ammonia were evolved indicating that only reaction (2) was occurring. The authors studied the kinetics of the desorption of nitrogen from the catalyst surface and found the desorption process obeyed second order kinetics. The kinetics were attributed to the desorption of nitrogen atoms adsorbed on the catalyst and following on from this they postulated that the initial step in the decomposition reaction to be the formation of nitrogen to iridium bonds and the fission of the nitrogen-nitrogen bond of the hydrazine molecule. In support of this postulate they suggested that as the interatomic distance for the nitrogen atoms of the hydrazine molecule is 1.50 Å while the interatomic distance of iridium is 2.70 Å the hydrazine molecule cannot be adsorbed on an iridium surface without nitrogen-nitrogen bond fission. However it should be noted that Cosser and Tompkins observed the same reaction on tungsten films, which has interatomic distances similar to those of iridium, and found the adsorbed hydrazine molecule only occupied one adsorption site. The dissociative chemisorption of hydrazine on tungsten films resulted in the appearance of hydrogen as the only product. Pannetier and Contour did not observe hydrogen as a product and their interpretation of their data may be open to some doubt.

1.4 The use of ^{15}N as a tracer

All the reactions which have been used to represent the decomposition of hydrazine under various experimental conditions involve the formation of nitrogen as one of the major products. By using ^{15}N as a label it is possible to study the formation of the nitrogen molecule from a mechanistic viewpoint and to show whether the nitrogen molecule is formed from the nitrogen atoms of the same or from different hydrazine molecules.

This technique was used by Higginson and Sutton[57] to study the oxidation of hydrazine in aqueous solutions. They prepared a sample of hydrazine rich in ^{15}N and by diluting this with an excess of normal hydrazine they obtained a stock solution of hydrazine for which the distribution of $^{15}N_2H_4$, $^{15}NH_2{}^{14}NH_2$ and $^{14}N_2H_4$ was not in accordance with the statistical distribution calculated from the expression:-

$$\left[{}^{15}NH_2\ {}^{14}NH_2\right]^2 \Big/ \left[\left({}^{15}N_2H_4\right)\left({}^{14}N_2H_4\right)\right] = 4 \qquad (19)$$

From the results of the mass spectrometric analysis of the nitrogen gas evolved by the oxidation of the stock solution of hydrazine it was possible to calculate the percentage of nitrogen-nitrogen bond fission occurring in the formation of the nitrogen molecule.

Higginson and Sutton observed that in all the oxidation experiments when the nitrogen molecule was the sole nitrogen containing product then the isotope distribution of the nitrogen gas was the same as that of the stock solution of hydrazine. Therefore no nitrogen-nitrogen bond fission had occurred and both the atoms of the nitrogen molecule came from one hydrazine molecule. When ammonia was also formed as a reaction product the isotope distribution of the nitrogen gas was different to that of the stock solution of hydrazine showing that some nitrogen-nitrogen bond fission had occurred. However the observed isotope distribution was not the same as that calculated on the basis of the expression (19) and therefore not all the nitrogen-nitrogen

bonds were broken during the reaction. Calculations based on the ^{15}N distribution in the stock solution of hydrazine and in the nitrogen gas showed that approximately 50% of the nitrogen molecules were formed following nitrogen-nitrogen bond fission. To account for this finding the authors postulated a mechanism in which the initial step was the formation of N_2H_3 radicals which dimerised to form N_4H_6 then broke down to yield nitrogen and ammonia. In detail the mechanism was:-

$$H_2N^a\text{-}N^aH_2 + H_2N^b\text{-}N^bH_2 \longrightarrow H_2N^a\text{-}N^aH + HN^b\text{-}N^bH_2 \longrightarrow$$

$$H_2N^a\text{-}N^aH\text{-}N^bH\text{-}N^bH_2 \longrightarrow N^aH_3 + [\, HN^a{=}N^b\text{-}N^bH_2 \rightleftharpoons H_2N^a\text{-}N^b{=}N^bH \,]$$

$$\longrightarrow [\, H_2N^a\text{-}N^a{=}N^bH \rightleftharpoons HN^a{=}N^a\text{-}N^bH_2 \,] + N^bH_3$$

$$HN^a{=}N^b\text{-}N^bH_2 \longrightarrow N^a{\equiv}N^b + N^bH_3 \quad \text{etc.} \qquad (20)$$

The superscripts a and b were used to identify the particular hydrazine molecules from which the atoms so marked originated. The intermediate $NH_2\text{-}N{=}NH$ was always produced with the double bond linking nitrogen atoms from different hydrazine molecules. The formation of ammonia was postulated to involve the loss of the terminal NH_2 group from the intermediate and for the doubly bound nitrogen atoms to form the nitrogen molecule. Such a mechanism would lead to a statistical isotope distribution for the nitrogen gas. To explain the result of 50% randomisation the authors postulated rapid interconversion of the intermediate by proton transfer:-

$$H_2N^a\text{-}N^a{=}N^bH \rightleftharpoons HN^a{=}N^a\text{-}N^bH_2 \qquad (21)$$

and all that was necessary was that the rate of interconversion should be fast compared to the rate of loss of the NH_2 group.

Stief and DeCarlo[58] also used ^{15}N as a tracer in order to study the ratio of the disproportionation to combination of the N_2H_3. Under the

experimental conditions the initial step was the formation of N_2H_3 by the reaction:-

$$N_2H_4 + H \rightarrow N_2H_3 + H_2 \qquad (12)$$

and the N_2H_3 radicals could disappear by either disproportionation:-

$$2N_2H_3 \rightarrow N_2H_4 + H_2H_2 \rightarrow N_2H_4 + N_2 + H_2 \qquad (22)$$

or by combination:-

$$2N_2H_3 \rightarrow N_4H_6 \rightarrow N_2 + 2NH_3 \qquad (20)$$

In the first case the nitrogen molecule was formed from the two nitrogen atoms of one hydrazine molecule and therefore no randomisation occurred. The second reaction was assumed to occur by the same mechanism as postulated by Higginson and Sutton and would result in 50% radomisation. From their results of the isotope distribution of the nitrogen gas resulting from the reaction of ^{15}N labelled N_2H_3 radicals Stiet and DeCarlo were able to calculate that the ratio of disproportionation to combination was approximately four.

CHAPTER TWO

EXPERIMENTAL

2.1 Materials

In all experiments propellant grade hydrazine of greater than 97.5% w/w purity, obtained from Olin Mathieson Corporation, USA, was used diluted when necessary using de-ionised water. The concentrations of the resulting solutions were determined by two methods:

a) Andrews titration

A small quantity of the hydrazine solution was weighed out into a stoppered flask and sufficient concentrated hydrochloric acid solution to maintain an acid concentration in excess of 5 N throughout the titration was added. Chloroform or carbon tetrachloride, 5 ml, was added as an adsorption indicator and the hydrazine was titrated using 0.5 M potassium iodate solution. Between each addition of iodate solution the flask was vigourously shaken and the stopper then carefully removed to release the evolved nitrogen. The titration was continued until the purple colour of the iodine in the organic layer was just discharged. Under the conditions of the Andrews titration the reaction between hydrazine and potassium iodate may be represented as:-

$$KIO_3 + N_2H_4 + 2HCl \longrightarrow KCl + N_2 + 1Cl + 3H_2O$$

Therefore:

$$KIO_3 \equiv N_2H_4$$

and

$$1 \text{ ml } 0.5 \text{ M } KIO_3 \text{ solution} \equiv 1.6 \times 10^{-2} \text{ g } N_2H_4 \quad .$$

b) Measurement of the refractive index

Two drops of the hydrazine solution were placed on the lower face of the refractometer and the refractive index determined with respect to the d-lines of sodium. The concentration of the hydrazine solution was found by reference to standard graphs of the variation of the refractive index at 20°C with respect to hydrazine concentration.

The propellant grade hydrazine was used as received and no attempts were made to further purify the hydrazine.

For experiments using ^{15}N as a tracer a sample of hydrazine rich in ^{15}N was obtained from Isotopes Incorporated, USA, as an aqueous solution. The nitrogen isotope content was 96.2 atom % ^{15}N and 3.8 atom % ^{14}N. A stock solution of hydrazine was prepared by diluting the ^{15}N-enriched sample of hydrazine with an excess of normal propellant grade hydrazine to produce a solution in which the nitrogen isotope distribution was non-random. The solution was diluted to 25 ml using de-ionised water and the concentration of the resulting solution was 9.65 mole dm^{-3}. The weight of ^{15}N-enriched hydrazine was 0.119 gm and the weight of normal propellant grade hydrazine was 7.776 gm; thus the molar dilution ratio was 1 mole of ^{15}N-enriched hydrazine to 65.3 mole of propellant grade hydrazine. Assuming the nitrogen isotopes in the ^{15}N-enriched hydrazine sample were distributed in the statistical proportions according to the expression:

$$\frac{[H_2\ {}^{15}N\ {}^{14}N\ H_2]^2}{[({}^{14}N_2H_4)({}^{15}N_2H_4)]} = 4$$

Then the mole percentage distribution of the isotopically different forms of hydrazine in the ^{15}N-enriched sample was:-

$^{15}N_2H_4$	$^{15}NH_2.{}^{14}NH_2$	$^{14}N_2H_4$
92.55%	7.31%	0.14%

For normal propellant hydrazine the ^{15}N content was assumed to be 0.38 atom % the same as for the nitrogen of the atmosphere[59], and on the basis of the expression above the isotope distribution was calculated to be:-

$^{15}N_2H_4$	$^{15}NH_2.{}^{14}NH_2$	$^{14}N_2H_4$
0.00144%	0.757%	99.2%

The calculated ^{15}N isotope content of the stock solution of hydrazine was 1.824 atom % and the isotope distribution, calculated from the isotope distributions of the ^{15}N-enriched and the normal hydrazine sample and the molar dilution ratio, was:-

$^{15}N_2H_4$	$^{15}NH_2.^{14}NH_2$	$^{14}N_2H_4$
1.396%	0.856%	97.73%

This is a non-random distribution of the nitrogen isotopes. Based on the nitrogen isotope content the random distribution would be:-

$^{15}N_2H_4$	$^{15}NH_2.^{14}NH_2$	$^{14}N_2H_4$
0.033%	3.581%	96.39%

Theoretical isotope distributions for the nitrogen gas evolved by the decomposition of the stock solution of hydrazine may be calculated making assumptions as to the possible mechanisms for the formation of the nitrogen molecule. If, for example, the decomposition of hydrazine follows a reaction mechanism in which the two nitrogen atoms of one hydrazine molecule remain bonded together and form the nitrogen molecule, then the isotope distribution of the nitrogen gas will be the same as that of the stock solution of hydrazine. The calculated isotope distribution for this mechanism is given in Table 2.1 for 0% N-N bond fission.

On the other hand, if all the nitrogen-nitrogen bonds in the hydrazine molecules are broken in the decomposition reaction then the nitrogen molecule can only be formed by the recombination of nitrogen containing species. Such a recombination process may be assumed to be a purely random process, hence the isotope distribution of the resulting nitrogen gas may be calculated from the statistical expression (19) and the ^{15}N content of 1.824 atom %. The isotope distribution calculated on this basis is given in Table 2.1 for 100% N-N bond fission.

These are the two extreme mechanisms for the formation of the nitrogen molecule but a third, intermediate, mechanism will also be considered. This mechanism was postulated by Higginson and Sutton[57] to account for a result of approximately 50% randomisation observed as a result of the oxidation of aqueous hydrazine solutions in the presence of acid. A detailed mechanism is presented in the introduction. The isotope distribution calculated on the basis of such a mechanism is given in Table 2.1 for 50% N-N bond fission.

A second stock solution of hydrazine was prepared by diluting the 9.65 mole dm^{-3} stock solution with normal propellant grade hydrazine to give a solution of 14.1 mole dm^{-3} hydrazine. For this stock solution the molar dilution ratio was 1 mole ^{15}N-enriched to 122.3 mole normal hydrazine and the ^{15}N content was calculated to be 1.157 atom %. The isotope distributions calculated for this solution on the basis of the three mechanisms given above are presented in Table 2.1.

TABLE 2.1

Calculated nitrogen isotope distributions

Hydrazine solution mole dm^{-3}	Percentage of N-N bond fission	% distribution of nitrogen isotopes			^{15}N content atom %
		$^{14}N_2$	$^{15}N\ ^{14}N$	$^{15}N_2$	
9.65	0	97.73	0.856	1.396	)
9.65	50	97.1	2.218	0.715	) 1.824
9.65	100	96.39	3.581	0.033	)
14.1	0	98.4	0.81	0.75	)
14.1	50	98.05	1.55	0.38	) 1.157
14.1	100	97.69	2.29	0.013	)

To show that randomisation could be detected an experiment was carried out in which a sample of the 9.65 mole dm^{-3} stock hydrazine solution was

oxidised using ceric sulphate in acid solution. The mass spectrometric analysis of the resulting nitrogen gas samples gave a nitrogen isotope distribution of:-

$^{14}N_2$	$^{15}N\,^{14}N$	$^{15}N_2$
97.0	2.20	0.74

This result is in good agreement with the isotope distribution calculated on the basis of 50% randomisation. It thus proved that randomisation could be detected in the system in use and, as the result was in good agreement with that of Higginson and Sutton, also demonstrated the accuracy of the system.

The catalyst samples, in the form of $\frac{1}{8}$ inch alumina pellets impregnated with metal, were obtained from two sources:

a) The Shell Development Company, USA

Samples of the Shell 405 catalyst consisting of 33% iridium on an alumina support were obtained from the Shell Development Company.

b) Engelhard Industries Ltd

Engelhard Industries supplied the samples of iridium, rhodium, ruthenium, platinum and palladium catalysts all of which were supplied on the same alumina support. The iridium catalyst samples were obtained in a range of metal loadings while the remaining catalysts were obtained with a metal loading of 20% w/w.

Most of the catalyst samples were used as received from the manufacturers without any further treatment. However some of the samples of iridium catalyst were observed to have much lower catalytic activity than expected on the basis of early work. This loss of activity was traced to over oxidation of the iridium metal when the catalyst had been exposed to the atmosphere after the reduction of the impregnated iridium salts to the metal. These samples were reduced in a furnace using a mixture of hydrogen and nitrogen at 400°C and allowing the catalyst to remain in the furnace in a flow atmosphere

of nitrogen overnight. The small quantity of oxygen in the nitrogen supply was found to oxidise the catalyst very slowly to the point at which no further oxidation occurred when the catalyst was exposed to the air. After such treatment the normal catalytic activity was observed with respect to the decomposition of hydrazine.

Some characterisation of the Shell 405 catalyst has been carried out by Brooks who found the total surface area to be in the range 119-141 $m^2\ g^{-1}$ by nitrogen adsorption. The metal surface area, calculated from the results of hydrogen chemisorption experiments, was observed to be 38.0 $m^2\ g^{-1}$ and from his results Brooks[60] calculated a mean crystallite size of 26 to 29 $\times\ 10^{-6}$ cm. Work carried out at the Warren Spring Laboratory of the Department of Trade and Industry on the characterisation of the Shell 405 catalyst gave a total surface area result of 112 $m^2\ g^{-1}$. The metal surface area, measured by hydrogen chemisorption, was determined as 38.6 $m^2\ g^{-1}$ and the mean crystallite size was calculated to be 25 $\times\ 10^{-6}$ cm. A sample of 30% iridium catalyst prepared by Engelhard Industries was observed to have a total surface area of 129 $m^2\ g^{-1}$, a metal surface area of 19.6 $m^2\ g^{-1}$ and a mean crystallite size of 34 $\times\ 10^{-6}$ cm.

2.2 Experimental techniques

2.2.1 Product analysis

Possible products of the decomposition of hydrazine are hydrogen, nitrogen and ammonia. As ammonia is soluble in aqueous hydrazine solutions (see Appendix A) it is not possible to use any single technique to analyse for all three products. It was decided to use gas chromatography to analyse the evolved permanent gas for the relative proportions of hydrogen and nitrogen and to use a titrimetric method to determine the number of mole of ammonia produced by the decomposition of each mole of hydrazine.

The gas chromatograph consisted of a Pye Series 104 gas sampling valve which could be fitted with a series of different sample volumes ranging from

0.5 cc to 5.0 cc. The sample volumes were calibrated by filling with water and weighing to determine the volume and errors of up to 20% on the nominal calibration were found. The column consisted of a glass tube of 4 mm internal diameter and 1.5 metre in length. The column was packed with Linde Type 5A molecular sieve and was operated at laboratory temperature and using argon as the carrier gas at a flow rate of 50 cc/minute. A Pye Series 104 katherometer detector was used, the output being recorded on a Rikadenki B241 potentiometric recorder which was fitted with a retransmitting slide wire to drive the electron integrator used to measure the peak areas. The chromatograph was calibrated using the series of calibrated volumes to inject samples of nitrogen and hydrogen, obtained from cylinders of compressed gas. The areas of the peaks corresponding to the injected volumes of nitrogen and hydrogen were measured using the electronic integrator and calibration graphs of the integrator counts with respect to the volume of gas were prepared. Under the experimental conditions the hydrogen peak was recorded about 40-50 seconds after injection and the nitrogen peak about 140 seconds later.

The apparatus used in conjunction with the gas chromatograph for the analysis of the evolved permanent gas is shown in Fig. 2.1. The hydrazine solution was placed in the glass reaction vessel and the required number of pellets were placed in the side arm. The apparatus was then purged with argon until analysis showed that all traces of air had been removed. The catalyst pellets were then dropped into the hydrazine solution by rotating the side arm through 180^{o}. The evolved permanent gas was sampled and injected into the gas chromatograph using the gas sampling valve. For catalysts which only decomposed hydrazine very slowly the second apparatus shown in Fig. 2.1 was used. This apparatus had a much smaller ullage volume allowing samples to be collected and analysed with shorter time intervals than the original apparatus would allow.

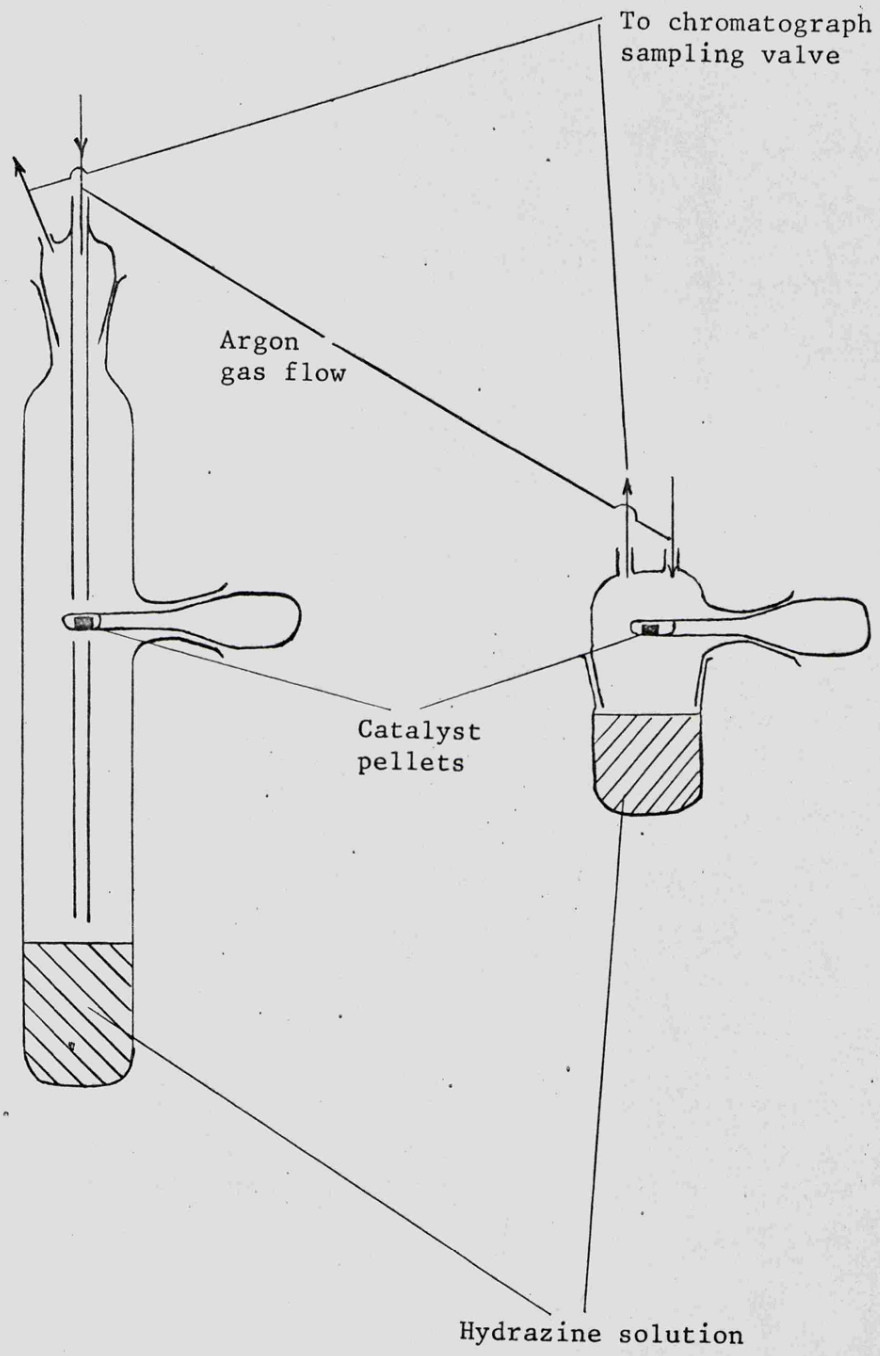

Fig. 2.1 Apparatus used to determine the composition of the evolved permanent gas

The apparatus used to prepare samples for the titrimetric analysis to determine the number of moles of ammonia produced by the decomposition of each mole of hydrazine is shown in Fig. 2.2. The hydrazine solution to be used in the test was analysed for hydrazine concentration by Andrews titration and the total alkali content was determined by acid-base titration using standard hydrochloric acid solution and bromo-cresol green indicator. The volume of hydrazine used for each experiment was 50 ml and on the basis of the initial titrations the moles of hydrazine and of total alkali used in the experiment were calculated. Any difference between the mole of hydrazine and moles of total alkali was the number of moles of ammonia present in the hydrazine solution as an impurity. The standard volume of hydrazine was pipetted into the reaction vessel, catalyst pellets added and a slow current of air was then drawn through the apparatus to remove any ammonia evolved from the solution. Two acid receiver flasks, containing standardised hydrochloric acid solution, were used to remove the ammonia from the stream of air. After a suitable time interval the reaction was stopped and the hydrazine solution was analysed for hydrazine content by Andrews titration and for total alkali content by an acid-base titration. The two acid receiver solutions were titrated with standardised sodium hydroxide solution to determine the number of moles of ammonia adsorbed.

The number of moles of ammonia formed by the reaction was given by the difference between the total moles of alkali (sum of the moles of alkali in the hydrazine solution and those trapped in the acid solution) and the moles of hydrazine remaining at the end of the reaction. The number of moles of hydrazine decomposed was given by the difference between the initial and final moles of hydrazine determined by Andrews titrations.

2.2.2 The use of ^{15}N as a tracer

The samples of nitrogen gas produced by the decomposition of the stock solutions of ^{15}N-enriched hydrazine on the supported metal catalysts were

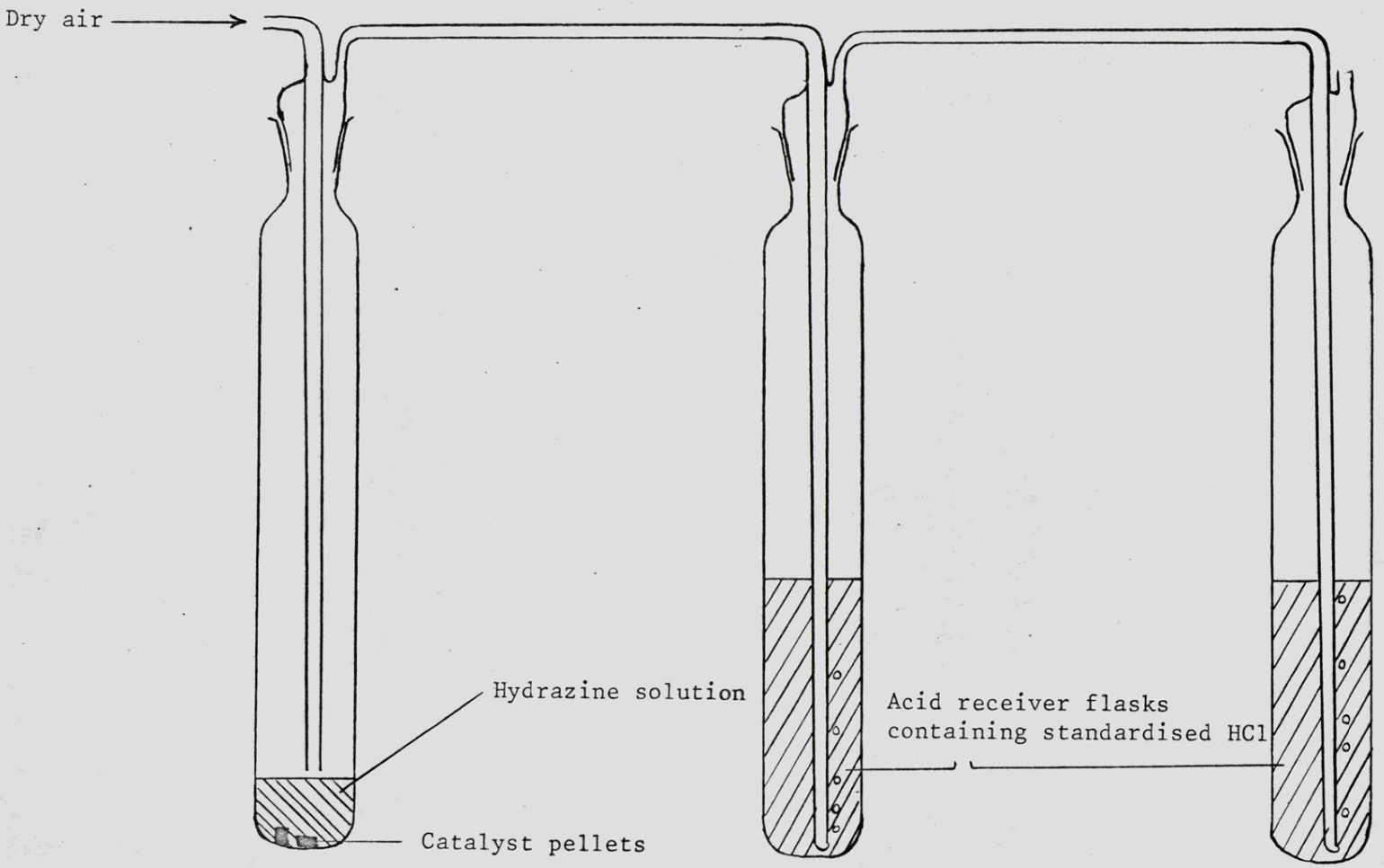

Fig. 2.2 Apparatus used to prepare samples for titrimetric analysis

prepared using the apparatus shown in Fig. 2.3. Sufficient hydrazine to produce, on decomposition, a pressure in the apparatus of greater than one atmosphere was placed in the reaction vessel. The catalyst pellets were placed in the side arm. The solution of hydrazine was frozen by immersion in liquid nitrogen and the apparatus was evacuated by pumping. The apparatus was then isolated from the pump and checked for leaks. When the apparatus was proved to be free from leaks the hydrazine was allowed to melt and then immersed in a beaker of water at 70°C to boil out any dissolved air. The solution was then refrozen by immersion in liquid nitrogen and the freeze-pump-thaw cycle repeated four times. The hydrazine solution was then allowed to reach temperature equilibrium in a thermostatically controlled water bath and the catalyst pellets were dropped into the hydrazine solution by rotating the side arm through 180°. The pressure in the apparatus was monitored using the mercury manometer and when the pressure in the system reached 780 mm Hg the gas sample bottle was sealed and the reaction stopped by immersing the solution in liquid nitrogen. The pressure in the apparatus was taken above atmospheric so that any leakage of gas through the stopcock would be from the sample to the atmosphere. The nitrogen gas samples were then analysed for the three nitrogen mass numbers 28, 29 and 30, and also for oxygen 32, on a Metropolitan-Vickers type MS2 mass spectrometer. Only rarely was the oxygen 32 peak observed above the background noise level of the instrument and the results of those samples were ignored in calculating the nitrogen isotope distributions.

2.2.3 Measurement of the rate of decomposition of hydrazine

It was decided to measure the rate of decomposition of hydrazine by measuring the rate of gas evolution with respect to time and then extrapolating the rate of gas evolution to the theoretical start of the reaction. In some cases this extrapolation was not necessary as the rate of decomposition was found to be independent of the time of reaction over the time of an

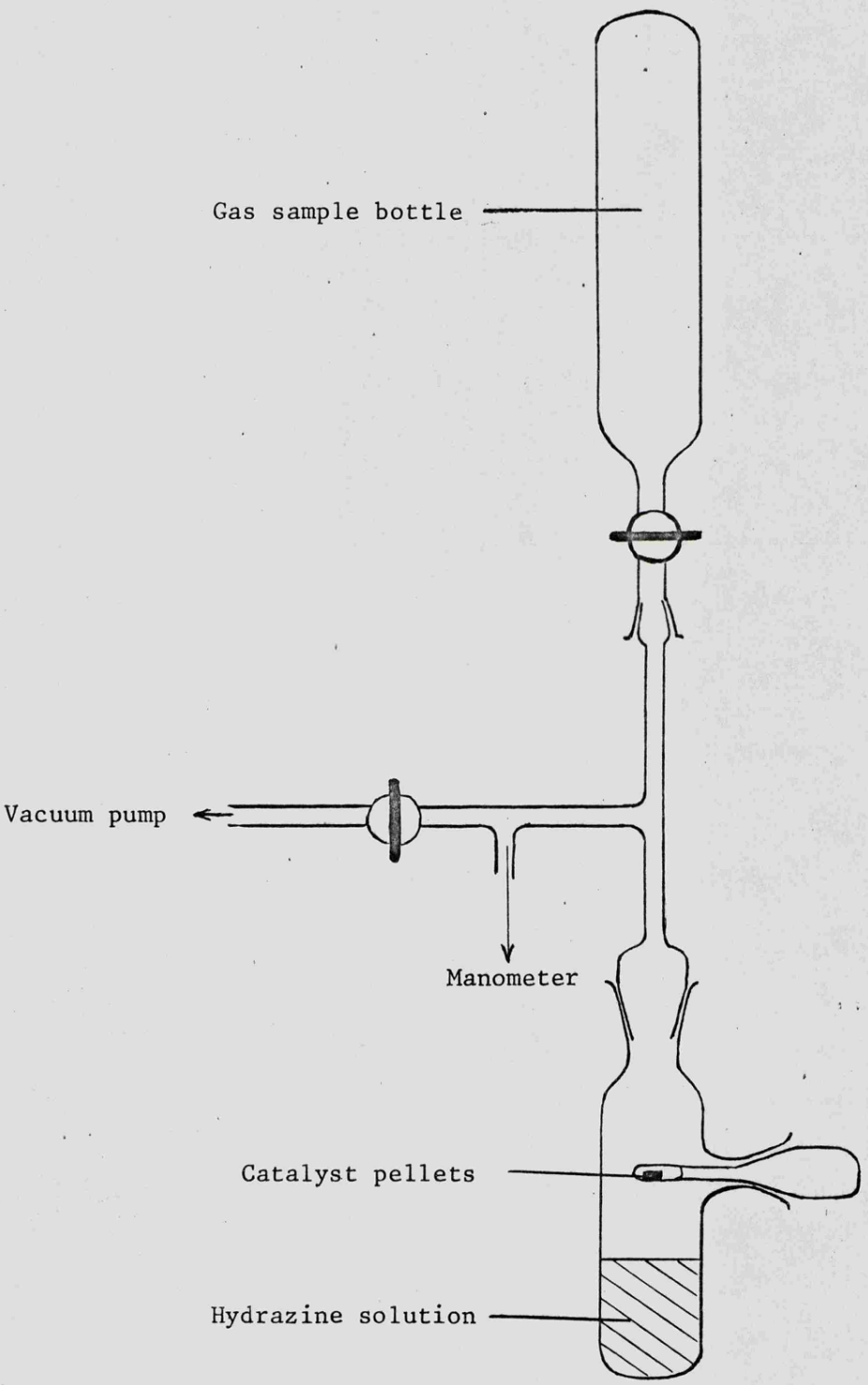

Fig. 2.3 Apparatus used to prepare samples of nitrogen gas for mass spectrometric analysis

experiment. As ammonia is soluble in aqueous hydrazine solutions the proportion of the ammonia observed in the gaseous products will vary with time of reaction and so any evolved ammonia was adsorbed using a molecular sieve filter. Over the range of experimental conditions studied the decomposition of hydrazine on the five supported metal catalysts result in a range of gas evolution rates from 1 to 3000 cc gas gm^{-1} min^{-1}. No single technique was available to cover such a range of gas flow rates and it was necessary to use two different techniques to cover the range. For high rates of gas evolution calibrated flowmeters were used while for measuring low rates of gas evolution gas burettes were used.

The only catalyst which decomposed hydrazine at a sufficiently high rate to require the use of the calibrated flowmeters was the Shell 405 catalyst and this was the first to be studied. The decomposition of hydrazine is a highly exothermic reaction and a high rate of reaction necessarily involves a high rate of heat production. Therefore it was necessary to use well-stirred reaction systems when studying the decomposition of hydrazine on the Shell 405 catalyst in order to try to maintain isothermal conditions.

The first apparatus used to study the decomposition of hydrazine on the Shell 405 catalyst is shown in Fig. 2.4. The glass reaction vessel was constructed with an internal cooling coil and the hydrazine solution was stirred by means of a magnetic stirrer. The catalyst holder was manufactured from PTFE and up to eight pellets could be used, held in place by the PTFE disc which was screwed into the shaft. A glass sheath was located in the shaft and the end of this sheath occupied a position between two catalyst pellets and a thermocouple was placed in the sheath to measure the temperature close to the catalyst pellets. For each experiment 250 ml hydrazine solution was placed in the reaction vessel and the required number of catalyst pellets were loaded into the catalyst holder. The catalyst holder was then lowered into the hydrazine solution and the rate of decomposition

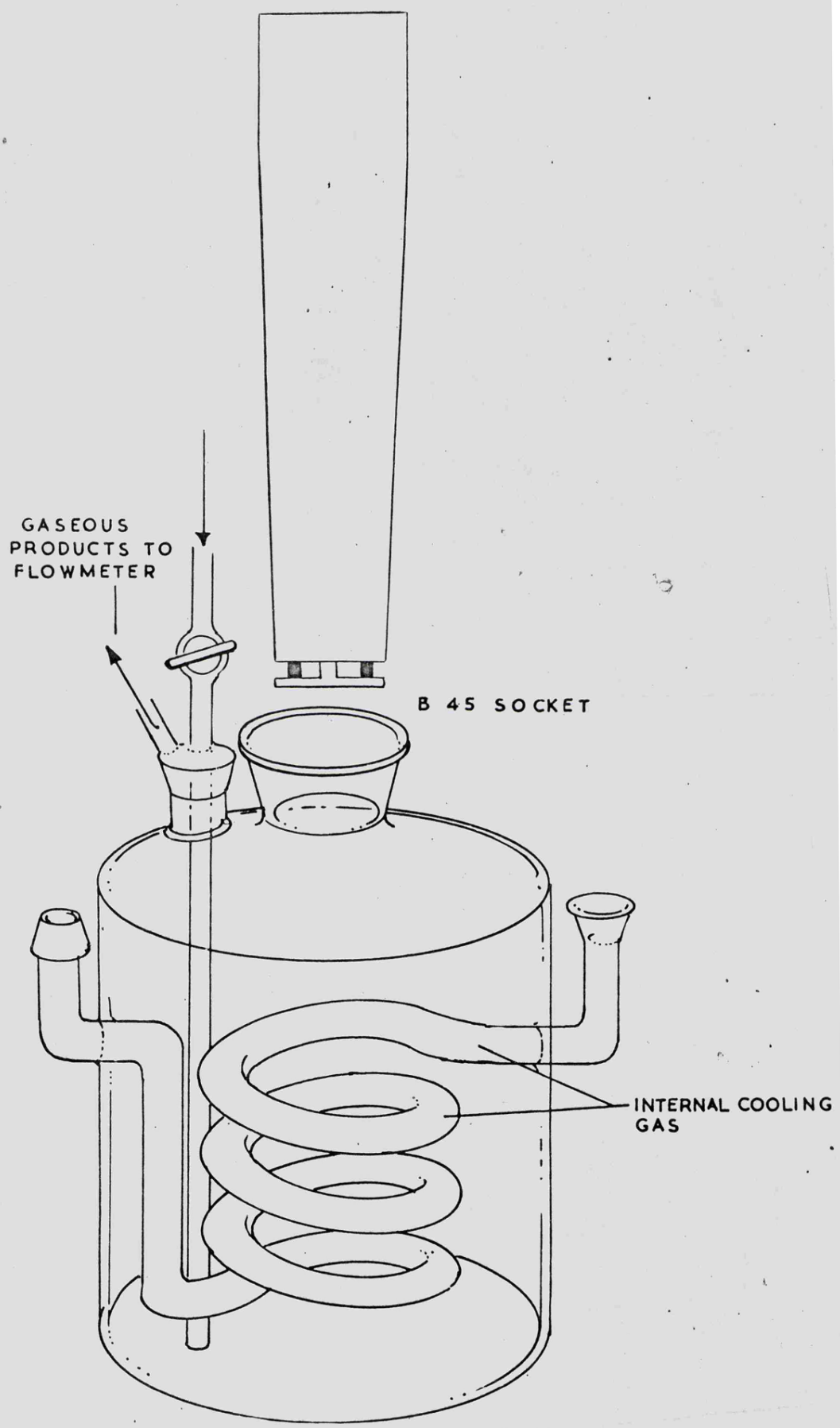

Fig. 2.4 Apparatus used to study decomposition of hydrazine on the Shell 405 catalyst

determined by measuring the rate of gas evolution. For hydrazine solutions of less than 20 to 22 mole dm^{-3} the rate of gas evolution, and the temperature recorded by the thermocouple, increased with time of reaction. For anhydrous hydrazine the rate of gas evolution was extremely erratic, sometimes falling to zero for a few seconds and it was noted that the temperature recorded by the thermocouple increased rapidly with respect to time. Observation of the reaction zone showed bubbles of gas forming around the catalyst pellets giving rise to vapour blanketing and the gas bubble would eventually break down and allow the liquid to contact the catalyst pellets again. There was no way in which the apparatus could be modified to overcome this problem and so a new apparatus was designed.

In place of the stationary catalyst holder a combined catalyst holder/stirrer was made as shown in Fig. 2.5, this also replaced the magnetic stirrer. The combined catalyst holder/stirrer was made from PTFE and the stirrer blade screwed into the shaft and was tightened onto the catalyst retaining disc. A polythene block was machined to form a B45 size cone to fit the glass reaction vessel and a brass drive shaft passed through the polythene cone, via bearings and gas seals, to connect the PTFE shaft to an electric motor. The rotational speed of the stirrer was measured using a tachometer and the speed was varied by means of a voltage regulator in the electric motor power supply line. The weakest point in the design was considered to be the gas seals between the rotating brass drive shaft and the stationary polythene cone. Tests were carried out to establish the efficiency of these seals by flowing nitrogen gas into the apparatus and monitoring the rate of nitrogen flow out of the apparatus while the stirring speed was varied over the range 0 to 500 rpm. The entry and exit rates of nitrogen gas flow were monitored using calibrated flow meters. It was found that over the range of stirring speeds and nitrogen flow rates studied there was no evidence of any gas leakage. As both the testing of the gas seals and actual experiments on the

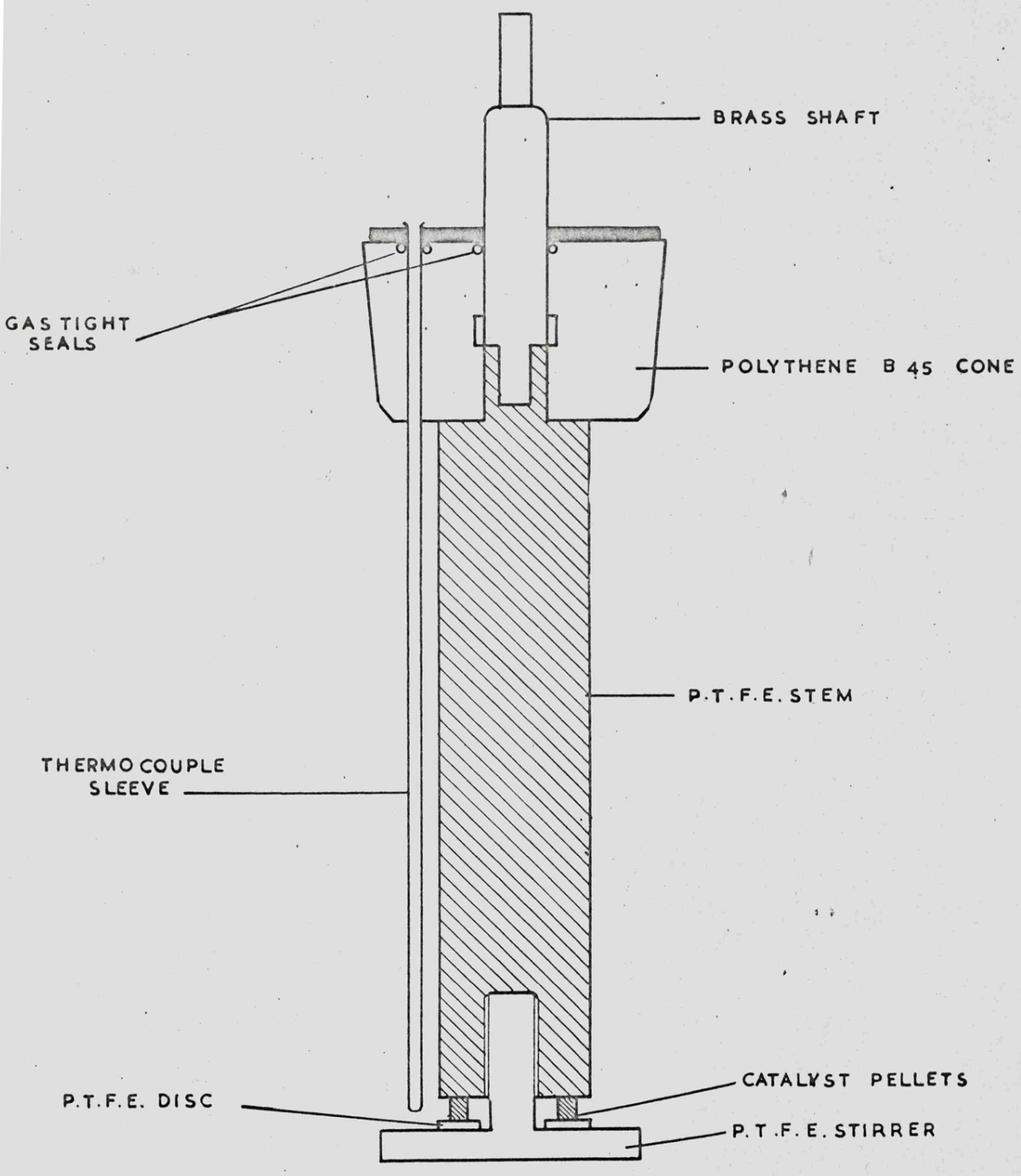

Fig. 2.5 Combined catalyst holder/stirrer

decomposition of hydrazine involve nitrogen gas exhausting to atmosphere through a flow meter it was concluded that under actual experimental conditions the measured flow rate would be the rate of gas evolution from the reaction.

The next experimental parameter to be studied was the effect of stirring speed on the rate of decomposition of hydrazine. 200 ml hydrazine solution was placed in the reaction vessel and this was immersed in a thermostatically controlled water bath. The catalyst holder was loaded with pellets and inert alumina pellets used to fill the remaining spaces to give a total of eight pellets. The catalyst holder was placed in a glass sheath and immersed in the water bath. When temperature equilibrium had been reached the catalyst holder was removed, attached to the drive from the electric motor and then lowered into the hydrazine solution while rotating at the required speed. A series of experiments were carried out using different stirring speeds and the rate of gas evolution was recorded as a function of time. At low stirring speeds the tendency for vapour blanketing to occur was reduced and the rate of gas evolution was smooth but increased rapidly with respect to time. Increasing the stirring speed to 250 rpm plus resulted in a steady rate of gas evolution for low and medium concentrations of hydrazine with respect to both stirring speed and time. For anhydrous hydrazine the rate of gas evolution increased slowly with respect to time to reach a steady value and this was constant with respect to stirring speed. These results are shown in Fig. 2.6. It was decided to use a stirring speed in the range 300-350 rpm and, when the rate of gas evolution exhibited a slow change with respect to time, to determine the theoretical rate of gas evolution at the start of the reaction by extrapolation to zero time.

The above system was considered suitable for the study of the variation of the rate of decomposition of hydrazine with respect to hydrazine concentration at laboratory temperature. However, the study of the temperature

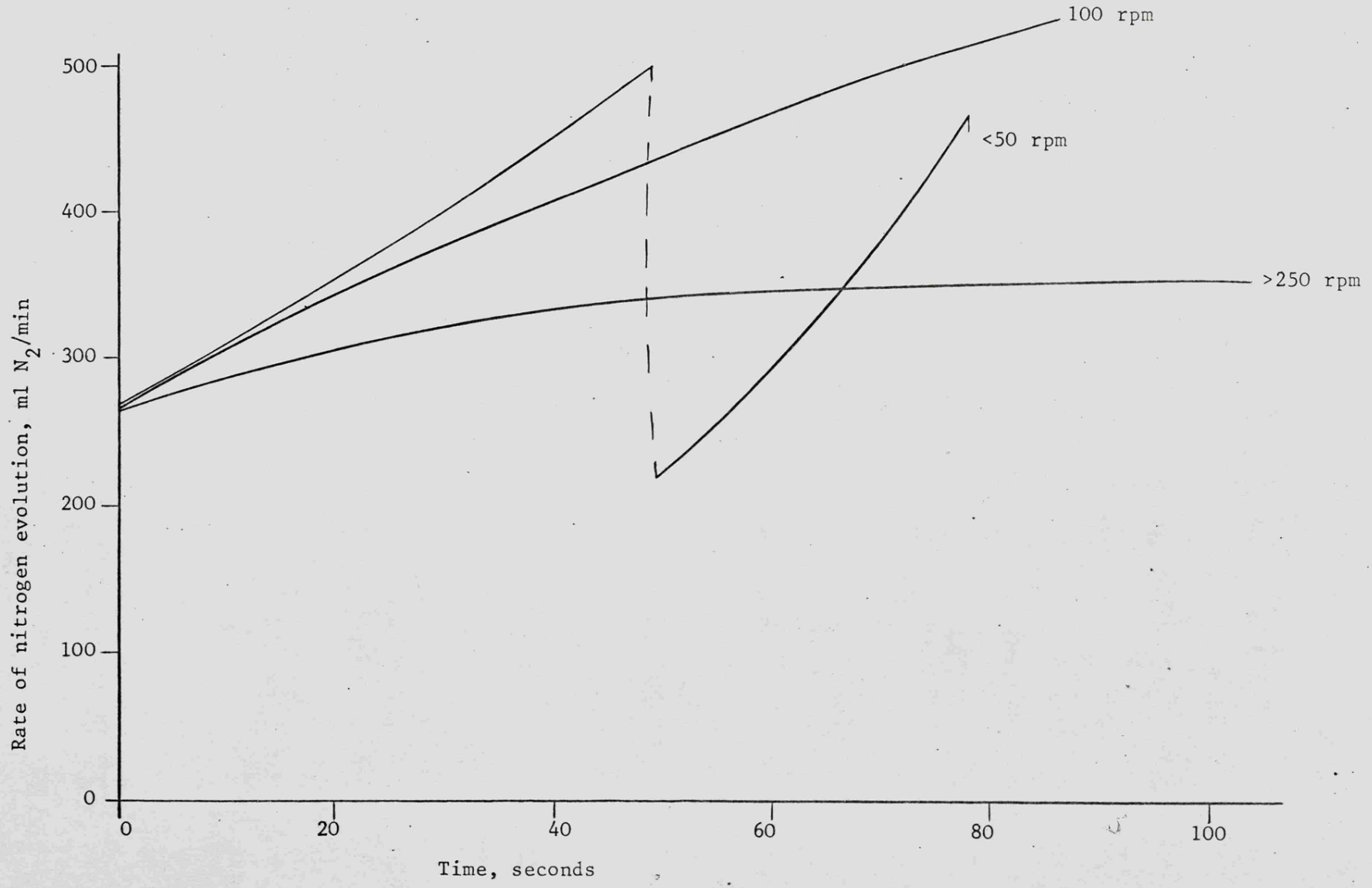

Fig. 2.6 Variation of rate of nitrogen evolution as a function of stirring speed

dependence of the rate of decomposition would involve the exposure of the cooled, or heated, catalyst pellets to the laboratory atmosphere for some time interval between the removal of the sheath and the catalyst holder being immersed in the hydrazine solution. Therefore there is the possibility of the temperature of the catalyst pellets changing during the exposure to the laboratory atmosphere and this would have some effect on the rate of decomposition. The effect would increase with increasing temperature differential thus effecting the accuracy of the calculated activation energy. To overcome this the apparatus shown in Fig. 2.7 was used to study the variation of the rate of decomposition with respect to temperature. The same catalyst holder/stirrer was used. The experimental procedure was to pipett 50 ml hydrazine solution into the side arm and to place the catalyst holder/stirrer in the reaction compartment. The apparatus was then immersed in a thermostatically controlled water bath. When temperature equilibrium had been reached the electric motor was switched on and the stirring speed set in the range 300-350 rpm. The hydrazine solution was transferred to the reaction compartment by means of helium gas pressure and the rate of gas evolution was measured using calibrated flow meters.

The apparatus used with the gas burettes to measure the rate of decomposition of hydrazine on the palladium, platinum, rhodium and ruthenium catalysts is shown in Fig. 2.8. 50 ml hydrazine solution was pipetted into the reaction vessel and the required number of catalyst pellets were placed in the side arm. The apparatus was immersed in a thermostatically controlled water bath and allowed to reach temperature equilibrium. The catalyst pellets were dropped into the solution by rotating the side arm through 180^{o}. The course of the reaction was followed by measuring the volume of permanent gas evolved with respect to time using the gas burette. The rate of reaction was calculated from the slope of the volume of gas evolved with respect to time. The rates of reaction in cc $[N_2 + H_2]$ per gm of catalyst per second were

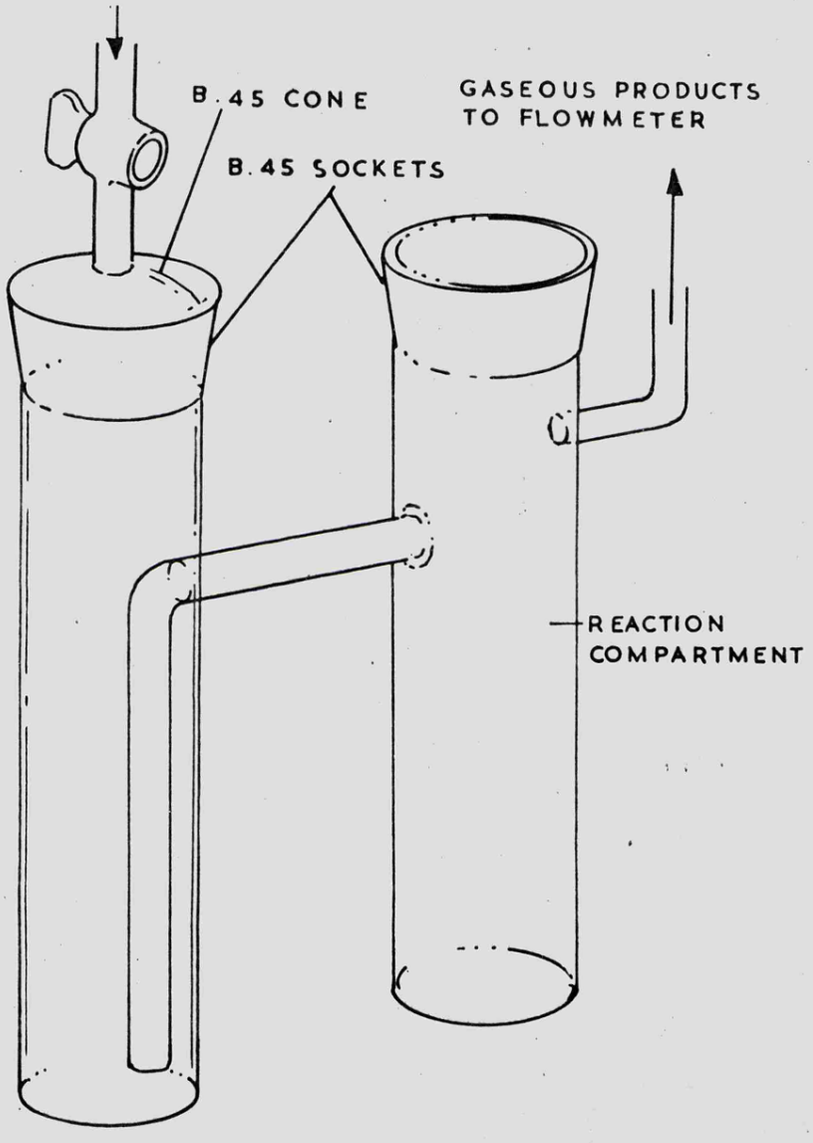

Fig. 2.7 Modified apparatus to study temperature dependence of the decomposition of hydrazine on the Shell 405 catalyst

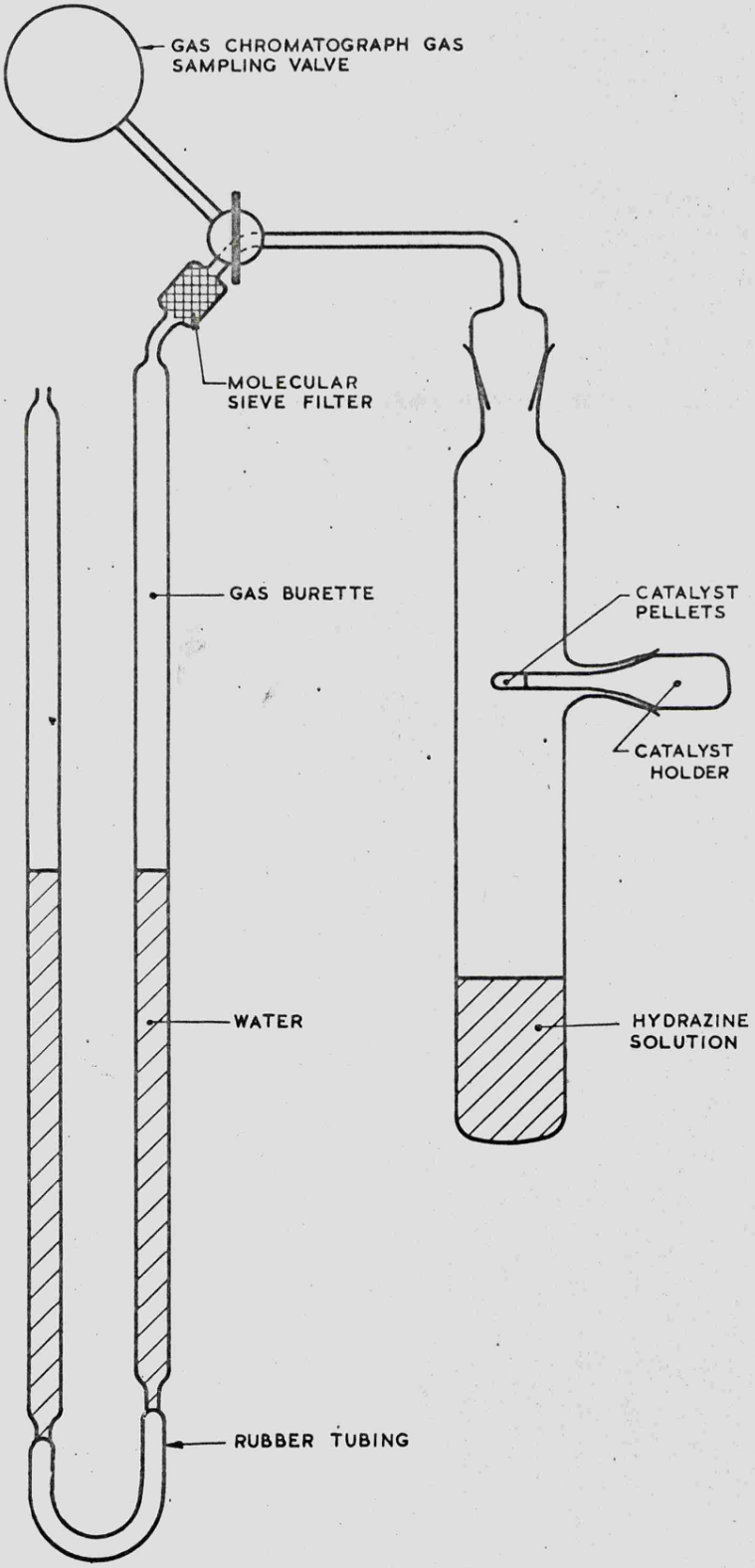

Fig. 2.8 Apparatus used to measure the rate of decomposition of hydrazine

corrected to standard temperature and pressure. Each experiment was terminated before the concentration of hydrazine had changed appreciably.

2.2.4 Preparation of samples of oxidised iridium catalyst

The Shell 405 catalyst as prepared consists of a mixture of iridium and oxygen in the atomic ratio of 1 to 0.4. This atomic ratio is stable in air at normal temperatures and is formed when the reduced catalyst is slowly exposed to the air. A Stanton Massflow Thermal Balance was used to prepare samples of the Shell 405 catalyst having higher oxygen to iridium ratios. The thermal balance used had a temperature range up to 1000°C and could take a sample of up to 20 gm and measure weight changes of down to 1.0 mgm. The sample holder is situated in a sealed sheath which permits the use of controlled atmospheres.

The experimental procedure was to accurately weigh out a sample of Shell 405 catalyst pellets into a crucible. This was then placed on the rise rod of the balance the the sheath placed in position. The appropriate weights were removed from the balance weight chamber and the balance was then set up for weight loss followed by weight gain in accordance with the manufacturers instructions. Nitrogen gas was flowed through the sheath of the balance and the hydrogen lines purged to remove all traces of air. The furnace was then switched on and the furnace temperature was programmed to rise at 6°C per minute. The loss in weight due to dehydration of the catalyst was recorded when the catalyst reached a steady weight at a temperature of 350°C. Hydrogen was then added to the gas flow and the further decrease in weight due to the reduction of the iridium oxide was recorded. The weight of iridium in the fully reduced catalyst was calculated and the weight increase corresponding to the required iridium to oxygen ratio was determined. The temperature of the furnace was reduced and the hydrogen gas flow was stopped. A calibrated flow rate of air or oxygen was added to the nitrogen gas flow and when the weight increment corresponding to the required amount of oxygen had been

achieved the air flow was turned off and the catalyst allowed to cool in nitrogen. It was possible to vary the extent of oxidation by controlling the partial pressure of oxygen and the temperature of the furnace. The atmosphere of nitrogen was then replaced with air to ensure that there was no further oxidation of the catalyst resulting from the exposure to the air and the catalyst then used in experiments.

2.2.5 The decomposition of hydrazine on the reduced iridium catalyst

The reduced iridium catalyst is not stable in air but readily chemisorbs oxygen to partially oxidise the metal. If the oxidation process is carefully controlled to prevent excessive heating of the catalyst then the lowest iridium to oxygen atomic ratio, which is stable with respect to the air at ambient temperature, is approximately 1:0.4. Any attempts to carry out experiments using a catalyst having lower atomic ratio than 1:0.4 must, therefore, be carried out under an inert atmosphere. A batch of Shell 405 catalyst pellets were placed in a U-bend of a glass tube which was fitted inside a furnace. The nitrogen and hydrogen supply lines were purged to remove all traces of air and the catalyst pellets were then heated to 350^{o}C in a stream of nitrogen gas. Hydrogen was then added to the gas flow to give a reducing atmosphere of approximately 25% hydrogen and 75% nitrogen and the reduction process was carried on for 1 hour. Experiments using the thermal balance had shown the reduction process to be complete in about 15 minutes but extra time was added on to ensure complete reduction. The catalyst was allowed to cool in nitrogen and the glass tube was then removed from the furnace and the centre section containing the catalyst sample was sealed off using a flame. The catalyst sample was transferred to a glove box which was filled with nitrogen and the glass tube was cut open and the catalyst pellets were transferred to a stoppered glass bottle. The reaction vessel shown in Fig. 2.8 was then prepared as usual except that the atmosphere above the hydrazine solution was pumped away and replaced with argon. The reaction vessel was passed through

the transfer port into the glove box, the appropriate number of pellets were loaded into the side arm and the reaction vessel was then removed from the glove box. The rate experiment was then carried out in the usual way.

The second system to be used is shown in Fig. 2.9, for each experiment the catalyst pellets would be reduced in the furnace and then transferred immediately to the reaction vessel keeping the pellet in a reducing atmosphere at all times. The furnace was set up and the reduction process carried out as in the preceding section. The catalyst pellet was allowed to cool in the hydrogen/nitrogen atmosphere and then transferred, by tilting the appropriate section of the apparatus to roll the pellet along the tubing, to point A. The stopcock B was closed and the pellet was dropped into the hydrazine solution by tilting the apparatus. Stopcock C was turned to connect only the reaction vessel and the gas burette and the rate of reaction was measured in the usual way.

2.2.6 Measurement of the induction period of the decomposition of hydrazine on the Shell 405 catalyst

The apparatus used is shown in Fig. 2.10 and consists of a glass reaction vessel which was fitted with two photoelectric cells and a pressure transducer. The outputs from these instruments were recorded on a galvanometer recorder. The pressure transducer was calibrated against a standard column of mercury and before each experiment calibration steps corresponding to 20, 40 and 60 mm Hg were recorded. For each experiment 10 ml hydrazine solution was pipetted into the apparatus and one catalyst pellet was placed in the catalyst holder. The apparatus was immersed in a thermostatically controlled water bath and allowed to reach temperature equilibrium. The distances of d_1 and d_2 were measured using a cathatometer. When temperature equilibrium had been reached the recorder was switched on, using a paper speed of 750 mm/sec, and the pellet was dropped down the tube by rotating the catalyst holder through 180°. The timer trace shown in Fig. 2.11 was activated and

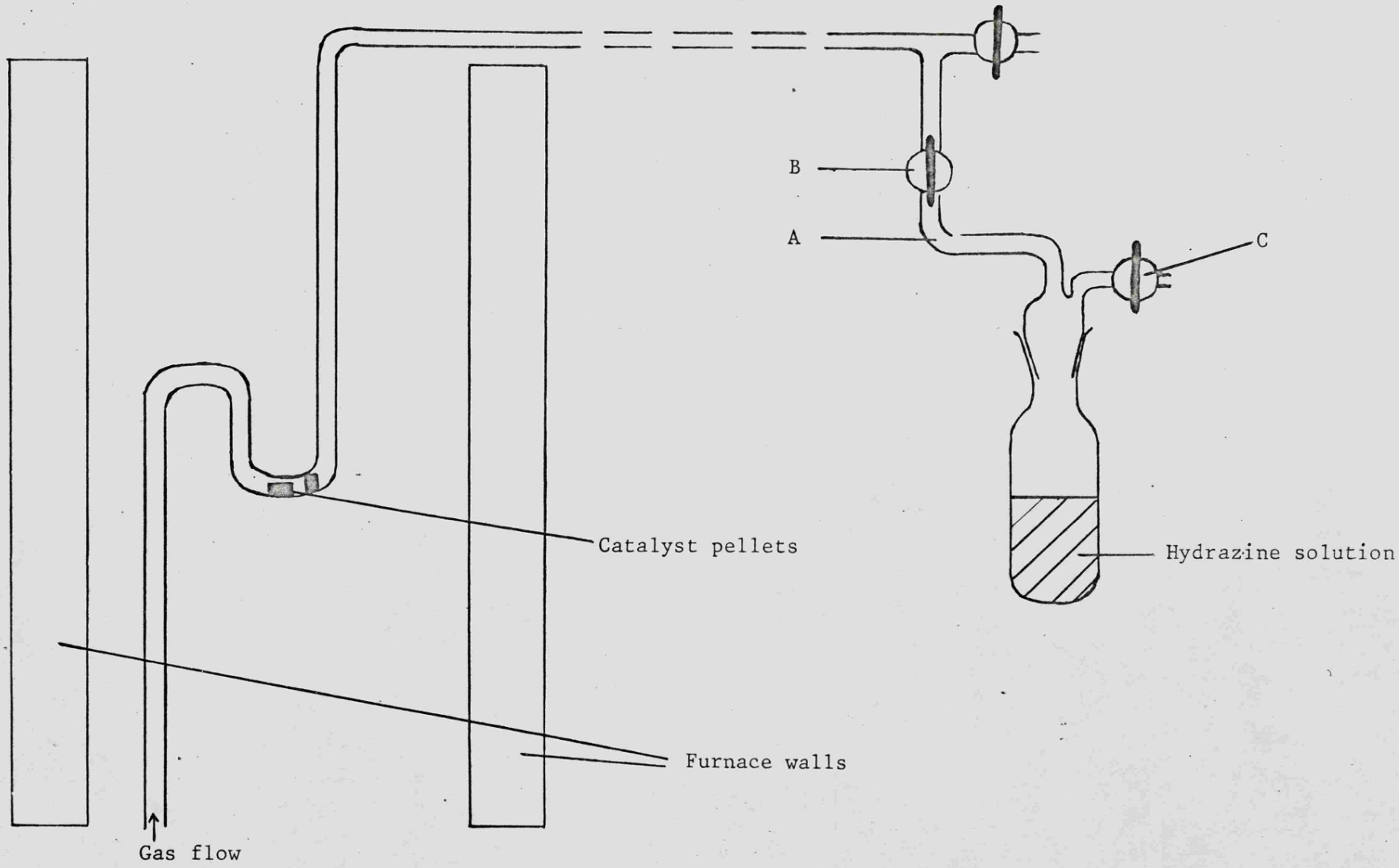

Fig. 2.9 Schematic diagram of apparatus used to study decomposition of hydrazine on reduced iridium catalyst

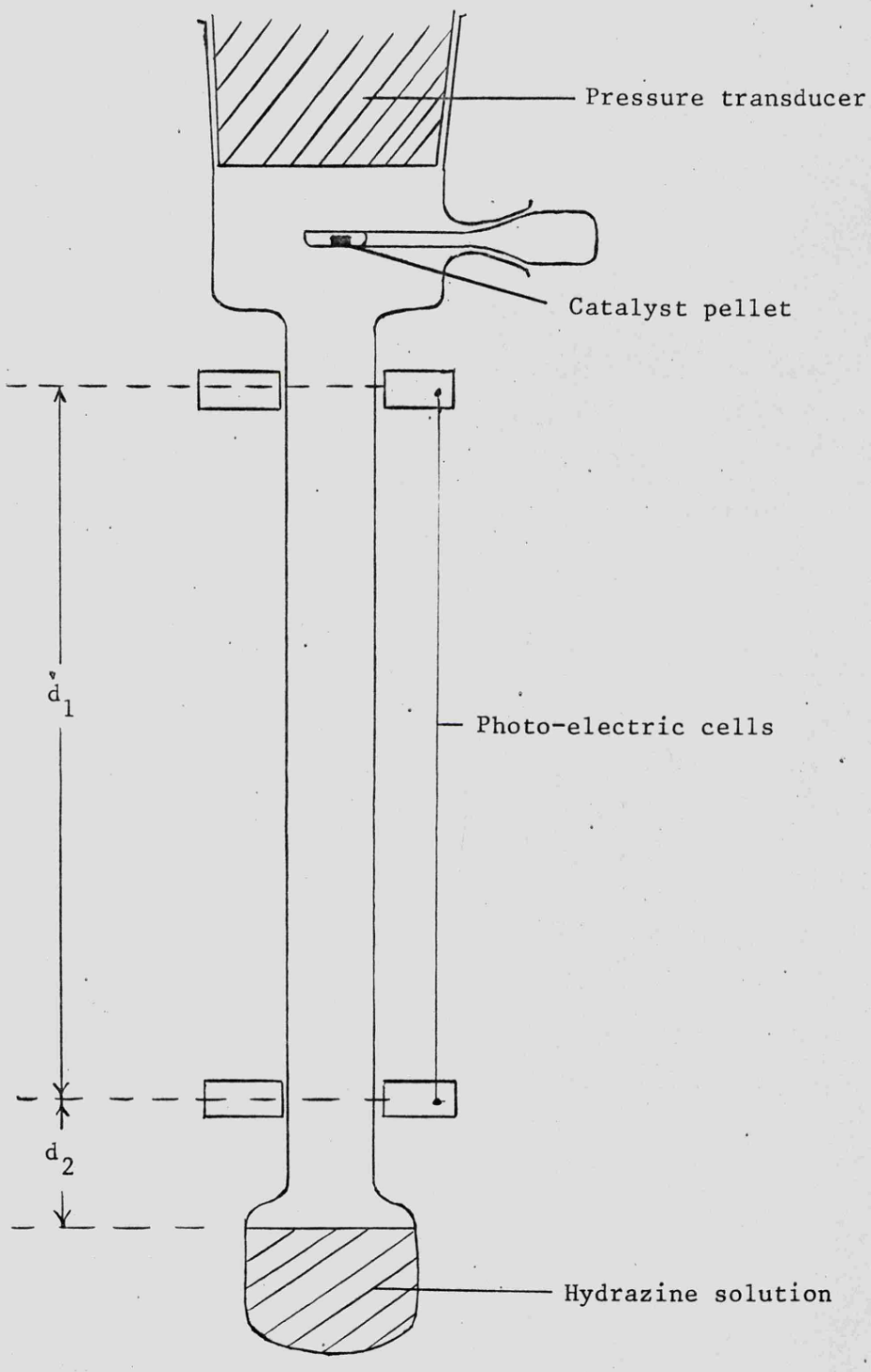

Fig. 2.10 Apparatus used to determine the induction period of the decomposition of hydrazine on Shell 405 catalyst

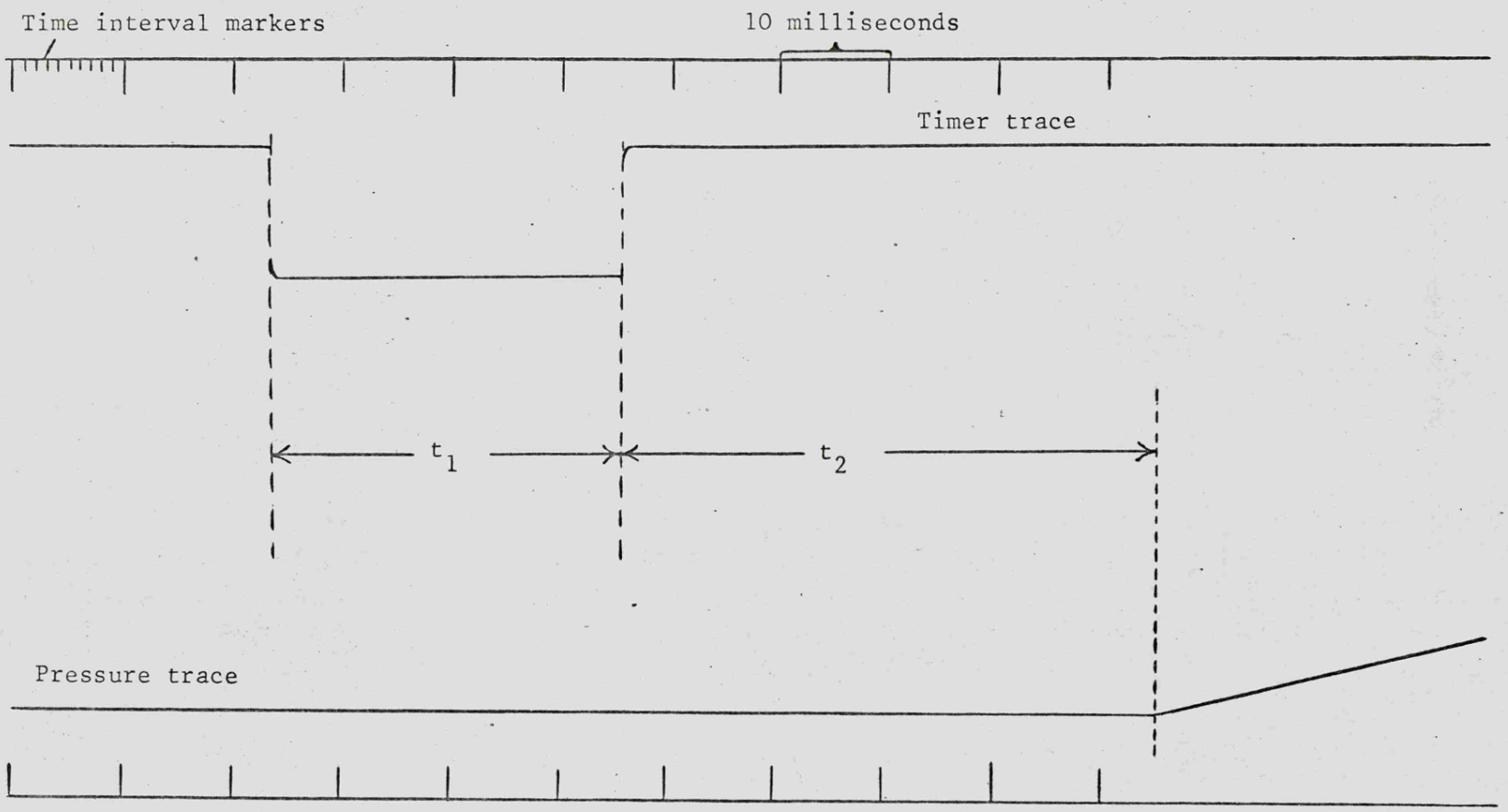

Fig. 2.11 Timer tracer from apparatus shown in Fig. 2.10

deactivated by the catalyst pellet passing photocells 1 and 2 respectively. Assuming that the acceleration of the catalyst pellet in the tube was 981 cm/sec^2 and knowing the distance d_1 and the time, t_1, required for the pellet to cover that distance the velocity, v_2, of the pellet as it passed the second photocell may be calculated from the two equations:-

$$s = v_1 t_1 + \tfrac{1}{2} a t_1^2$$

where v_1 is the velocity of the pellet as it passed the first photocell and a is 981 cm/sec^2, therefore:-

$$v_1 = (s - \tfrac{1}{2} a t_1^2)/t_1$$

and secondly:-

$$v_2 = v_1 + a t_1$$

The time interval t_3 for the pellet to travel the distance d_2 may be calculated from:-

$$s = v_2 t_3 + \tfrac{1}{2} a t_3^2 \quad .$$

The induction period, defined as the time interval from the contact of the pellet and the hydrazine solution to the appearance of gaseous products as indicated by the start of the pressure trace, was given by $(t_2 - t_3)$ seconds. The rate of decomposition of hydrazine was calculated in $d[N_2H_4]/dt$ mole gm^{-1} sec^{-1} from the rate of pressure rise with respect to time on the assumption that the pressure rise was due only to nitrogen evolution.

2.2.7 Search for radicals in solution

There were two techniques used to try to locate and identify any radicals present in the hydrazine solution while the decomposition reaction was occurring. The first was to use a Varian Associates electron spin resonance spectrometer to scan the hydrazine solution and the second was to use a

scavenger which was suggested to be specific for di-imide.

The esr experiments had to be carried out in a flow system as the iridium would give a spectrum and so a catalyst pellet was lodged in a sample cell above the scanned volume and hydrazine flowed past the pellet into the scanned volume. From the measured flow rates of hydrazine solution and the dimensions of the cell it was calculated that the time interval between the solution contacting the catalyst and then reaching the scanned volume was of the order of 10 milliseconds.

It has been shown that di-imide will reduce the double bond of unsaturated organic compounds to produce the saturated compound. One such system is the reduction of cis-4-cyclohexene-1:2-dicarboxylic acid to cyclohexane-1:2-dicarboxylic and the mixture of acids may be separated by thin layer chromatography. A reaction mixture of hydrazine solution, catalyst pellets and cis-4-cyclohexene-1:2-dicarboxylic acid was agitated for several days and then acidified and the organic acids extracted by repeated extractions with ether. The ether solution was then reduced in volume and spots applied to a thin layer plate together with spots of the pure acids in ether solution and the plate was developed in dioxane. The plate was then sprayed with an indicator, bromocresol green, and the products of the reaction system were compared to the pure acids to identify them. Artificial mixtures of the acids were also tested and the difference in distance travelled by the acids was sufficient for positive identification.

C H A P T E R T H R E E

THE USE OF A SUPPORTED RUTHENIUM CATALYST

3.1 Results

3.1.1 Product analysis

The permanent gas evolved by the decomposition of hydrazine solutions on the supported ruthenium catalyst was analysed for hydrogen and nitrogen using the gas chromatograph. The variation of the permanent gas composition with respect to hydrazine concentration was studied at 24°C and the results are given in Table 3.1.

TABLE 3.1

Variation of the permanent gas composition with respect to hydrazine concentration at 24°C

Hydrazine concentration, mole dm^{-3}	% H_2	% N_2
1.2	24.1	75.9
3.1	25.6	74.4
6.1	25.1	74.9
9.3	26.5	73.5
12.3	23.0	77.0
14.7	25.1	74.9
18.3	25.0	75.0
21.4	25.7	74.3
24.4	25.1	74.9
26.4	24.9	75.1

The results show that the relative proportions of hydrogen and nitrogen are independent of hydrazine concentration.

The effect of temperature on the permanent gas composition was studied for two concentrations of hydrazine solution, 6.1 and 18.3 mole dm^{-3}, and the results are presented in Tables 3.2 and 3.3 respectively.

TABLE 3.2

Variation of the permanent gas composition with respect to temperature for the decomposition of 6.1 mole dm^{-3} hydrazine solution on the ruthenium catalyst

Temperature, ^{o}C	% H_2	% N_2
17.5	25.5	74.5
24.0	25.1	74.9
36.0	18.6	81.4
44.0	18.3	81.7
51.0	16.1	83.9
58.0	14.0	86.0
63.0	12.0	88.0
69.0	12.5	87.5

TABLE 3.3

Variation of the permanent gas composition with respect to temperature for the decomposition of 18.3 mole dm^{-3} hydrazine solution on the ruthenium catalyst

Temperature, ^{o}C	% H_2	% N_2
-10.0	34.4	65.6
- 6.0	35.7	64.3
0	30.1	69.9
5.0	30.5	69.5
7.0	30.7	69.3
12.0	27.8	72.2
17.5	25.0	75.0
24.0	25.0	75.0

These results show that the relative proportions of nitrogen and hydrogen vary with respect to temperature, the percentage of nitrogen in the permanent gas increasing with increasing temperature.

A third parameter to be studied was the effect on the permanent gas composition of the pre-adsorption of the products of the reaction on the catalyst surface. The effect of the pre-adsorption of hydrogen on the catalyst on the permanent gas composition is shown in Table 3.4.

TABLE 3.4

The effect of hydrogen pre-adsorption on the permanent gas composition

Hydrogen pre-adsorbed	Hydrazine concentration, mole dm^{-3}	Temperature, ^{o}C	% H_2	% N_2
No	9.3	24.0	26.5	73.5
Yes	9.3	24.0	48.5	51.5
No	18.3	24.0	25.0	75.0
Yes	18.3	24.0	49.5	50.5
No	26.4	24.0	24.9	75.1
Yes	26.4	24.0	50.3	49.7
No	18.3	-10.0	34.4	65.6
Yes	18.3	-10.0	50.2	49.8
No	6.1	36.0	18.6	81.4
Yes	6.1	36.0	47.7	52.3
No	6.1	69.0	12.5	87.5
Yes	6.1	69.0	51.3	48.7

Compared to the standard catalyst condition the effect of the pre-adsorption of hydrogen is to increase the proportion of hydrogen in the permanent gas. The effect of the pre-adsorption of ammonia on the permanent gas composition was also studied and the results are given in Table 3.5. The pre-adsorption of ammonia has no effect on the permanent gas composition.

TABLE 3.5

The effect of ammonia pre-adsorption on the permanent gas composition

Ammonia pre-adsorption	Hydrazine concentration mole dm^{-3}	Temperature, ^{o}C	% H_2	% N_2
No	18.3	-10.0	34.4	65.6
Yes	18.3	-10.0	33.1	66.9
No	18.3	5.0	30.5	69.5
Yes	18.3	5.0	27.5	72.5
No	18.3	24.0	25.0	75.0
Yes	18.3	24.0	26.3	73.7
No	26.4	24.0	24.9	75.1
Yes	26.4	24.0	23.8	76.2

3.1.2 The use of ^{15}N as a tracer

The results of the mass spectrometric analysis of the nitrogen gas evolved by the decomposition of the stock ^{15}N enriched hydrazine solutions on the supported ruthenium catalyst are given in Table 3.6. Also included in Table 3.6 are the calculated isotope distributions from Section 2 for 0% and 100% N-N bond fission.

TABLE 3.6

Results of the mass spectrometric analysis of nitrogen gas samples

Hydrazine solution, mole dm^{-3}	% N-N bond fission (theoretical)	% distribution of nitrogen isotopes			Per cent ^{15}N
		28	29	30	
9.65	100%	96.39	3.581	0.033	1.824
9.65	0%	97.73	0.856	1.396	
9.65	observed	97.7	0.91	1.4	1.85
14.1	100%	97.69	2.29	0.013	1.157
14.1	0%	98.4	0.81	0.75	
14.1	observed	98.5	0.77	0.74	1.13

The results are in good agreement with the theoretical isotope distributions calculated on the basis of no N-N bond fission in forming the nitrogen molecule.

3.1.3 Results of the kinetic experiments

The variation of the overall rate of decomposition of hydrazine on the supported ruthenium catalyst with respect to hydrazine concentration is given in Table 3.7. The results are also presented in Fig. 3.1 where it can be seen that the overall rate of decomposition is a linear function of the hydrazine concentration.

TABLE 3.7

Variation of the overall rate of decomposition of hydrazine at 24°C on the supported ruthenium catalyst with respect to hydrazine concentration

Hydrazine concentration, mole dm^{-3}	Overall rate of decomposition $d[N_2 + H_2]/dt$ mole gm^{-1} sec^{-1} $\times 10^6$
1.2	7.2
3.1	14.3
6.1	28.3
9.3	39.0
12.3	52.0
14.7	64.0
18.3	82.0
21.4	96.0
24.4	101.0
26.4	116.0

The variation of the overall rate of decomposition of hydrazine on the supported ruthenium catalyst with respect to temperature was studied using 6.1 and 18.3 mole dm^{-3} hydrazine solutions. The temperature variation of the rate of decomposition of 6.1 mole dm^{-3} hydrazine solution is given in Table 3.8 and the results are also plotted in Fig. 3.2.

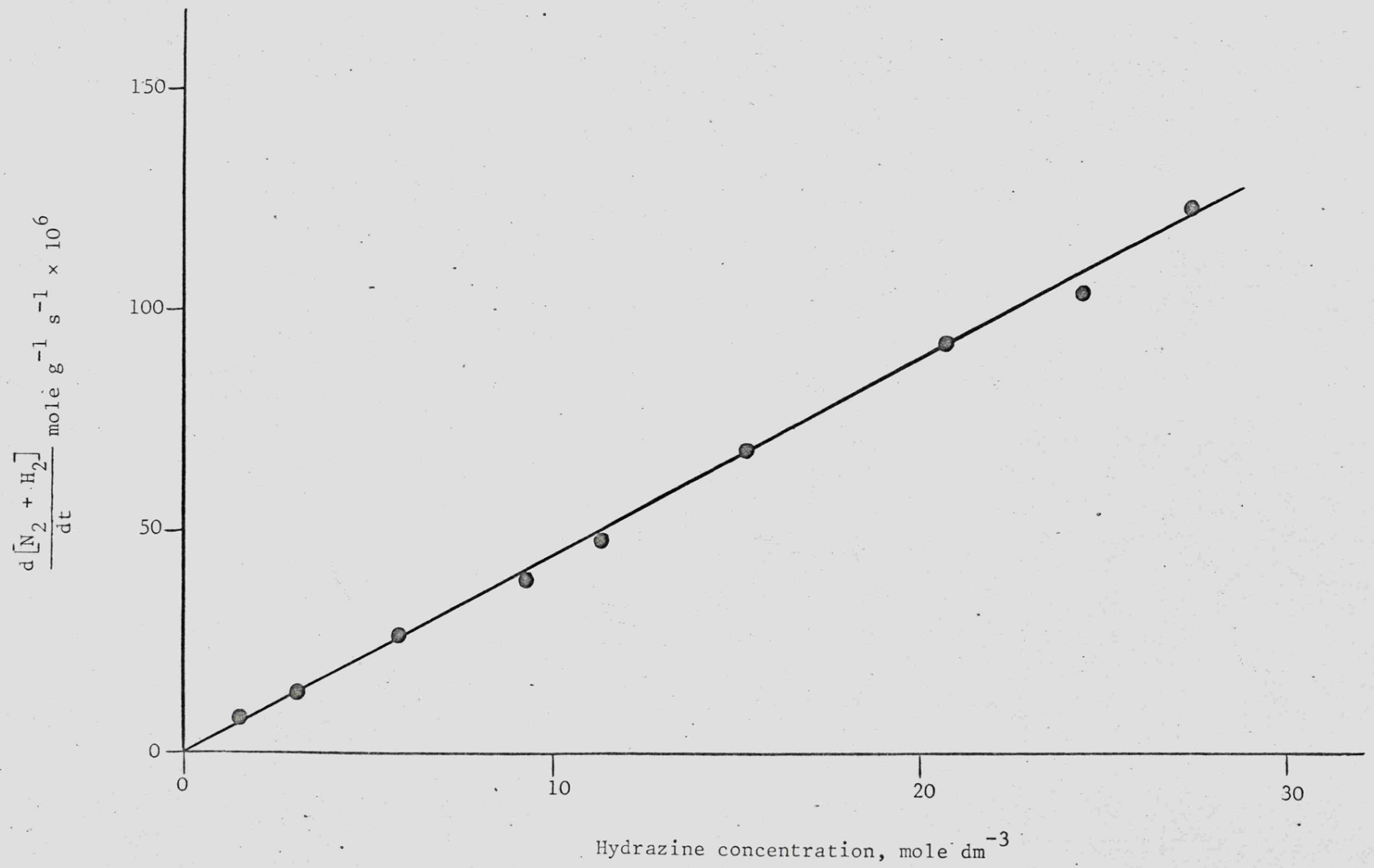

Fig. 3.1 Overall rate of decomposition of hydrazine at 24°C on the ruthenium catalyst

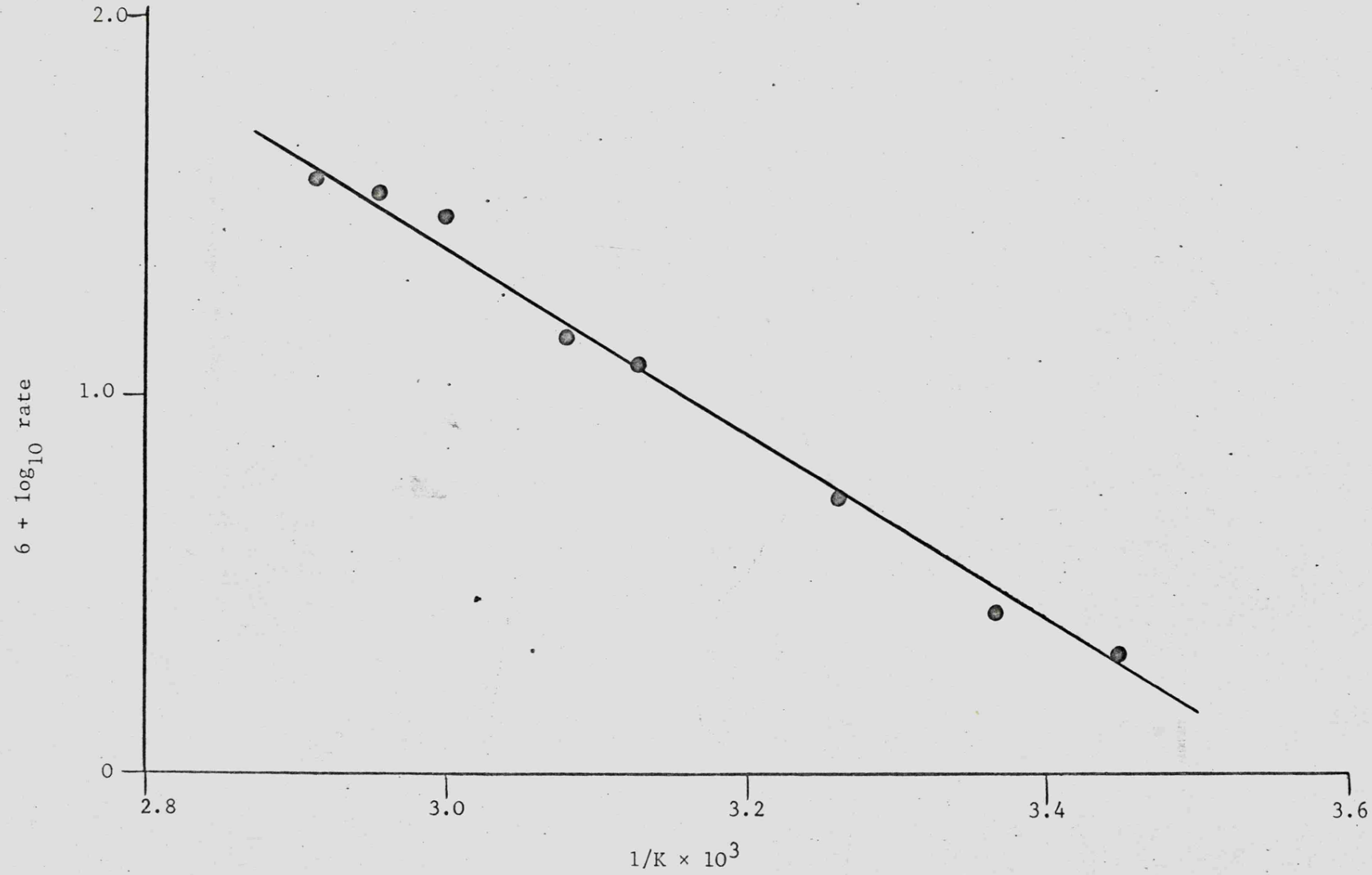

Fig. 3.2 Arrhenius plot for the decomposition of 6.1 mole dm^{-3} hydrazine solution on the ruthenium catalyst

TABLE 3.8

Variation of the rate of decomposition of 6.1 mole dm^{-3} hydrazine solution with respect to temperature

Temperature, ^{o}C	Temperature, ^{o}K	$1/K \times 10^{3}$	Overall rate of decomposition $d[N_2 + H_2]/dt$ mole gm^{-1} $sec^{-1} \times 10^{6}$	$6 + \log_{10}$ rate
17.5	290.7	3.440	20.6	1.314
24.0	297.2	3.365	28.3	1.452
36.0	309.2	3.234	62.0	1.792
44.0	317.2	3.153	102.0	2.009
51.0	324.2	3.084	138.0	2.140
58.0	331.2	3.019	267.0	2.427
63.0	336.2	2.974	293.0	2.467
69.0	342.2	2.922	339.0	2.530

The variation of the rate of decomposition of 18.3 mole dm^{-3} hydrazine solution with respect to temperature is given in Table 3.9 and the results are also plotted in Fig. 3.3.

TABLE 3.9

Variation of the rate of decomposition of 18.3 mole dm^{-3} hydrazine solution with respect to temperature

Temperature, ^{o}C	Temperature, ^{o}K	$1/K \times 10^{3}$	Rate of decomposition $d[N_2 + H_2]/dt$ mole gm^{-1} $sec^{-1} \times 10^{6}$	$6 + \log_{10}$ rate
-10.0	263.2	3.800	10.3	1.013
- 5.0	267.2	3.742	13.2	1.121
0.0	273.2	3.661	19.0	1.279
5.0	278.2	3.595	31.4	1.497
7.0	280.2	3.569	26.8	1.428
12.0	285.2	3.507	46.9	1.671
17.5	290.7	3.440	58.2	1.765
24.0	297.2	3.365	82.0	1.914

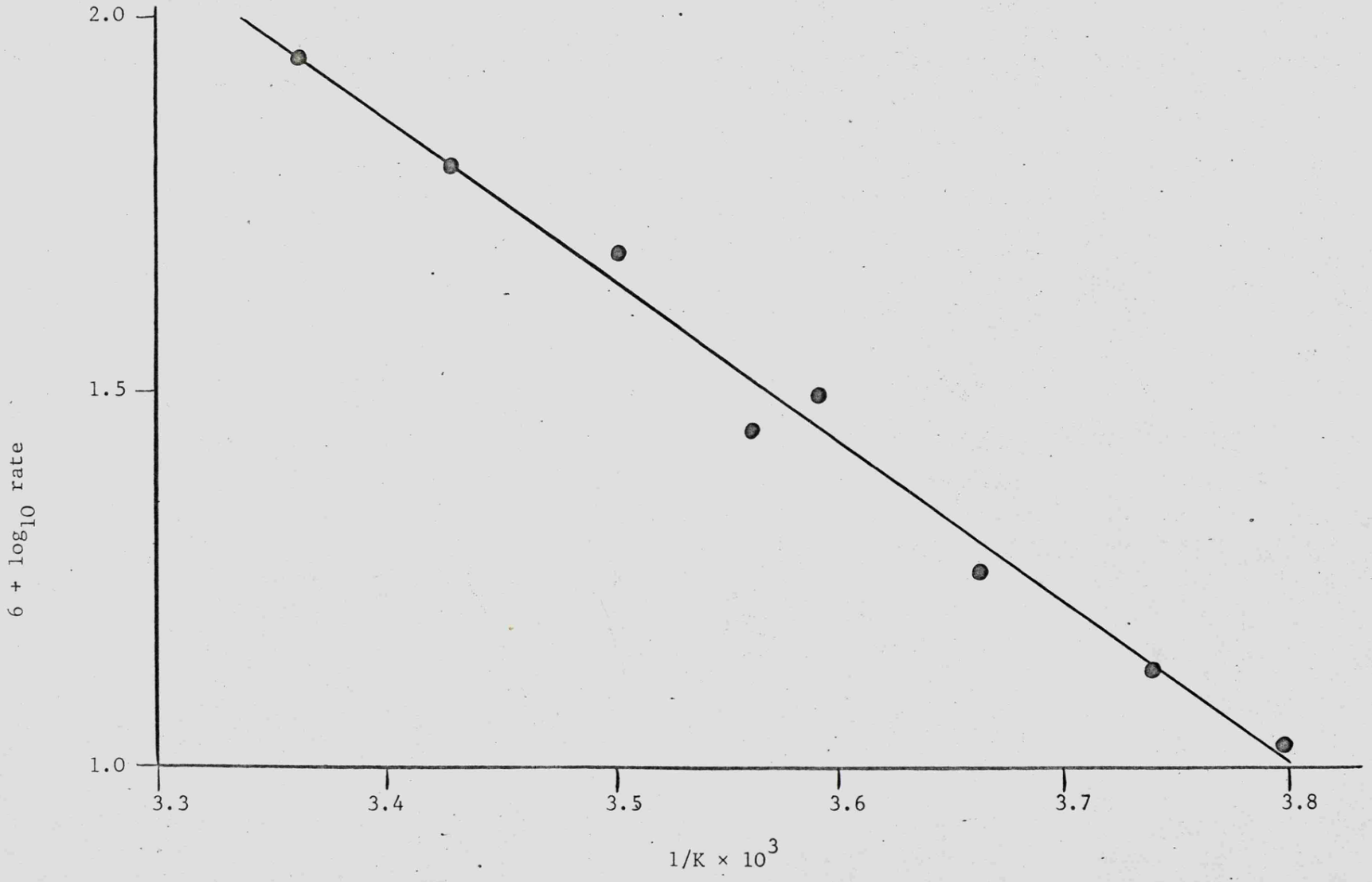

Fig. 3.3 Arrhenius plot for the decomposition of 18.3 mole dm^{-3} hydrazine on the ruthenium catalyst

3.2 Discussion

3.2.1 Results

Four reactions have previously been used to represent the decomposition of hydrazine under various experimental conditions. These reactions are:-

$$3N_2H_4 \longrightarrow N_2 + 4NH_3 \quad (2)$$

$$3N_2H_4 \longrightarrow 2N_2 + 3H_2 + 2NH_3 \quad (7)$$

$$2N_2H_4 \longrightarrow N_2 + H_2 + 2NH_3 \quad (6)$$

$$N_2H_4 \longrightarrow N_2 + 2H_2 \quad (8)$$

The only permanent gas produced by reaction (2) is nitrogen while the remaining three reactions all produce nitrogen and hydrogen in varying proportions. For reaction (6) the percentage of hydrogen in the permanent gas is 50%, for reaction (7) it is 60% while for reaction (8) it is 67%.

The decomposition of hydrazine on the supported ruthenium catalyst produced permanent gas containing between 12 and 36% hydrogen depending on the experimental conditions. Pretreating the catalyst with hydrogen resulted in an increase in the proportion of hydrogen in the evolved permanent gas up to a maximum of approximately 50%. These results are not consistent with the occurrence of only one of the above reactions and therefore it can only be assumed that the decomposition of hydrazine on the supported ruthenium catalyst follows two, or more, reaction paths simultaneously. As only reaction (2) produces a smaller propertion of hydrogen in the permanent gas than the experimentally observed proportions this reaction must occur. The remaining reactions all produce a greater proportion of hydrogen than the observed range and therefore any one, or more, of these reactions may occur. It will be seen in future chapters that on the supported rhodium, palladium and platinum catalysts the decomposition of hydrazine follows reaction (6). Taking this into account and that the limiting concentration of hydrogen in the permanent gas evolved from the use of the ruthenium catalyst is 50% it will be assumed that reaction (6) is the second contributory reaction.

The rates of the individual reactions may be calculated from the overall rate of reaction using the stoichiometries of the reactions (2) and (6) and the composition of the permanent gas. All the hydrogen in the evolved permanent gas is produced by reaction (6) and an equivalent quantity of nitrogen is also produced by this reaction. Therefore the percentage of the overall rate of decomposition which is due to reaction (6) is twice the observed percentage of hydrogen. The remainder of the overall rate of decomposition is the rate of nitrogen formation resulting from reaction (2).

The calculations of the variation of the rates of reactions (2) and (6) with respect to hydrazine concentration are shown in Table 3.10. The variation of the rates of reactions (2) and (6) with respect to hydrazine concentration are also presented in Figs. 3.4 and 3.5 respectively. In both cases the rate of reaction is a linear function of the hydrazine concentration, this result was expected as the overall rate is a linear function and the ratio of the individual rates remained constant as indicated by the constant permanent gas composition.

The calculation of the rate of reaction (2) with respect to temperature is shown in Table 3.11 and the results are also presented in the form of an Arrhenius plot in Fig. 3.6. From this data the activation energy for reaction (2) was calculated to be 54.4 ± 0.5 kJ $mole^{-1}$ and the pre-exponential factor 2.6×10^4 dm^3 gm^{-1} sec^{-1}.

The calculation of the rate of reaction (6) with respect to temperature is shown in Table 3.12 and the results are also presented in Fig. 3.7 in the form of an Arrhenium plot. From this data the activation energy for reaction (6) was calculated to be 34.1 ± 0.4 kJ $mole^{-1}$ and the pre-exponential factor 3.0 dm^3 gm^{-1} sec^{-1}.

The observation that for each reaction the rate of decomposition is a linear function of hydrazine concentration may be explained on the basis of the reactions being either diffusion or first order chemically controlled.

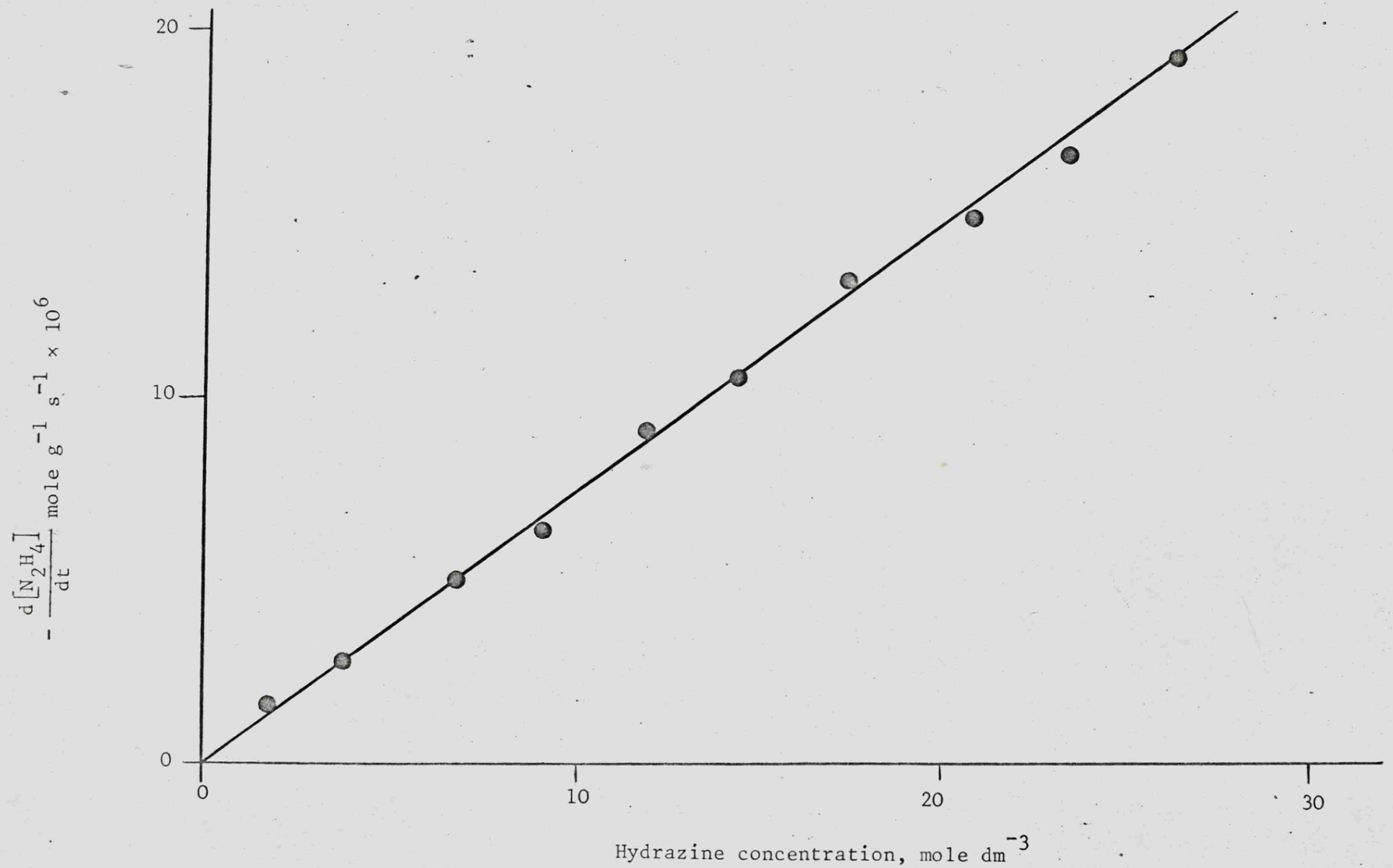

Fig. 3.4 Rate of reaction (2) with respect to hydrazine concentration at 24°C

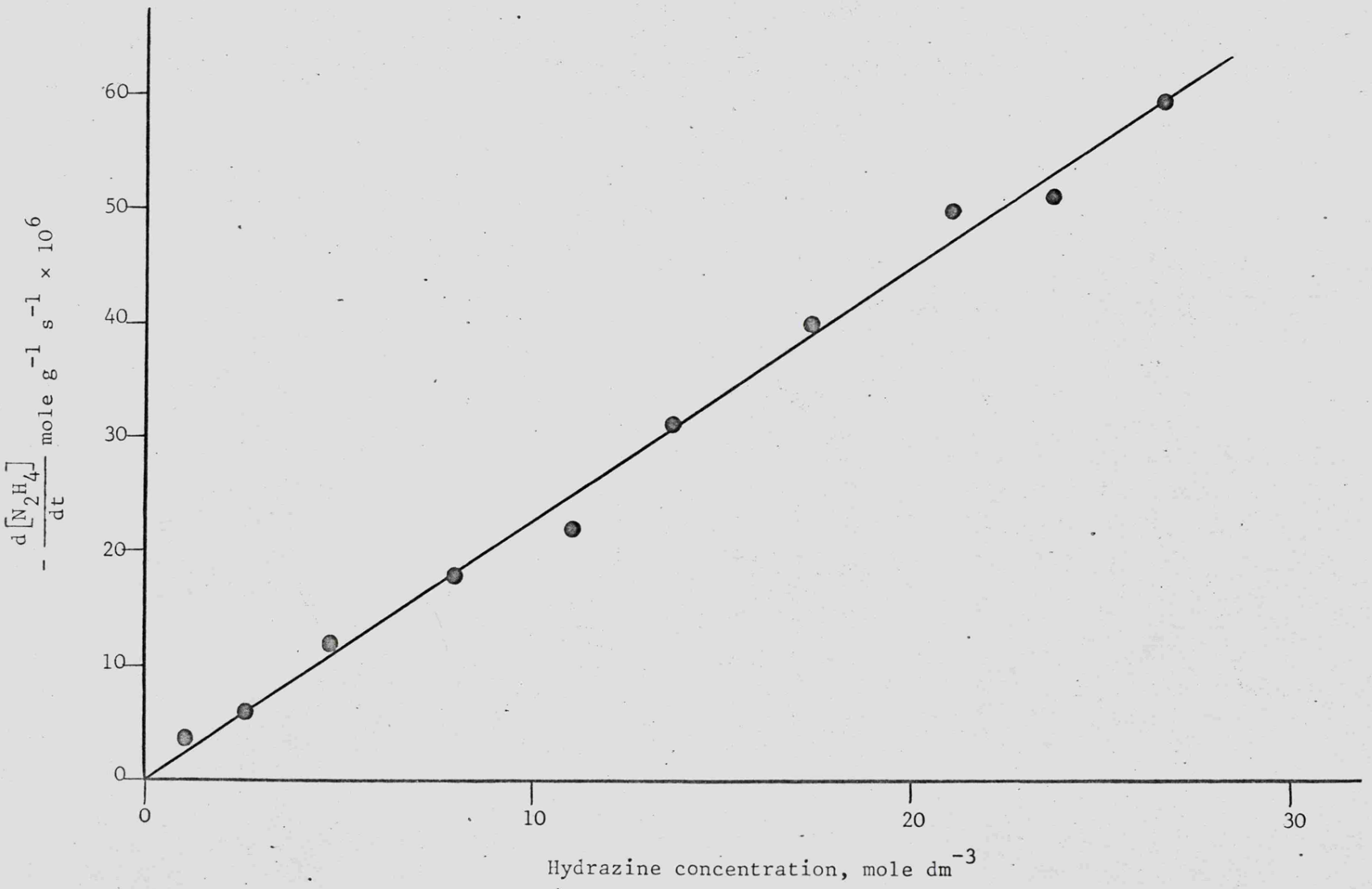

Fig. 3.5 Rate of reaction (6) with respect to hydrazine concentration at 24°C

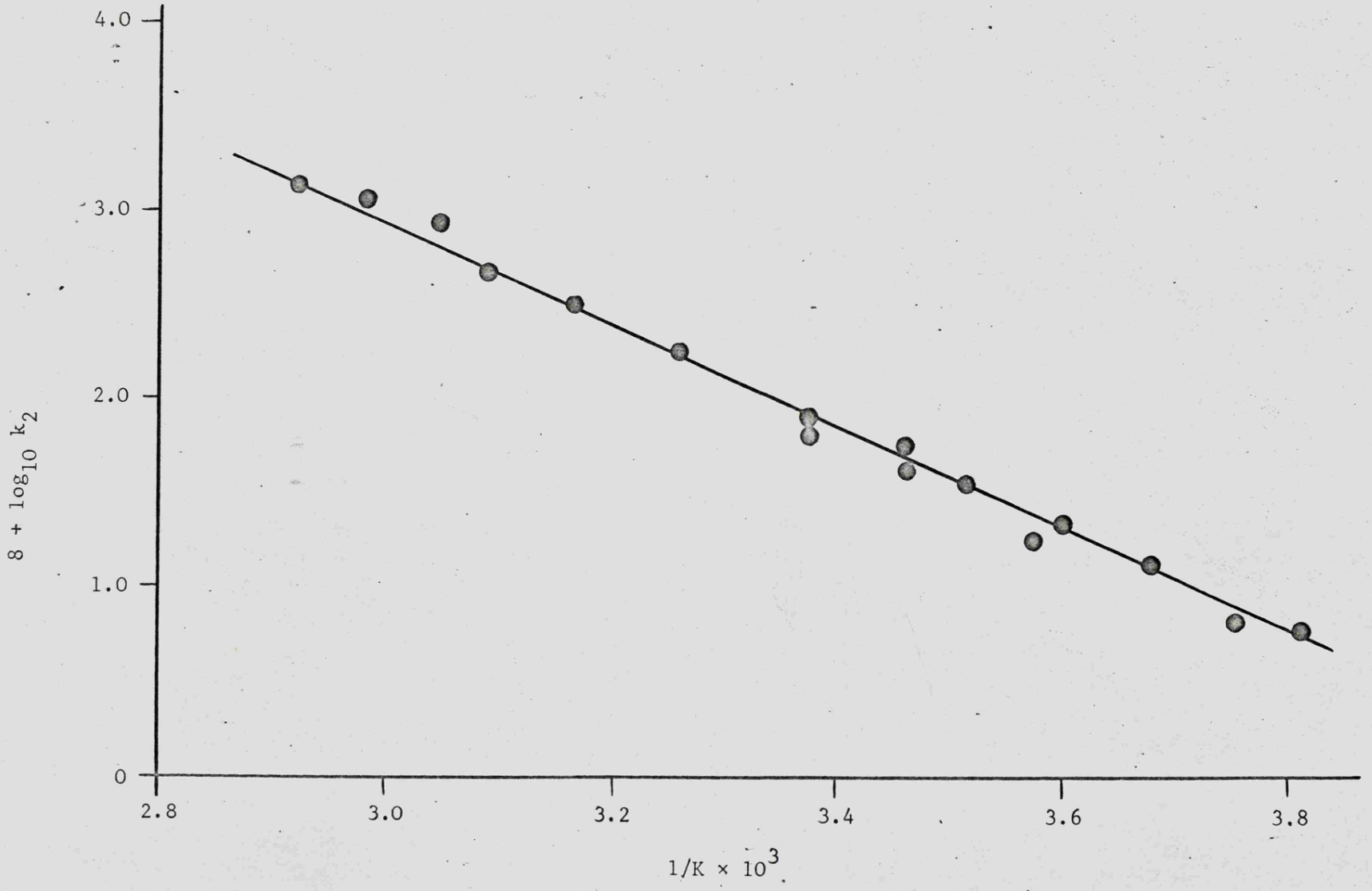

Fig. 3.6 Arrhenius plot for reaction (2) on the ruthenium catalyst

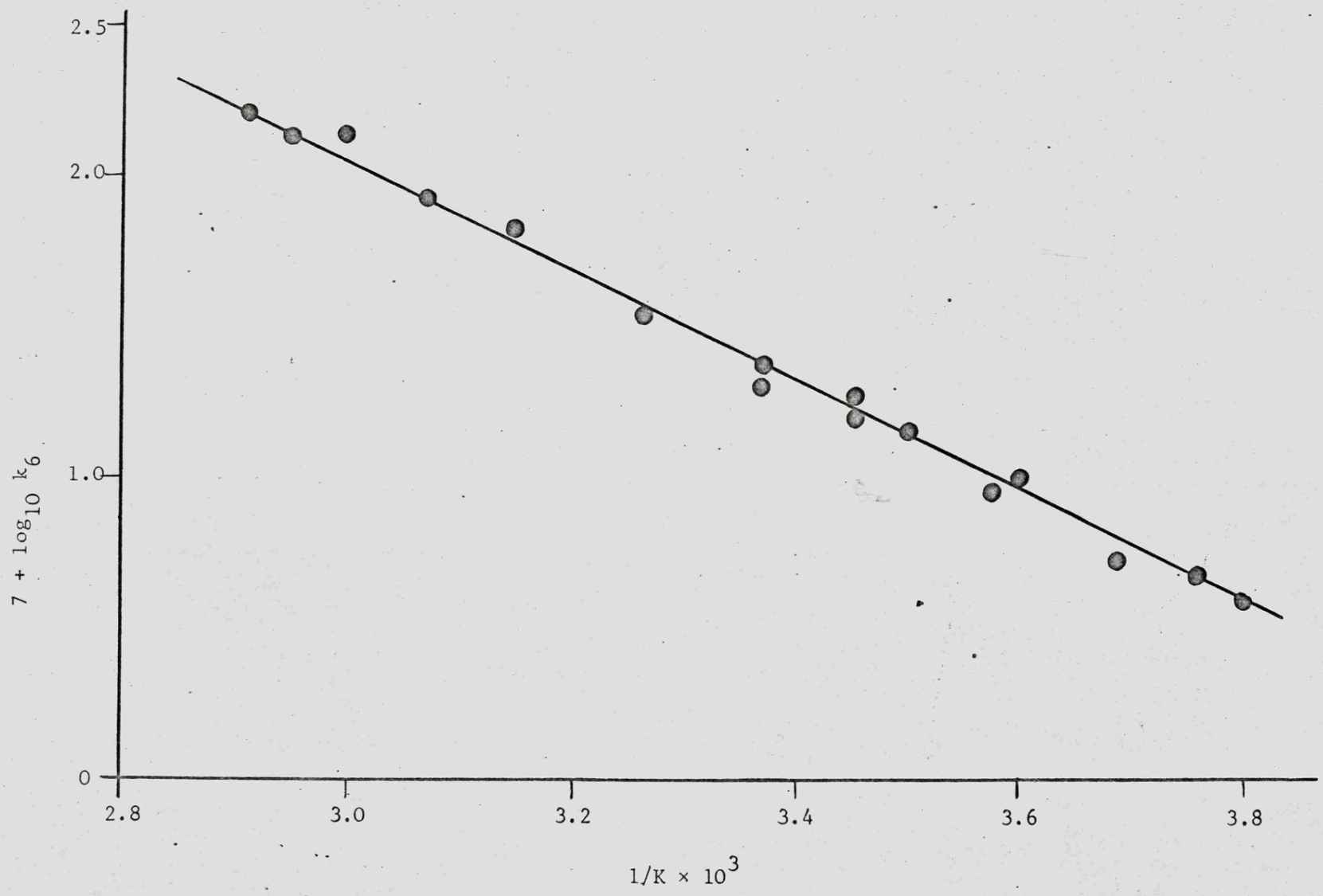

Fig. 3.7 Arrhenius plot for reaction (6) on the ruthenium catalyst

TABLE 3.10

Variation of the rates of reactions (2) and (6) on the supported ruthenium catalyst at 24°C with respect to hydrazine concentration

Hydrazine concentration mole dm^{-3}	Overall rate of decomposition $\frac{d[N_2 + H_2]}{dt}$ mole gm^{-1} sec^{-1} $\times 10^6$	Hydrogen content of permanent gas, %	Percentage of overall rate due to reaction (6)	Rate of reaction (6) $\frac{d[N_2 + H_2]}{dt}$ mole gm^{-1} sec^{-1} $\times 10^6$	Rate of reaction (6) $-\frac{d[N_2H_4]}{dt}$ mole gm^{-1} sec^{-1} $\times 10^6$	rate of reaction (2) $\frac{d[N_2]}{dt}$ mole gm^{-1} sec^{-1} $\times 10^6$	Rate of reaction (2) $-\frac{d[N_2H_4]}{dt}$ mole gm^{-1} sec^{-1} $\times 10^6$
1.2	7.2	24.1	48.2	3.48	3.48	3.72	1.24
3.1	14.3	25.6	51.2	7.3	7.3	7.0	2.33
6.1	28.3	25.1	50.2	14.2	14.2	14.1	4.7
9.3	39.0	26.5	53.0	20.6	20.6	18.4	6.1
12.3	52.0	23.0	46.0	24.0	24.0	28.0	9.3
14.7	64.0	25.1	50.2	32.2	32.2	31.8	10.6
18.3	82.0	25.0	50.0	41.0	41.0	41.0	13.7
21.4	96.0	25.7	51.4	49.5	49.5	46.5	15.5
24.4	101.0	25.1	50.2	50.8	50.8	50.2	16.7
26.4	116.0	24.9	48.8	57.8	57.8	58.2	19.4

TABLE 3.11

Variation of the rates of reaction (2) on the supported ruthenium catalyst with respect to temperature

Hydrazine concentration mole dm^{-3}	Temperature, ^{o}K	$\frac{1}{K} \times 10^{3}$	Overall rate of reaction $\frac{d[N_2 + H_2]}{dt}$ mole $gm^{-1}\ sec^{-1} \times 10^{6}$	Hydrogen % in permanent gas	% of overall rate due to reaction (2)*	Rate of reaction (2) $-\frac{d[N_2H_4]}{dt}$ mole $gm^{-1}\ sec^{-1} \times 10^{6}$	$k_2 \times 10^{6}$	$8 + \log_{10} k_2$
6.1	290.7	3.442	20.6	25.5	49.0	3.4	0.558	1.747
6.1	297.2	3.365	28.3	25.1	49.8	4.7	0.77	1.886
6.1	309.2	3.234	62.0	18.6	62.8	13.0	2.13	2.320
6.1	317.2	3.153	102.0	18.3	63.4	21.6	3.55	2.550
6.1	324.2	3.084	138.0	16.1	67.8	31.2	5.11	2.708
6.1	331.2	3.019	267.0	14.0	72.0	64.2	10.55	3.023
6.1	336.2	2.974	293.0	12.0	76.0	74.2	11.9	3.073
6.1	342.2	2.922	339.0	12.5	75.0	84.7	13.9	3.141
18.3	263.2	3.800	10.3	34.4	31.2	1.07	0.059	0.767
18.3	267.2	3.742	13.2	35.7	28.6	1.26	0.069	0.838
18.3	273.2	3.661	19.0	30.1	39.8	2.52	0.138	1.140
18.3	278.2	3.595	31.4	30.5	39.0	4.07	0.223	1.348
18.3	280.2	3.569	26.8	30.7	38.6	3.45	0.188	1.274
18.3	255.2	3.507	46.9	27.8	44.4	6.60	0.36	1.556
18.3	290.7	3.442	58.2	25.0	50.0	9.70	0.53	1.724
18.3	297.2	3.365	82.0	25.0	50.0	13.7	0.75	1.874

*% of overall rate due to reaction (2) is $[\,100 - (2 \times \%\ H_2$ in permanent gas$)\,]$ % .

TABLE 3.12

Variation of the rate of reaction (6) on the supported ruthenium catalyst with respect to temperature

Hydrazine concentration mole dm^{-3}	Temperature, ^{o}K	$\frac{1}{K} \times 10^{3}$	Overall rate of reaction $\frac{d[N_2 + H_2]}{dt}$ mole gm^{-1} sec^{-1} $\times 10^{6}$	Hydrogen % in permanent gas	% of overall rate due to reaction (6)	Rate of reaction (6) $-\frac{d[N_2H_4]}{dt}$ mole gm^{-1} sec^{-1} $\times 10^{6}$	$k_6 \times 10^{6}$	$7 + \log_{10} k_6$
6.1	290.7	3.442	20.6	25.5	51.0	10.5	1.72	1.235
6.1	297.2	3.365	28.3	25.1	50.2	14.2	2.23	1.345
6.1	309.2	3.234	60.0	18.6	37.2	23.0	3.77	1.576
6.1	317.2	3.153	102.0	18.3	36.6	37.2	6.10	1.785
6.1	324.2	3.084	138.0	16.1	32.2	44.5	7.3	1.863
6.1	331.2	3.019	267.0	14.0	28.0	74.5	12.2	2.086
6.1	336.2	2.974	293.0	12.0	24.0	70.5	11.6	2.064
6.1	342.2	2.922	339.0	12.5	25.0	85.0	14.0	2.146
18.3	263.2	3.800	10.3	34.4	68.8	7.05	0.385	0.585
18.3	267.2	3.742	13.2	35.7	71.4	9.4	0.512	0.709
18.3	273.2	3.661	19.0	30.1	60.2	11.5	0.628	0.780
18.3	278.2	3.595	31.4	30.5	61.0	19.2	1.05	1.021
18.3	280.2	3.569	26.8	30.7	61.4	16.4	0.896	0.952
18.3	285.2	3.507	46.9	27.8	55.6	26.1	1.42	1.152
18.3	290.7	3.442	58.2	25.0	50.0	29.1	1.59	1.201
18.3	297.2	3.365	82.0	25.0	50.0	41.0	2.24	1.350

It seems most improbable that the reactions are diffusion controlled because the associated activation energy would normally be less than 16 kJ mole^{-1}. Therefore it is assumed that both reactions for the decomposition of hydrazine on the supported ruthenium catalyst are first order chemically controlled.

The results of the experiments using ^{15}N as a tracer have shown that all the nitrogen formed by the decomposition of hydrazine on the supported ruthenium catalyst is formed without N-N bond fission. Therefore both reaction mechanisms involve two nitrogen atoms of one hydrazine molecule remaining bonded together to form the nitrogen molecule.

The effect of the pre-adsorption of hydrogen on the catalyst, shown in Table 3.4, is to increase the proportion of hydrogen in the evolved permanent gas to approximately 50%, and at the same time the rate of reaction is reduced to a low level. The stoichiometry of the evolved permanent gas corresponds to reaction (6) and it appears that the effect of the pre-adsorption of hydrogen on the catalyst is to completely inhibit reaction (2) and also to inhibit reaction (6).

The pre-adsorption of ammonia on the ruthenium catalyst had little or no effect on the composition of the evolved permanent gas (see Table 3.5). The rate of decomposition of hydrazine was depressed by the pre-adsorption of ammonia but the rate increased with time of reaction until the observed rate of reaction was almost the same as that measured using the standard catalyst. It is suggested that ammonia is only weakly adsorbed on the supported ruthenium catalyst and after immersion of the treated catalyst the adsorbed ammonia molecules desorb and are replaced by hydrazine molecules. After some time interval the surface is effectively free from adsorbed ammonia molecules and the decomposition of hydrazine occurs as though the catalyst had not been pre-treated with ammonia.

3.2.2 Mechanism of the decomposition reactions

Any reaction mechanisms postulated to account for the decomposition of

hydrazine on the supported ruthenium catalyst must be consistent with the observation that the decomposition consists of the simultaneous occurrence of two reactions, the stoichiometries of which are:-

$$3N_2H_4 \longrightarrow N_2 + 4NH_3 \qquad (2)$$

$$2N_2H_4 \longrightarrow N_2 + H_2 + 2NH_3 \qquad (6)$$

This situation is analogous to the decomposition of hydrazine on tungsten and molybdenum films. Cosser and Tompkins[52] postulated a dual plane mechanism in which the overall reaction path was determined by the mode of adsorption of the hydrazine molecule. On certain planes the dissociative chemisorption of hydrazine occurred giving adsorbed NH_2 radicals which, on further dissociation, produced hydrogen and these planes were designated as active. On the inactive planes associative adsorption of the hydrazine molecules occurred to form an activated complex which broke down to yield nitrogen and ammonia in accordance with reaction (2).

It has been postulated that reaction (2) is one of the contributory reactions in the decomposition of hydrazine on the ruthenium catalyst. In considering a mechanism for this reaction the following experimental observations must be explained:-

(1) The reaction exhibits overall first order kinetics,

(2) The nitrogen molecule is formed from the two nitrogen atoms of one hydrazine molecule without N-N bond fission.

The overall first order kinetics show that the rate controlling step involves one hydrazine molecule from solution but this may be either an adsorption process or a reaction between some adsorbed species and a solution phase hydrazine molecule.

If it is assumed that the adsorption of the hydrazine molecule is the rate controlling step then the rate equations may be derived from the Langmuir adsorption isotherm. If θ is the fraction of surface which is

covered, then $(1 - \theta)$ is the fraction which is bare. Let c be the concentration of reactant and k_1 and k_{-1} are the rate constants for the absorption and desorption steps respectively, then the rate of adsorption is:-

$$v_1 = k_1 c (1 - \theta)$$

and the rate of desorption is:-

$$v_{-1} = k_{-1} \theta \quad .$$

At equilibrium the rates are equal so that:-

$$k_1 c (1 - \theta) = k_{-1} \theta$$

$$\frac{\theta}{1 - \theta} = \frac{k_1 c}{k_{-1}} = K c \qquad (\text{where } K = k_1/k_{-1})$$

$$\theta = \frac{K c}{1 + K c} \quad .$$

The rate, R, of a heterogeneous reaction is proportional to the fraction of the surface which is covered:-

$$R = k_2 \theta = \frac{k_2 K c}{1 + K c}$$

where k_2 is the rate constant for the reaction. Now:-

(1) at low concentrations c is small and $K c \ll 1$, so

$$R \approx k_2 K c$$

and the rate of reaction is proportional to the concentration of reactant and the reaction is first order.

(2) at high concentrations c is large and $K c \gg 1$, so

$$R \approx k_2$$

and the reaction is zero order.

Therefore, in order for reaction (2) on the ruthenium catalyst to be adsorption controlled it is necessary that the surface is always sparsely covered by adsorbed hydrazine molecules. The formation of the activated

complex and its breakdown to yield the products must be fast in comparison to the adsorption step.

The second possibility is that the surface of the catalyst is effectively covered by adsorbed hydrazine molecules and therefore the rate of reaction is independent of the adsorption process. The overall first order kinetics arise from reaction between adsorbed hydrazine molecules and a hydrazine molecule from solution to form the activated complex which then breaks down to form ammonia and nitrogen.

It is not possible to decide which of the two alternative mechanisms is the correct one but it is suggested that the second case, in which the formation of the activated complex is the rate controlling step, is the more likely. In this case the reaction mechanism involves the adsorption of hydrazine molecules to saturate the surface followed by reaction between a solution hydrazine molecule and two adsorbed hydrazine molecules to form an activated complex. This then breaks down and the nitrogen molecule is formed from the two nitrogen atoms of solution phase hydrazine molecule without N-N bond fission.

The second contributory reaction was postulated to be reaction (6) on the basis that the percentage of hydrogen in the permanent gas never exceeded 50% even under the most favourable conditions for the production of hydrogen and secondly, that this reaction occurred on the rhodium, palladium and platinum catalysts. Reaction (6) occurs following the dissociative chemisorption of hydrazine on these catalysts and it is postulated that this is also the initial step in the decomposition mechanism on the ruthenium catalyst. It will be seen in Chapter 4 that when the dissociative chemisorption of hydrazine is the rate controlling step then the overall reaction exhibits half order kinetics. As reaction (6) on the ruthenium catalyst is first order the adsorption step is not rate controlling. The NH_2 radicals formed by the dissociative chemisorption of hydrazine may further dissociate to form

adsorbed imide radicals and hydrogen atoms, the latter combine to be desorbed as hydrogen molecules. This is then followed by a Langmuir-Rideal reaction between the adsorbed imide radicals and a solution hydrazine molecule in which the imide radicals are hydrogenated to ammonia while the hydrazine molecule is dehydrogenated to form the nitrogen molecule without N-N bond fission. If the Langmuir-Rideal reaction is assumed to be the rate controlling step in the overall mechanism, this explains the first order kinetics as this step depends only on the concentration of hydrazine in the bulk solution.

The reaction may be represented as:-

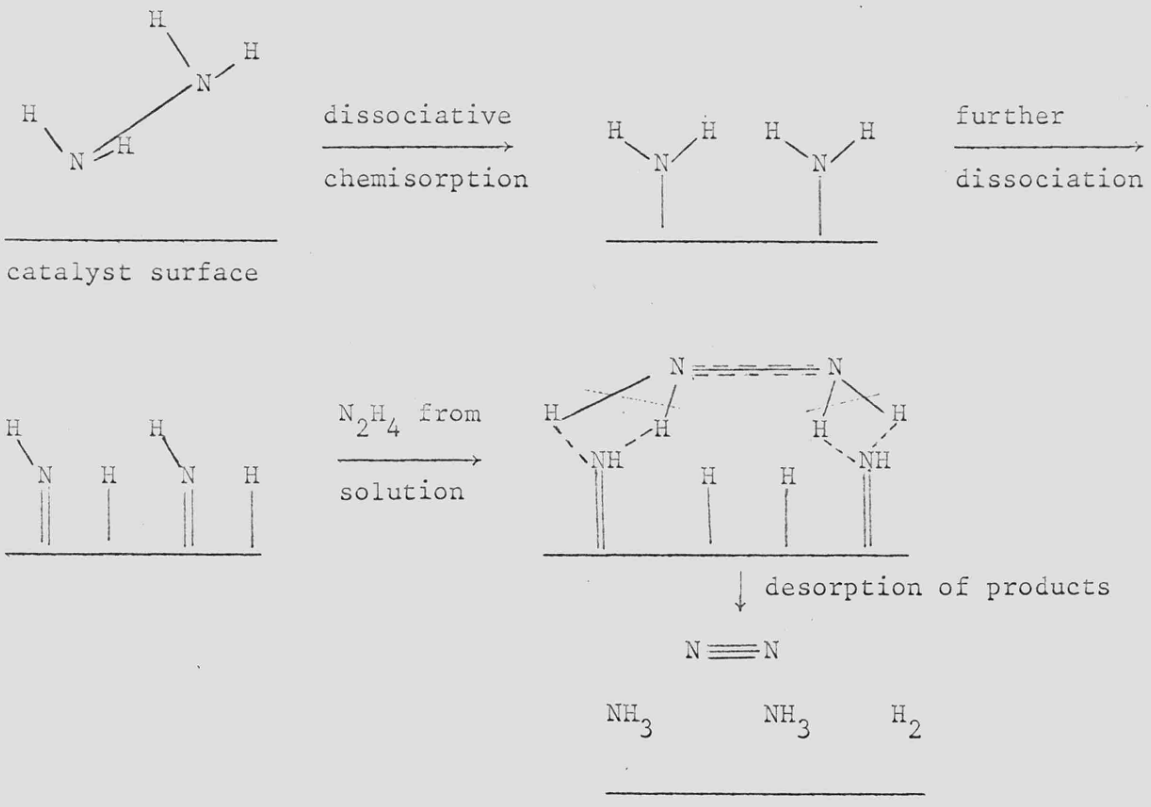

In conclusion the decomposition of hydrazine on the supported ruthenium catalyst is a complex situation which has been analysed in terms of the simultaneous occurrence of reactions (2) and (6). The experimental observations are consistent with mechanisms based on the dual plane theory of Cosser and Tompkins which envisages that the overall reaction path is determined by the mode of adsorption of hydrazine. Reaction (6) occurs following the dissociative chemisorption of hydrazine on the active planes of ruthenium

while on other planes the associative adsorption occurs resulting in reaction (2). For both reactions it is suggested that the first order kinetics arise from Langmuir-Rideal reactions between adsorbed species and a solution phase hydrazine molecule.

CHAPTER FOUR

THE USE OF A SUPPORTED RHODIUM CATALYST

4.1 Results

4.1.1 Product analysis

The permanent gas evolved by the decomposition of hydrazine solutions on the supported rhodium catalyst was analysed for hydrogen and nitrogen using the gas chromatograph. The variation of the permanent gas composition with respect to both hydrazine concentration and temperature is shown in Table 4.1.

TABLE 4.1

Results of the permanent gas analysis

Hydrazine concentration mole dm^{-3}	Temperature, ^{o}C	% H_2	% N_2
3.12	22	48.9	51.1
6.25	22	50.6	49.4
15.6	22	50.5	49.5
23.5	22	49.7	50.3
29.6	22	51.8	48.2
30.6	22	49.2	50.8
30.6	0	51.1	48.9
30.6	11	49.1	50.9
30.6	17	50.6	49.4
30.6	31	48.7	51.3

The results show that the composition of the permanent gas is independent of both hydrazine composition and temperature.

The ratio of the number of moles of ammonia formed by the decomposition of one mole of hydrazine was determined by titrimetric analysis. The results of the analysis for the decomposition of 6.25 mole dm^{-3} hydrazine solution on the supported rhodium catalyst are presented in Table 4.2.

TABLE 4.2

Determination of the conversion of hydrazine to ammonia

Moles of hydrazine			Total moles alkali[4]	Moles NH_3 produced[5]	N_2H_4:NH_3 ratio
Start[1]	Finish[2]	Decomposed[3]			
0.0232	0.0226	0.0006	0.0232	0.0006	1:1.0
0.0232	0.0194	0.0038	0.0231	0.0037	1:0.97
0.0232	0.0074	0.0156	0.0228	0.0154	1:0.97
0.0232	0.0056	0.0176	0.0235	0.0179	1:1.02

Notes

1. Starting number of moles of hydrazine, determined by Andrews titration.
2. Final number of moles of hydrazine, determined by Andrews titration.
3. Given by (1-2).
4. Total alkali (ammonia + hydrazine) after reaction, determined by acid titration.
5. Given by (4-2).

The titrametric analysis was carried out for four concentrations of hydrazine and three temperatures and the results are given in Table 4.3.

TABLE 4.3

Results of the titrametric analysis to determine the conversion of hydrazine to ammonia

Hydrazine concentration mole dm^{-3}	Temperature, ^{o}C	N_2H_4:NH_3 ratio
6.25	22	1:1.0
15.6	22	1:1.02
23.5	22	1:1.01
30.6	22	1:0.97
23.5	0	1:1.0
23.5	11	1:0.98

The results show that under all the experimental conditions studied the decomposition of one mole of hydrazine is accompanied by the formation of one mole of ammonia.

4.1.2 The use of ^{15}N as a tracer

The results of the mass spectrometric analysis of the nitrogen gas evolved by the decomposition of the stock ^{15}N enriched hydrazine solutions on the supported rhodium catalyst are presented in Table 4.4. Also included are the calculated nitrogen isotope distributions for 0% and 100% N-N bond fission.

TABLE 4.4

Results of the mass spectrometric analysis of nitrogen gas samples

Hydrazine solution mole dm^{-3}	% N-N bond fission (theoretical)	Distribution of nitrogen isotopes atom %			Per cent ^{15}N
		28	29	30	
9.65	100%	96.39	3.581	0.033	1.824
9.65	0%	97.73	0.856	1.396	
9.65	observed	97.6	0.97	1.40	1.90
14.1	100%	97.69	2.29	0.013	1.157
14.1	0%	98.4	0.81	0.75	
14.1	observed	98.4	0.77	0.74	1.14

The results are in good agreement with the theoretical nitrogen isotope distributions calculated on the basis of no N-N bond fission in forming the nitrogen molecule.

4.1.3 The kinetics of the decomposition of hydrazine

The variation of the rate of decomposition of hydrazine at 21°C on the supported rhodium catalyst with respect to hydrazine concentration is shown in Fig. 4.1 and the results are presented in Table 4.5.

The rate of decomposition of hydrazine is a curved function of the hydrazine concentration over the range 0-15 mole dm^{-3} and above 15 mole dm^{-3} the rate of reaction is independent of hydrazine concentration.

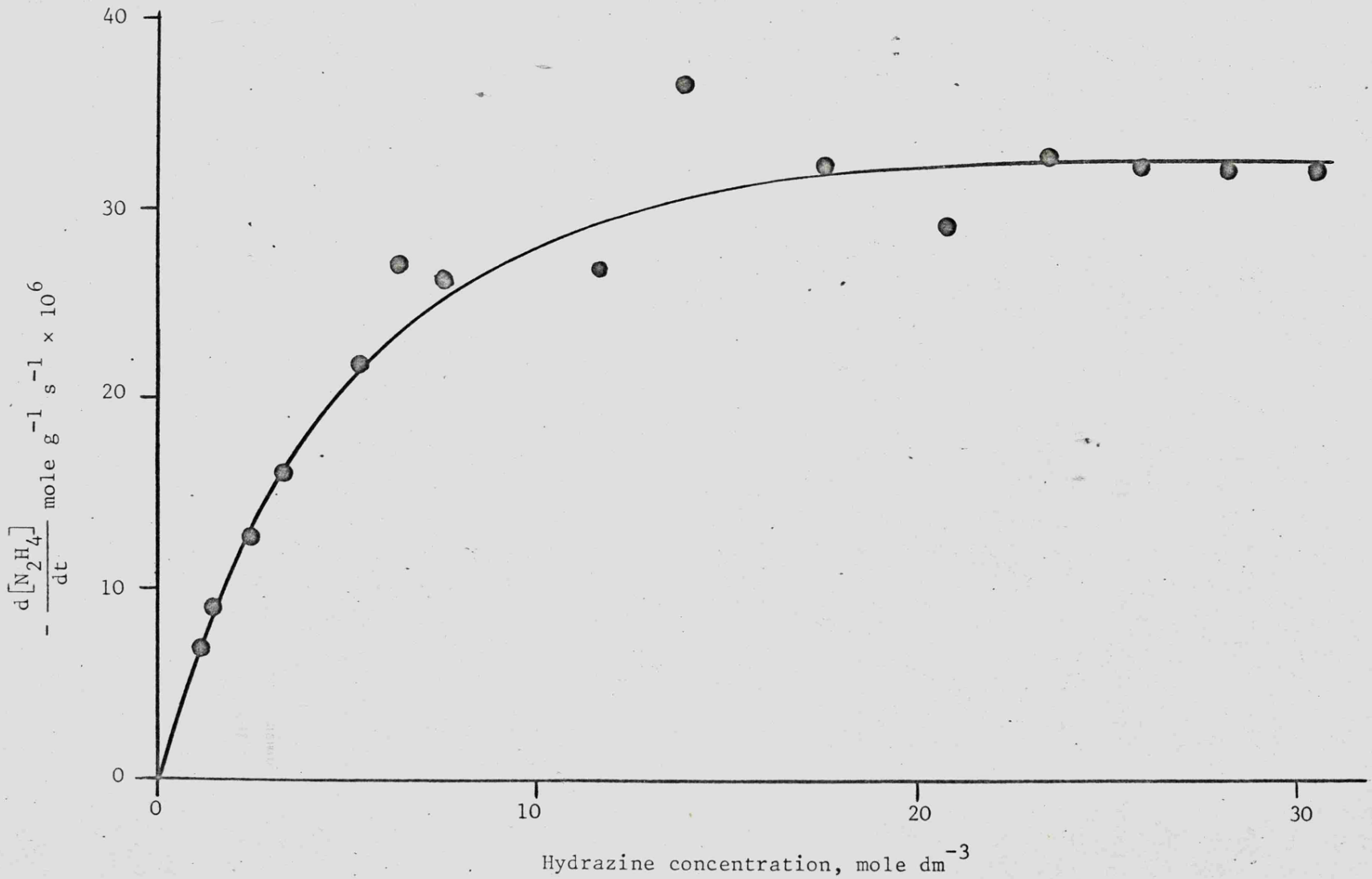

Fig. 4.1 Rate of decomposition of hydrazine at 21°C on the rhodium catalyst

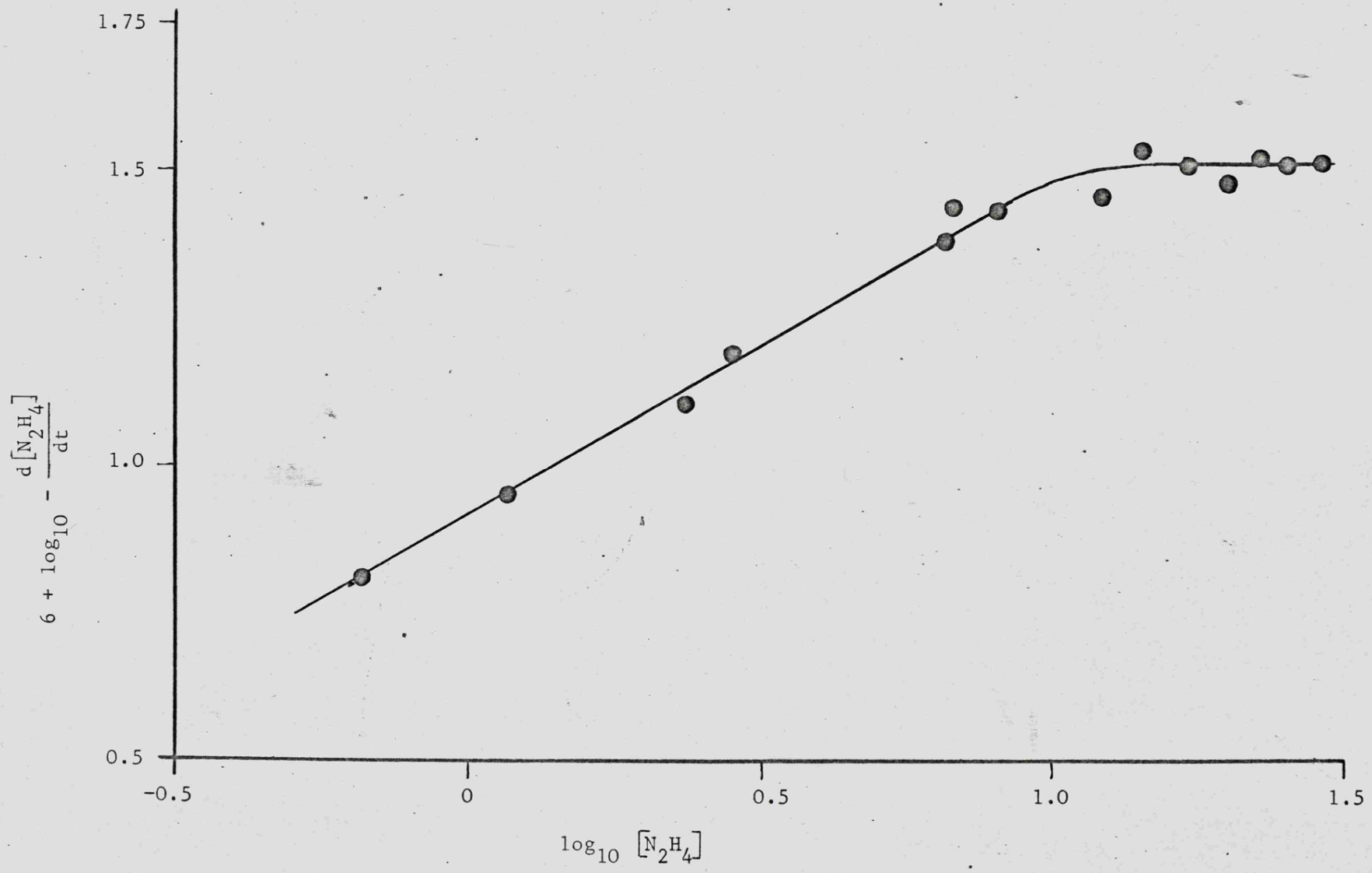

Fig. 4.2 Plot of $\log_{10}$ (rate of reaction) with respect to $\log_{10}$ (hydrazine concentration)

TABLE 4.5

The variation of the rate of decomposition of hydrazine at 21°C with respect to hydrazine concentration

Hydrazine concentration mole dm^{-3}	$\log_{10}[N_2H_4]$	Rate of decomposition $-\frac{d[N_2H_4]}{dt}$ mole $gm^{-1}\ sec^{-1} \times 10^6$	$6 + \log_{10}\frac{d[N_2H_4]}{dt}$
0.625	-0.204	6.4	0.806
1.22	0.086	9.5	0.971
2.44	0.387	13.0	1.114
3.0	0.477	16.0	1.204
6.25	0.796	24.0	1.380
6.43	0.808	28.0	1.447
8.1	0.908	27.2	1.435
11.9	1.076	27.2	1.435
14.1	1.149	35.1	1.545
17.7	1.248	32.0	1.505
20.6	1.314	28.0	1.447
24.0	1.380	32.5	1.512
27.1	1.433	32.0	1.505
30.6	1.486	32.0	1.505

The variation of the rate of decomposition of hydrazine on the supported rhodium catalyst with respect to temperature was studied for 22.7 mole dm^{-3} hydrazine solution. The results are given in Table 4.6 and are also presented in the form of an Arrhenius plot in Fig. 4.3. The activation energy calculated from the Arrhenius plot in Fig. 4.3 is 41.28 ± 0.33 kJ $mole^{-1}$ and the pre-exponential factor is 3.45×10^2 mole gm^{-1} sec^{-1}.

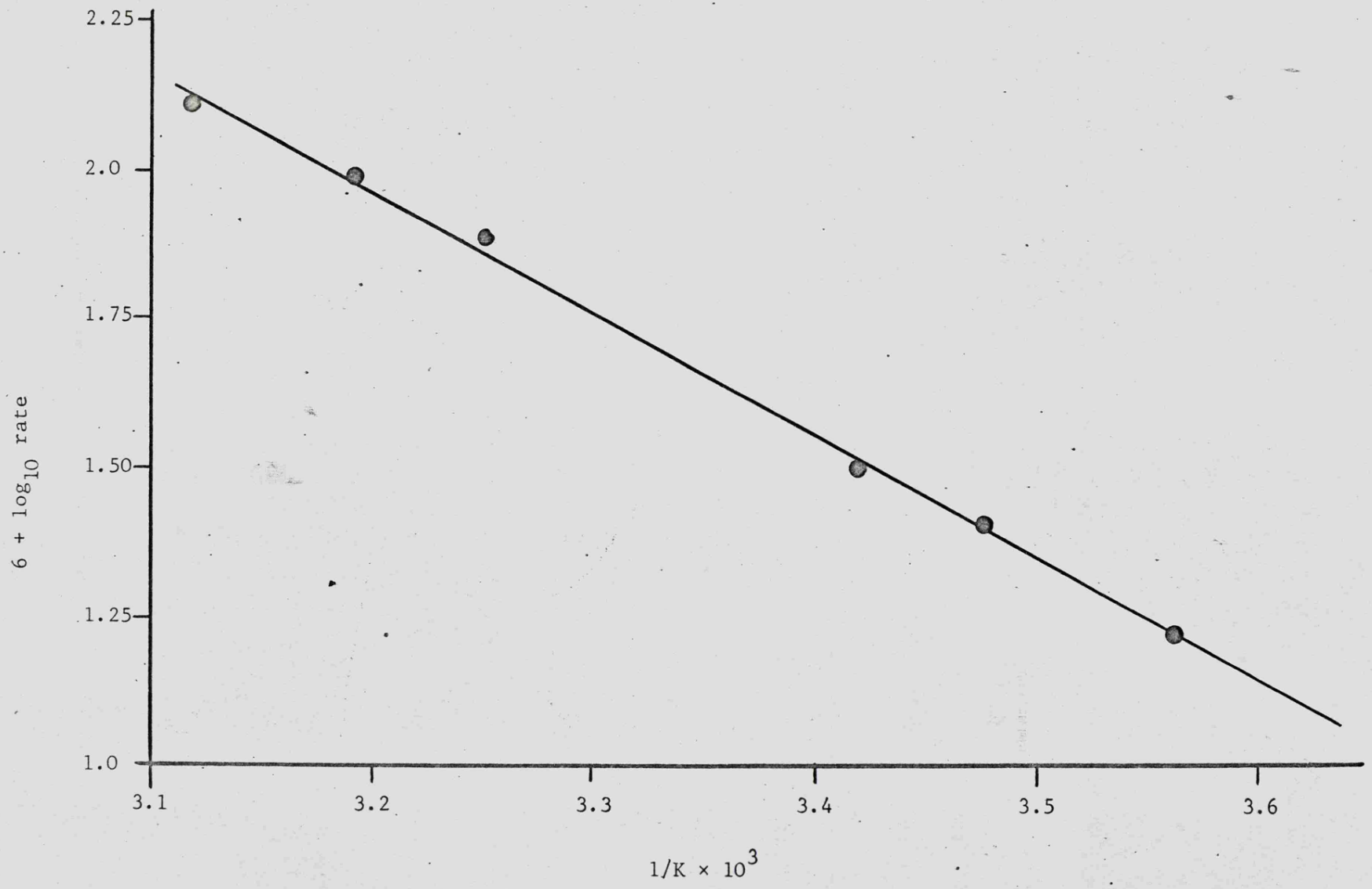

Fig. 4.3 Arrhenius plot for the decomposition of 30.8 mole dm^{-3} hydrazine on the rhodium catalyst

TABLE 4.6

The variation of the rate of decomposition of 22.7 mole dm^{-3} hydrazine solution on the supported rhodium catalyst with respect to temperature

Temperature		$\frac{1}{K} \times 10^3$	Rate of decomposition $-\frac{d[N_2H_4]}{dt}$ mole $gm^{-1}\ sec^{-1} \times 10^6$	$6 + \log_{10} k$
^oC	^oK			
3.9	277.1	3.611	12.6	1.111
7.7	280.9	3.560	16.3	1.212
15.0	288.2	3.470	26.1	1.416
20.0	293.2	3.411	32.7	1.514
34.5	307.7	3.250	77.6	1.890
41.0	314.2	3.183	101.0	2.006
48.0	321.2	3.113	146.5	2.116

4.2 Discussion

Under various experimental conditions four reactions have been used to represent the decomposition of hydrazine. These reactions are:-

$$3N_2H_4 \rightarrow N_2 + 4NH_3 \quad (2)$$

$$3N_2H_4 \rightarrow 2N_2 + 3H_2 + 2NH_3 \quad (7)$$

$$2N_2H_4 \rightarrow N_2 + H_2 + 2NH_3 \quad (6)$$

$$N_2H_4 \rightarrow N_2 + 2H_2 \quad (8)$$

On the supported rhodium catalyst the decomposition of hydrazine produces permanent gas having the composition of 50% hydrogen and 50% nitrogen. This permanent gas ratio corresponds to that of reaction (6). The titrimetric analysis showed that for each mole of hydrazine decomposed one mole of ammonia was produced and this ratio also corresponds to that of reaction (6). Therefore the results show that the decomposition of hydrazine on the supported rhodium catalyst may be represented by reaction (6).

The use of ^{15}N as a tracer has shown that the nitrogen molecule is formed from the two nitrogen atoms of one hydrazine molecule without N-N bond fission.

The rate of decomposition with respect to hydrazine concentration as shown in Fig. 4.1 is a curved function which becomes independent of concentrations in excess of 15 mole dm^{-3} hydrazine. The relationship between the rate of decomposition and hydrazine concentration may be written as:-

$$R = k\,c^{n}$$

where R is the rate of reaction, k is the rate constant, c is the concentration of hydrazine and n is the order of reaction. Taking logs:-

$$\log_{10} R = \log_{10} k + n \log_{10} c \quad .$$

The results are shown plotted in Fig. 4.2 in the form $\log_{10} R$ against $\log_{10} c$, where it can be seen that over the concentration range 0 to 6 mole dm^{-3} the value of n is $\frac{1}{2}$ and above 15 mole dm^{-3} the value of n is zero.

This type of relationship between the order of reaction and concentration for a heterogeneous reaction suggests that the rate controlling step is an adsorption process. In such cases the kinetics may be explained on the basis of the Langmuir adsorption isotherm. In adsorption controlled processes a one half order of reaction indicates that adsorption is occurring with dissociation to cover two surface sites and this must be taken into account in applying the Langmuir adsorption isotherm.

A brief derivation of the Langmuir adsorption isotherm is as follows. If θ is the fraction of the surface which is covered then $(1 - \theta)$ is the fraction which is bare. Let p be the pressure, or concentration, of the adsorbing species and k and k_{-1} are the rate constants for the adsorption and desorption respectively. Then for adsorption with dissociation to cover

two surface sites, the rate of adsorption is:-

$$v_1 = k_1 p (1 - \theta)^2 \quad .$$

Desorption involves the adsorbed species on two surface sites and the rate is:-

$$v_{-1} = k_{-1} \theta^2 \quad .$$

At equilibrium the rates are equal, so that

$$k_1 p (1 - \theta)^2 = k_{-1} \theta^2$$

$$\frac{\theta}{1 - \theta} = \left[\frac{k_1 p}{k_{-1}}\right]^{\frac{1}{2}} = K^{\frac{1}{2}} p^{\frac{1}{2}}$$

and

$$\theta = \frac{K^{\frac{1}{2}} p^{\frac{1}{2}}}{1 + K^{\frac{1}{2}} p^{\frac{1}{2}}} \quad .$$

The rate R of a heterogeneous reaction is proportional to the fraction of the surface which is covered, i.e.

$$R = k_2 \theta = \frac{k_2 K^{\frac{1}{2}} p^{\frac{1}{2}}}{(1 + K^{\frac{1}{2}} p^{\frac{1}{2}})}$$

where k_2 is the rate constant for the decomposition reaction. Now

(a) at low concentrations p is small and $K^{\frac{1}{2}} p^{\frac{1}{2}} \ll 1$, so

$$R \approx k_2 K^{\frac{1}{2}} p^{\frac{1}{2}}$$

and the rate of reaction is proportional to the square root of the concentration of the reactant.

(b) at high concentrations p is large and $K^{\frac{1}{2}} p^{\frac{1}{2}} \gg 1$, so

$$R \approx k_2$$

and the rate of reaction is independent of the concentration of the reactant.

At intermediate concentrations the rate of reaction is proportional to the concentration of the reactant to some power between one-half and zero.

The observed kinetics of the decomposition of liquid hydrazine on a supported rhodium catalyst may therefore be explained by assuming that the dissociative chemisorption of hydrazine is the rate controlling step and applying this to the Langmuir adsorption isotherm to derive the rate equations. For any hydrazine solution of less than 15 mole dm^{-3} the rate equation contains two temperature dependent rate constants k_2 and K. Therefore to determine the temperature variation of k_2 and hence the true activation energy for the reaction, hydrazine solutions of greater than 15 mole dm^{-3} concentration must be used. Fig. 4.3 shows the Arrhenius plot for the temperature variation of the rate of decomposition of 22.7 mole dm^{-3} hydrazine solution on the supported rhodium catalyst. The activation energy calculated from this data is 41.28 ± 0.34 kJ $mole^{-1}$ and the pre-exponential factor is 3.45×10^2 mole gm^{-1} sec^{-1}

Any mechanism postulated to account for the decomposition of hydrazine on the supported rhodium catalyst must be consistent with the following experimental observations:-

1. The stiochiometry of the reaction is

$$2N_2H_4 \longrightarrow N_2 + H_2 + 2NH_3 \quad .$$

2. The nitrogen molecule is formed from the two nitrogen atoms of one hydrazine molecule without N-N bond fission.

3. The kinetics have shown that in the adsorption step dissociation of the hydrazine molecule occurs.

The initial step in the reaction mechanism is the dissociative chemisorption of hydrazine in the form of amide radicals. These further dissociate on the surface to form imide radicals and hydrogen atoms, the latter are mobile and combine to be desorbed as hydrogen molecules. To account for the

observation that the nitrogen molecule is formed without N-N bond fission the next step is postulated to be a Langmuir-Rideal reaction between the adsorbed imide radicals and a hydrazine molecule from solution. In this step the imide radicals are hydrogenated to ammonia while the hydrazine molecule is dehydrogenated to form the nitrogen molecule without N-N bond fission. The reaction mechanism may be represented as follows:-

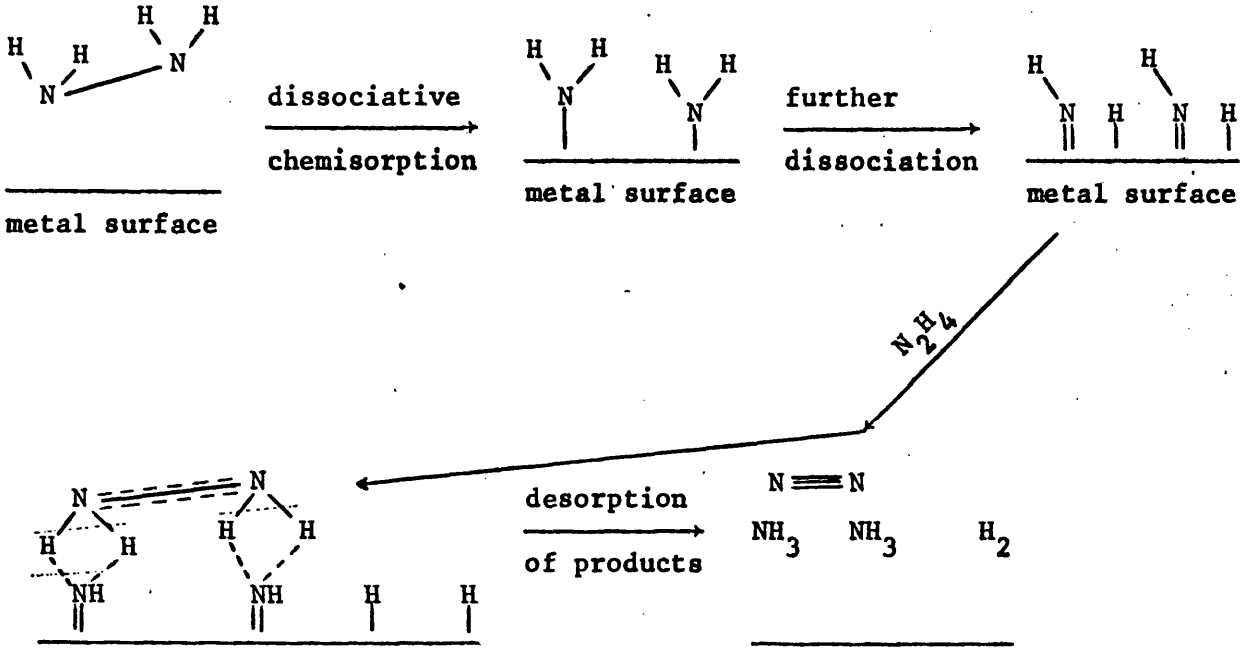

Such a mechanism is consistent with all the experimental observations and also with dual plane theory of Cosser and Tompkins on the basis that reaction only occurs on those planes of rhodium which are active for the dissociative chemisorption of hydrazine.

CHAPTER FIVE

THE USE OF A SUPPORTED PALLADIUM CATALYST

5.1 Results

5.1.1 Product analysis

The permanent gas evolved by the decomposition of hydrazine solutions on a supported palladium catalyst was analysed for hydrogen and nitrogen content using the gas chromatograph. The variation of the permanent gas composition with respect to hydrazine concentration was studied at 24°C and the results are presented in Table 5.1.

TABLE 5.1

Variation of the permanent gas composition with respect to hydrazine concentration

Hydrazine concentration mole dm^{-3}	Permanent gas composition	
	% H_2	% N_2
1.2	7.0	93.0
3.1	12.3	87.7
4.8	16.2	83.8
6.1	20.1	79.9
9.3	32.0	68.0
12.3	36.0	64.0
16.5	40.5	59.5
18.8	45.0	55.0
23.0	47.0	53.0
28.3	47.5	52.5
31.0	53.0	47.0

The results show that the percentage of hydrogen increases with respect to increasing hydrazine concentration.

The effect of temperature on the permanent gas composition was studied using 31.0 mole dm^{-3} hydrazine solution and the results are presented in Table 5.2.

TABLE 5.2

Variation of the permanent gas composition with respect to temperature for the decomposition of 31.0 mole dm^{-3} hydrazine solution on a supported palladium catalyst

Temperature, ^{o}C	Permanent gas composition	
	% H_2	% N_2
15.0	48.5	51.5
19.0	49.5	50.5
22.0	53.0	47.0
24.6	49.0	51.0
30.0	48.6	51.4
34.5	50.9	49.1
40.0	51.3	48.7
45.0	49.1	50.9

The results show that the relative proportions of hydrogen and nitrogen in the permanent gas are independent of temperature.

A third parameter to be studied was the effect on the permanent gas composition of the pre-adsorption of the products of the decomposition reaction on the catalyst. The effect of the pre-adsorption of hydrogen on the permanent gas composition is given in Table 5.3.

TABLE 5.3

The effect of hydrogen pre-adsorption on the permanent gas composition

Hydrogen pre-adsorbed	Hydrazine concentration mole dm^{-3}	Temperature, ^{o}C	Permanent gas composition	
			% H_2	% N_2
No	3.1	24.0	12.3	87.7
Yes	3.1	24.0	48.4	51.6
No	3.1	41.0	21.3	78.7
Yes	3.1	41.0	50.3	49.7
No	3.1	10.0	9.8	90.2
Yes	3.1	10.0	47.7	52.3
No	9.3	24.0	32.0	68.0
Yes	9.3	24.0	51.1	48.9
No	18.8	24.0	45.0	55.0
Yes	18.8	24.0	49.1	50.9
No	31.0	24.0	53.0	47.0
Yes	31.0	24.0	48.6	51.4

Compared to the standard catalyst conditions these results show that the effect of the pre-adsorption of hydrogen is to increase the proportion of hydrogen in the permanent gas to approximately one half. The effect of the pre-adsorption of ammonia on the permanent gas composition was also studied and the results are given in Table 5.4.

TABLE 5.4

The effect of ammonia pre-adsorption on the permanent gas composition

Ammonia pre-adsorbed	Hydrazine concentration mole dm^{-3}	Temperature, ^{o}C	Permanent gas composition	
			% H_2	% N_2
No	3.1	10.0	9.8	90.2
Yes	3.1	10.0	46.3	53.7
No	3.1	24.0	12.3	87.7
Yes	3.1	24.0	51.9	48.1
No	3.1	41.0	21.3	78.7
Yes	3.1	41.0	47.9	52.1
No	9.3	24.0	32.0	68.0
Yes	9.3	24.0	48.1	51.9
No	18.8	24.0	45.0	55.0
Yes	18.8	24.0	50.6	49.4

These results show that the pre-adsorption of ammonia also has the effect of increasing the proportion of hydrogen in the permanent gas to approximately one half.

It was also observed that the composition of the permanent gas changed with respect to the time of reaction. For all the concentrations of hydrazine studied the limiting composition of the permanent gas appeared to be 50% nitrogen and 50% hydrogen.

The ratio of the number of moles of ammonia formed by the decomposition of one mole of hydrazine was determined by titrimetric analysis. The results of the analysis carried out for the decomposition of 9.3 mole dm^{-3}

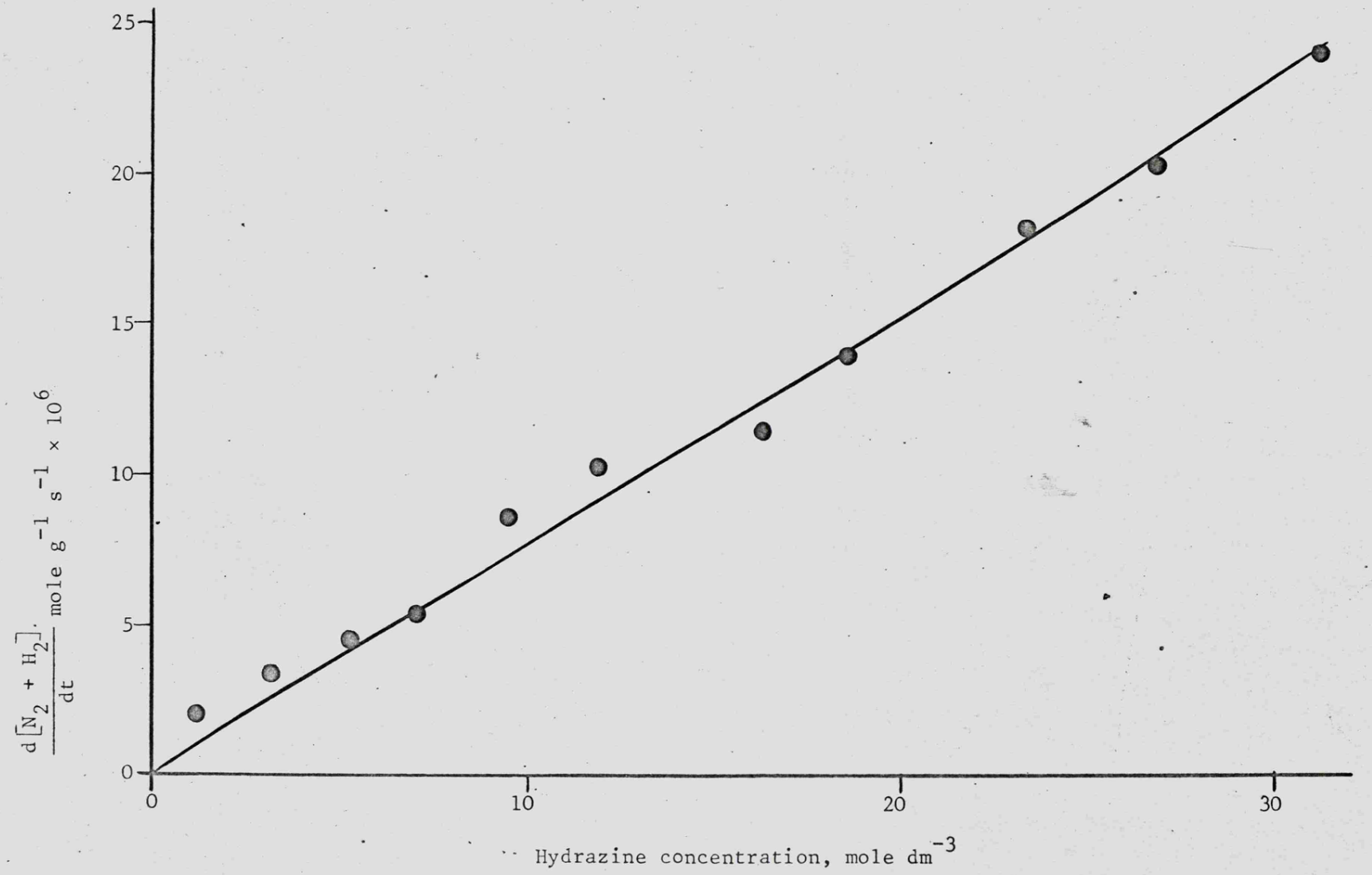

Fig. 5.1 Overall rate of decomposition of hydrazine on the palladium catalyst at 24°C

hydrazine solution on the supported palladium catalyst are shown in Table 5.5.

TABLE 5.5

Determination of the conversion of hydrazine to ammonia

Moles of hydrazine			Total moles of alkali[4]	Moles of ammonia produced[5]	$N_2H_4:NH_3$ ratio
Start[1]	Finish[2]	Decomposed[3]			
0.0347	0.0172	0.0175	0.0353	0.0181	1:1.04
0.0347	0.0119	0.0228	0.0360	0.0241	1:1.06
0.0347	0.0211	0.0136	0.0360	0.0149	1:1.10
0.0347	0.0071	0.0276	0.0369	0.0298	1:1.08

Notes

1. Starting number of moles of hydrazine determined by Andrews titration.
2. Final number of moles of hydrazine determined by Andrews titration.
3. Given by (1-2).
4. Total alkali (ammonia + hydrazine) after reaction determined by acid titration.
5. Given by (4-2).

These results show that the decomposition of one mole of hydrazine is accompanied by the formation of 1.07 moles of ammonia.

5.1.2 Results of the kinetic experiments

The variation of the overall rate of decomposition of aqueous hydrazine solutions on the supported palladium catalyst with respect to hydrazine concentration is given in Table 5.6. The experiments were carried out at 24°C. The results are also presented in Fig. 5.1 where it can be seen that the overall rate of decomposition is a curved function of the hydrazine concentration.

The variation of the overall rate of decomposition of 31.0 mole dm^{-3} hydrazine solution on the supported palladium with respect to temperature

is presented in Table 5.7. The results are also presented in Fig. 5.2 in the form of an Arrhenius plot.

TABLE 5.6

Variation of the overall rate of decomposition of hydrazine at 24°C on the supported palladium catalyst with respect to hydrazine concentration

Hydrazine concentration mole dm^{-3}	Overall rate of decomposition $\frac{d[N_2 + H_2]}{dt}$ mole $gm^{-1}\ sec^{-1} \times 10^6$
1.2	1.72
3.1	3.4
4.8	4.5
6.1	5.0
9.3	7.9
12.3	9.9
16.5	10.9
18.8	12.9
23.0	16.2
28.3	17.8
31.0	22.2

TABLE 5.7

Variation of the rate of decomposition of 31.0 mole dm^{-3} hydrazine solution with respect to temperature

Temperature, °C	Temperature, °K	$\frac{1}{K} \times 10^3$	Overall rate of decomposition $\frac{d[N_2 + H_2]}{dt}$ mole $gm^{-1}\ sec^{-1} \times 10^6$	$6 + \log_{10}$ rate
15.0	288.2	3.470	13.6	1.134
19.0	292.2	3.422	18.2	1.260
22.0	295.2	3.388	20.8	1.318
24.6	297.8	3.358	22.9	1.360
30.0	303.2	3.298	33.9	1.530
34.5	307.7	3.250	44.4	1.647
40.0	313.2	3.193	60.8	1.784
45.0	318.2	3.143	81.8	1.913

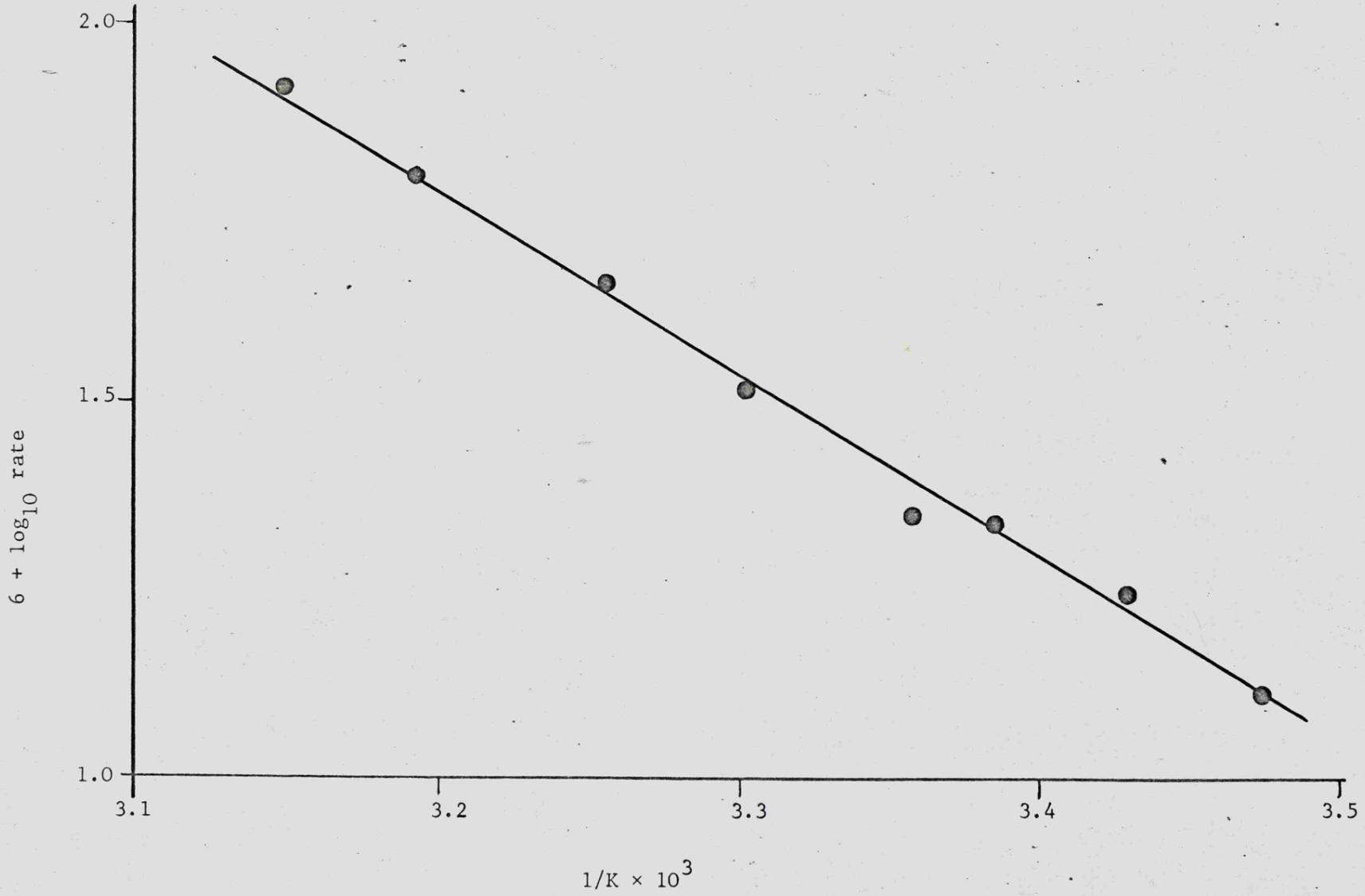

Fig. 5.2 Arrhenius plot for the overall reaction on the palladium catalyst

The effect of pre-adsorbing the products of the reaction on the rate of decomposition was also studied but the results were not reproducible and only qualitative results could be obtained. The pre-adsorption of hydrogen on the catalyst resulted in a decrease in the rate of decomposition to less than 30% of the decomposition rate observed using the standard condition catalyst. The effect of the pre-adsorption of ammonia was even more marked as some catalyst samples were apparently totally inactive with respect to the decomposition of hydrazine. However, it was observed that even the samples which were apparently inactive did begin to decompose hydrazine after a short time interval and for all the samples the rate of decomposition increased with respect to time. Ultimately the limiting rate of decomposition of hydrazine on the ammonia pre-treated catalyst was similar to the limiting rate observed with the standard catalyst.

5.2 Discussion

The decomposition of hydrazine on a supported rhodium catalyst was shown to follow reaction (6):-

$$2N_2H_4 \rightarrow N_2 + H_2 + 2NH_3 \qquad (6)$$

while on the supported ruthenium catalyst the overall decomposition reaction was shown to consist of two reactions which occurred simultaneously:-

$$3N_2H_4 \rightarrow N_2 + 4NH_3 \qquad (2)$$

and also reaction (6).

The analysis of the permanent gas evolved by the decomposition of aqueous hydrazine solutions on the palladium catalyst showed that the percentage of hydrogen increased with respect to hydrazine concentration up to a maximum of 50%. The permanent gas composition of equimolar quantities of nitrogen and hydrogen was found to be invariant for the decomposition of 30.8 mole dm^{-3} hydrazine solution with respect to temperature. Pretreating the palladium catalyst with hydrogen or ammonia results in the evolution of

TABLE 5.8

Calculation of the rates of reactions (2) and (6) from the overall rate of reaction

Hydrazine concentration mole dm^{-3}	Overall rate of reaction $\frac{[N_2 + H_2]}{dt}$ mole gm^{-1} sec^{-1} $\times 10^6$	% H_2 in permanent gas	% of overall reaction due to reaction (6)	Rate of reaction (6) $\frac{d[N_2 + H_2]}{dt}$ mole gm^{-1} sec^{-1} $\times 10^6$	Rate of reaction (6) $-\frac{d[N_2H_4]}{dt}$ mole gm^{-1} sec^{-1} $\times 10^6$	Rate of reaction (2) $\frac{d[N_2 + H_2]}{dt}$ mole gm^{-1} sec^{-1} $\times 10^6$	Rate of reaction (2) $-\frac{d[N_2H_4]}{dt}$ mole gm^{-1} sec^{-1} $\times 10^6$
1.2	2.0	7	14.0	0.28	0.28	1.72	0.57
3.1	3.4	12.3	24.6	0.84	0.84	2.56	0.85
4.8	4.5	16.2	32.4	1.46	1.46	3.04	1.01
6.1	5.0	20.1	40.2	2.0	2.0	3.0	1.0
9.3	7.9	32.0	64.0	5.1	5.1	2.8	0.93
12.3	9.9	36.0	72.0	7.1	7.1	2.8	0.93
16.5	10.9	40.5	81.0	8.8	8.8	2.1	0.7
18.8	12.9	45.0	90.0	11.6	11.6	1.3	0.43
23.0	16.2	47.0	94.0	15.0	15.0	1.2	0.40
28.3	17.8	47.5	95.0	16.9	16.9	0.9	0.30
31.0	22.2	53.0	106.0	23.5	23.5	-	-

permanent gas having a constant composition of equimolar quantities of nitrogen and ammonia. At first sight the variation of the permanent gas composition with respect to hydrazine concentration might be considered to indicate the simultaneous occurrence of two reactions as was observed using the ruthenium catalyst. However such an assumption leads to derived kinetic data which is very difficult to interpret in a rational manner. Analysing the results in terms of the simultaneous occurrence of reactions (2) and (6), see Table 5.8 and Fig. 5.3, produces a rate for reaction (2) which goes through a maximum with respect to hydrazine concentration and decreases to zero at high concentrations. It is difficult to envisage a mechanism which would produce such a result and so other reaction schemes will be considered.

Under various experimental conditions the composition of the evolved permanent gas is equimolar quantities of nitrogen and hydrogen which corresponds to the permanent gas composition for reaction (6). In addition the titrimetric analysis has shown that for each mole of hydrazine decomposed approximately one mole of ammonia is formed and this result is also consistent with reaction (6). However, if only reaction (6) occurs for the decomposition of hydrazine on the supported paladium catalyst then the non-stoichiometric composition of the permanent gas evolved under certain conditions has to be explained. In view of the readiness of palladium to adsorbed hydrogen and the effect of the pre-treatment of the catalyst with hydrogen on the permanent gas composition, it is postulated that under certain conditions an appreciable quantity of hydrogen is adsorbed on the catalyst surface. Hence the true reaction stoichiometry is only observed when the surface is effectively covered by adsorbed species and there are no vacant sites available to adsorbed hydrogen.

The kinetics of the decomposition of hydrazine on the supported paladium catalyst will now be considered in terms of the occurrence of reaction (6). When the observed stoichiometry of the permanent gas is different to

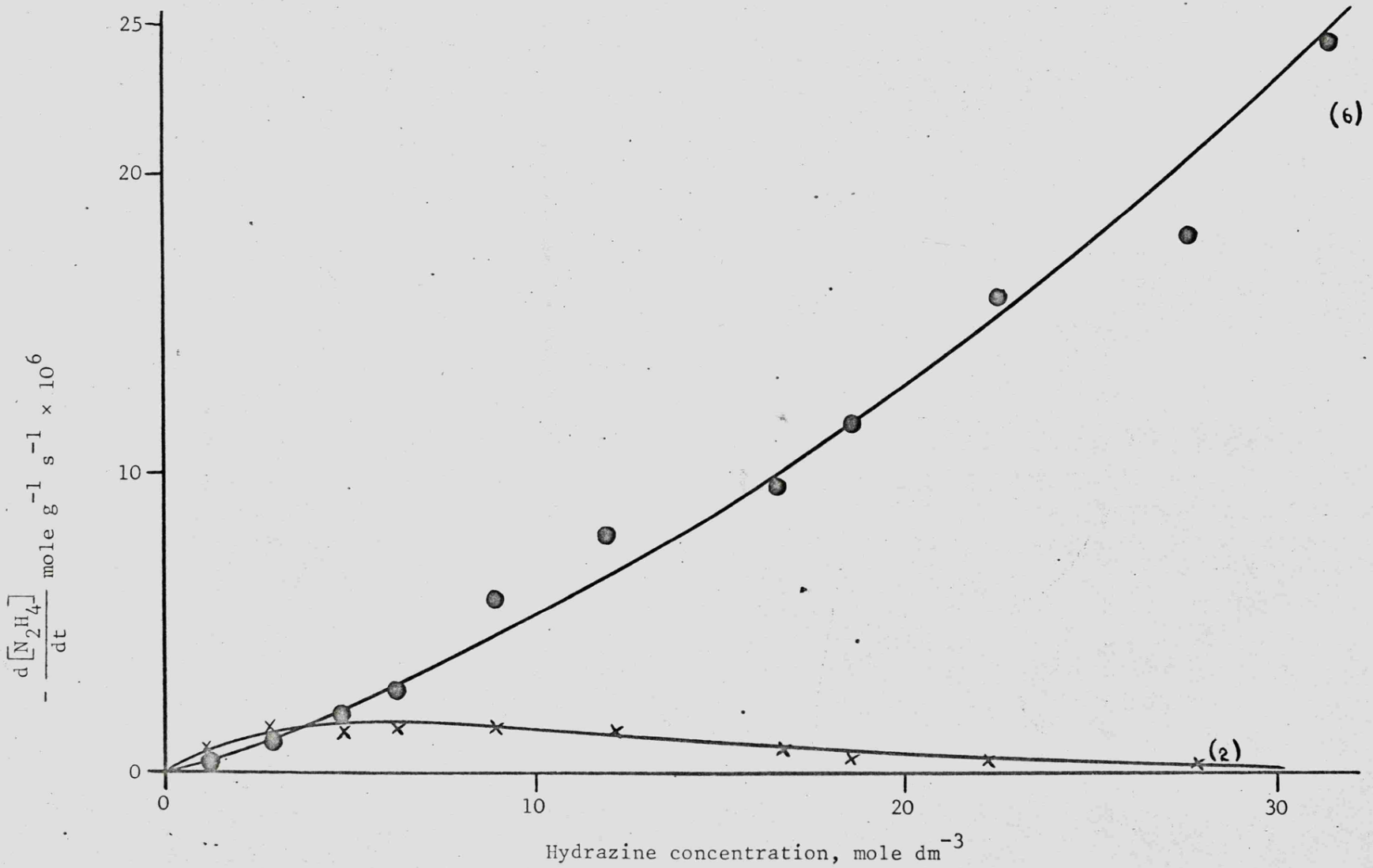

Fig. 5.3 Calculated rates of reactions (2) and (6) for the decomposition of hydrazine on the palladium catalyst

that of reaction (6), the rate of reaction will be calculated from the overall rate of reaction and the observed permanent gas composition. The true rate of reaction is twice the percentage of the overall rate of reaction which is due to nitrogen evolution. The true rate of reaction (6) with respect to hydrazine concentration is shown in Fig. 5.4 where it can be seen that the rate is a curved function of hydrazine concentration. The relationship between the rate of reaction, R, and the concentration, c, is:-

$$R = k c^n$$

where k is the rate constant for the reaction and n is the order of reaction. Taking logs:-

$$\log_{10} k = \log_{10} k + n \log_{10} c \quad .$$

The data of Table 5.9 and Fig. 5.4 is also plotted in Fig. 5.5 in log-log form where the value of n is approximately one-half. Hence the decomposition of hydrazine on the supported palladium catalyst obeys one half order kinetics.

The observed one half order kinetics for the decomposition of hydrazine on the supported rhodium catalyst (see Chapter 3) were explained on the basis that the dissociative chemisorption of hydrazine was the slow step. The rate equations were derived using the Langmuir adsorption isotherm and the half order rate equation was:-

$$R \approx k_2 K^{\frac{1}{2}} c^{\frac{1}{2}}$$

where k_2 is the reaction rate constant and K is the equilibrium constant for the adsorption process, both k_2 and K are temperature dependant. This rate equation also applies to the decomposition of hydrazine on the supported palladium catalyst and as the reaction is one half order throughout the hydrazine concentration range only an apparent activation energy may be calculated. Fig. 5.2 shows the Arrhenius plot for the temperature variation of the rate of decomposition of 31.0 mole dm^{-3} hydrazine solution and

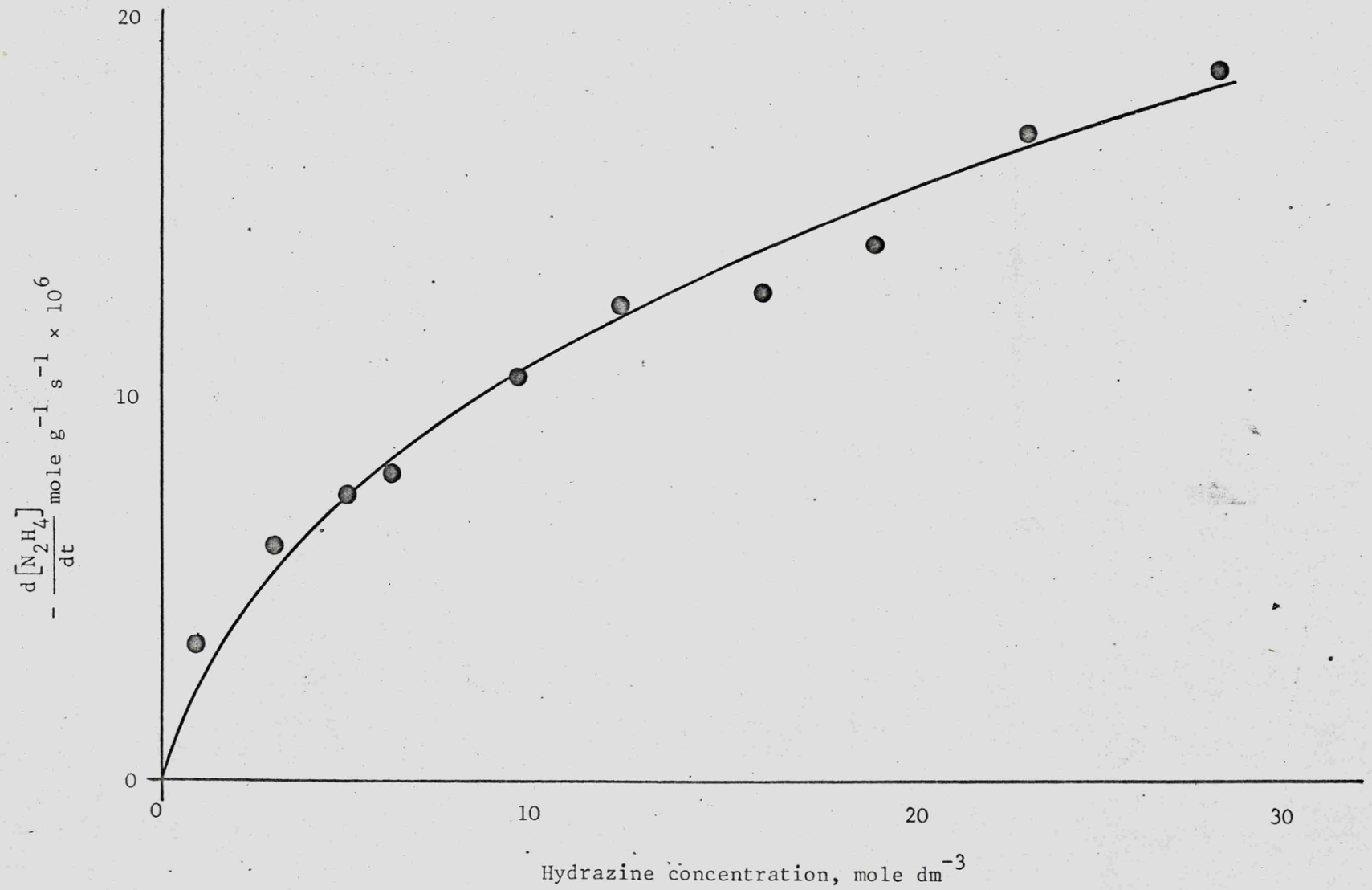

Fig. 5.4 Rate of reaction (6) on the palladium catalyst at 24°C

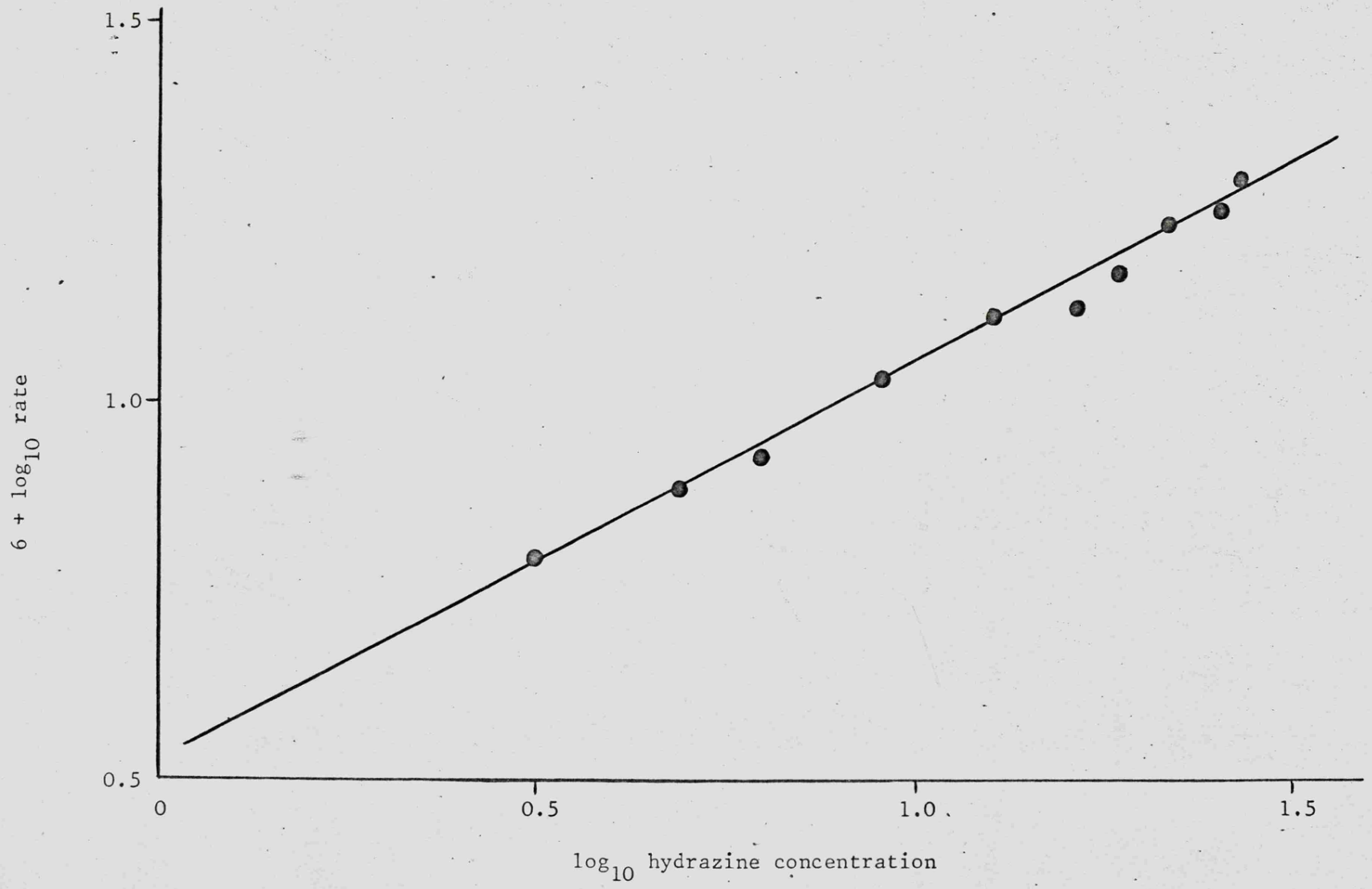

Fig. 5.5 $\log_{10}$ rate of reaction (6) with respect to $\log_{10}$ hydrazine concentration

TABLE 5.9

Calculation of the rate of reaction (6) for the decomposition of hydrazine on the supported palladium catalyst

Hydrazine concentration mole dm^{-3}	Overall rate of reaction $\frac{d[N_2 + H_2]}{dt}$ mole gm^{-1} sec^{-1} $\times 10^6$	% N_2 in permanent gas	Rate of nitrogen evolution $\frac{d[N_2]}{dt}$ mole gm^{-1} sec^{-1} $\times 10^6$	Rate of reaction (6) $-\frac{d[N_2H_4]}{dt}$ mole gm^{-1} sec^{-1} $\times 10^6$	$\log_{10}$ hydrazine concentration	$\log_{10}$ rate of reaction (6)
1.2	2.0	93.0	1.86	3.72	0.079	0.571
3.1	3.4	87.7	3.0	6.0	0.491	0.776
4.8	4.5	83.8	3.8	7.5	0.681	0.877
6.1	5.0	79.9	4.0	8.0	0.785	0.903
9.3	7.9	68.0	5.4	10.7	0.968	1.031
12.3	9.9	64.0	6.3	12.7	1.090	1.103
16.5	10.9	59.5	6.5	13.0	1.217	1.113
18.8	12.9	55.0	7.1	14.2	1.274	1.152
23.0	16.2	53.0	8.6	17.2	1.362	1.235
28.3	17.8	52.5	9.3	18.7	1.452	1.272
31.0	22.2	47.0	10.4	20.9	1.491	1.319

the activation energy calculated from this data is 44.6 ± 0.5 kJ mole^{-1}.

Any reaction mechanism postulated to account to the decomposition of hydrazine on the supported palladium catalyst must be consistent with the following experimental observations:-

(1) The stoichiometry of the overall reaction is:-

$$2N_2H_4 \rightarrow N_2 + H_2 + 2NH_3 \qquad (6)$$

(2) The kinetics show that the dissociative chemisorption of hydrazine is the rate controlling step.

(3) The effect of the pre-adsorption of the reaction products on the permanent gas composition and the rate of reaction.

The initial step is the dissociative chemisorption of hydrazine in the form of NH_2 radicals and this is also the rate controlling step. As one half order kinetics are observed throughout the concentration range the surfact is never completely covered by adsorbed NH_2 radicals. The overall reaction stoichiometry involves two hydrazine molecules and the next step is postulated to be reaction between the adsorbed radicals, either NH or NH_2, and a hydrazine molecule from solution to form nitrogen and ammonia. Although no ^{15}N tracer experiments were carried out with the palladium catalyst it is suggested by analogy with the results of the ^{15}N tracer work using rhodium and ruthenium catalysts that in the Langmuir-Rideal reaction the adsorbed species are hydrogenated to ammonia while the hydrazine molecule is dehydrogenated to nitrogen. The way in which the hydrogen molecule is formed is not known but there are two obvious paths, one that surface dissociation of the NH_2 radicals occurs to give adsorbed hydrogen atoms which then combine and desorb, secondly the hydrogen molecule may be formed directly in the course of the Langmuir-Rideal reaction. However the hydrogen molecule is formed it is postulated that under certain conditions of very sparse surface coverage an appreciable quantity of hydrogen is adsorbed on the catalyst surface resulting in a non-stoichiometric composition of the

evolved permanent gas. It is only when the catalyst surface is effectively covered by adsorbed species, either as a result of pre-treatment or previous reaction, that the true reaction stoichiometry is observed.

Pre-treatment of the catalyst with hydrogen results in a surface effectively covered by adsorbed hydrogen atoms and as a result there are few surface sites available for the adsorption of hydrazine molecules. Hence the the rate of decomposition is greatly reduced but, as the surface is effectively covered with respect to hydrogen, all the hydrogen produced by the reaction appears in the evolved gas. When ammonia is pre-adsorbed on the catalyst the rate of decomposition is decreased, in some cases the catalyst appears totally inactive, but after immersion in the hydrazine solution for a short time the rate of decomposition starts to increase, even the totally inactive catalyst decomposing the hydrazine. It is postulated that ammonia is only weakly adsorbed on the catalyst surface and is, therefore, easily desorbed and replaced by another molecule such as hydrazine. Ultimately the fraction of the surface covered by reacting hydrazine species is the same for both the normal and ammonia pre-treatment catalysts and the rates of decomposition are the same. The adsorbed ammonia molecules also block sites which would otherwise adsorb hydrogen formed by the reaction and therefore all the hydrogen appears in the evolved permanent gas.

The reaction mechanism postulated to account for the decomposition of hydrazine on the supported palladium catalyst is the same as that postulated to account for reaction (6) on both the rhodium and ruthenium catalysts. As was the case using the rhodium catalyst such a mechanism is consistent with the dual plane theory of Cosser and Tompkins on the assumption that reaction only occurs on those planes which are active for the dissociative chemisorption of hydrazine.

CHAPTER SIX

THE USE OF A SUPPORTED IRIDIUM CATALYST

6.1 Results

6.1.1 Product analysis

The permanent gas evolved by the decomposition of aqueous hydrazine solutions on the supported iridium catalyst was analysed by gas chromatography. The effect of the following parameters on the permanent gas composition was studied:

(1) Effect of the variation of hydrazine concentration over the range 1 to 30 mole dm^{-3}.

(2) Effect of the variation of temperature over the range -20^{o} to $+54^{o}C$.

(3) Effect of the variation of the iridium to oxygen ratio between the limiting ratios of 1:0.4 and 1:1.

(4) Effect of iridium metal content over the range 5 to 40% w/w.

Under all the experimental conditions which were studied the permanent gas was found to consist of nitrogen with a very small quantity of hydrogen present, the hydrogen content never exceeded 1% of the evolved permanent gas.

Titrimetric analysis was carried out to determine the number of moles of ammonia produced by the decomposition of each mole of hydrazine. The conversion of hydrazine to ammonia was studied over the hydrazine concentration range 1 to 30 mole dm^{-3} and the temperature range -20^{o} to $+54^{o}C$. The results for the analysis carried out using 6.3 mole dm^{-3} hydrazine solution at $22^{o}C$ are given in Table 6.1.

The results show that for each mole of hydrazine decomposed 1.3 moles of ammonia are formed and this result was found to be independent of hydrazine concentration and temperature.

TABLE 6.1

Determination of the conversion of hydrazine to ammonia

Moles of hydrazine			Total moles of alkali[4]	Moles of ammonia produced[5]	$N_2H_4:NH_3$ ratio
Start[1]	Finish[2]	Decomposed[3]			
0.0232	0.0092	0.0140	0.0279	0.0186	1:1.33
0.0232	0.0126	0.0106	0.0269	0.0144	1:1.35
0.0232	0.0091	0.0141	0.0279	0.0189	1:1.33
0.0232	0.0092	0.0140	0.0279	0.0187	1:1.33

Notes:

1. Starting number of moles of hydrazine determined by Andrews titration
2. Final number of moles of hydrazine determined by Andrews titration
3. Given by (1-2)
4. Total alkali (ammonia + hydrazine) after reaction determined by acid titration.
5. Given by (4-2).

6.1.2 The use of ^{15}N as a tracer

The results of the mass spectrometric analysis of the nitrogen gas evolved by the decomposition of the stock ^{15}N enriched hydrazine solutions on the supported iridium catalyst (Shell 405) are presented in Table 6.2. Also included are the calculated nitrogen isotope distributions for mechanisms involving 0% and 100% N-N bond fission.

The results are in good agreement with the theoretical isotope distributions calculated on the basis of no N-N bond fission in forming the nitrogen molecule.

TABLE 6.2

Results of the mass spectrometric analysis of the nitrogen gas samples

Hydrazine solution mole dm^{-3}	% N-N bond fission theoretical	Distribution of nitrogen isotopes, atom %			Atom per cent ^{15}N	
		$^{14}N_2$	$^{14}N\ ^{15}N$	$^{15}N_2$		
9.65	100	96.39	3.581	0.033	)	
9.65	0	97.73	0.856	1.396	) 1.824	
9.65	observed	97.70	0.88	1.419	1.855	
1.05	observed	97.77	0.87	1.40	1.84	Note 1
14.1	100	97.69	2.29	0.013	)	
14.1	0	98.4	0.81	0.75	) 1.157	
14.1	observed	98.47	0.79	0.74	1.135	

Note 1

Solution was prepared by diluting 9.65 mole dm^{-3} hydrazine solution with distilled water and therefore the theoretical isotope distribution and ^{15}N content are the same as for the original stock solution of hydrazine.

6.1.3 Results of the kinetic experiments

1. The decomposition of hydrazine on the Shell 405 catalyst.

The high rate of decomposition of hydrazine on the Shell 405 catalyst necessitated the use of the apparatus shown in Fig. 2.6 and flow meters to measure the rate of nitrogen evolution. The initial experiments were carried out to determine the effect of the number of catalyst pellets on the rate of decomposition and the results are presented in Table 6.3 and also in Fig. 6.1.

For a given concentration of hydrazine the rate of evolution of nitrogen is proportional to the number of catalyst pellets used and therefore the results may be normalised to the rate of decomposition per unit mass of catalyst per unit time. Such results may be consistent only for catalyst particles which are dimensionally similar as the proportion of the effective

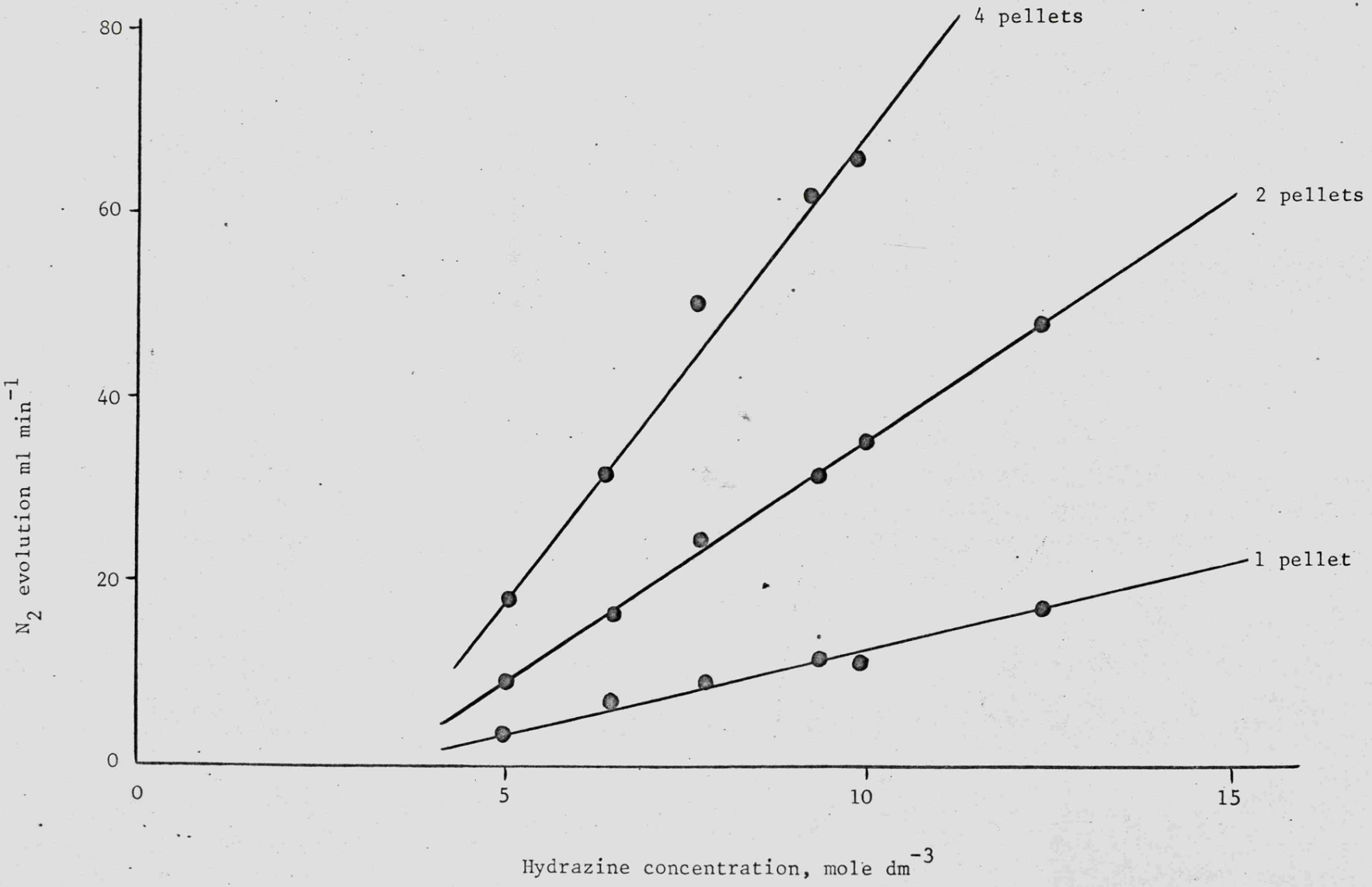

Fig. 6.1 Rate of nitrogen evolution as a function of the number of iridium catalyst pellets

TABLE 6.3

Rate of gas evolution at 22°C as a function of the number of catalyst pellets

Hydrazine concentration mole dm^{-3} \ Rate of nitrogen evolution ml/min	1 pellet	2 pellets	4 pellets
5.0	4.5	9.0	18.0
6.3	8.4	14.7	30.0
7.2	11.0	22.6	50.0
9.4	15.8	31.6	64.2
9.8	15.8	33.9	66.3
12.5	24.5	48.2	

mass of the catalyst particle may be different for different sizes of particle. In Fig. 6.1 the rate of decomposition may be seen to be a linear function of the hydrazine concentration over the limited range studied. The variation of the rate of decomposition of hydrazine with respect to concentration is given in Fig. 6.2, the results are also presented in Table 6.4, and it can be seen that the rate is a linear function of concentration over the range 5 to 31 mole dm^{-3} hydrazine.

The temperature variation of the rate of decomposition of 9.65 mole dm^{-3} hydrazine is presented in Table 6.5 and the results are also presented in the form of an Arrhenius plot in Fig. 6.3. The activation energy calculated from this data is 62.4 ± 0.4 kJ $mole^{-1}$. This result was obtained from experiments carried out using the apparatus shown in Fig. 2.6 which involved exposing the cooled catalyst to the laboratory and this was considered to be a potential source of inaccuracy. Using the reaction vessel shown in Fig. 2.7 the temperature variation of the rates of decomposition of 10.1 and 31.0 mole dm^{-3} hydrazine was studied and the results are presented in Tables 6.6 and 6.7 respectively. The Arrhenius plot for the temperature dependence of the rate

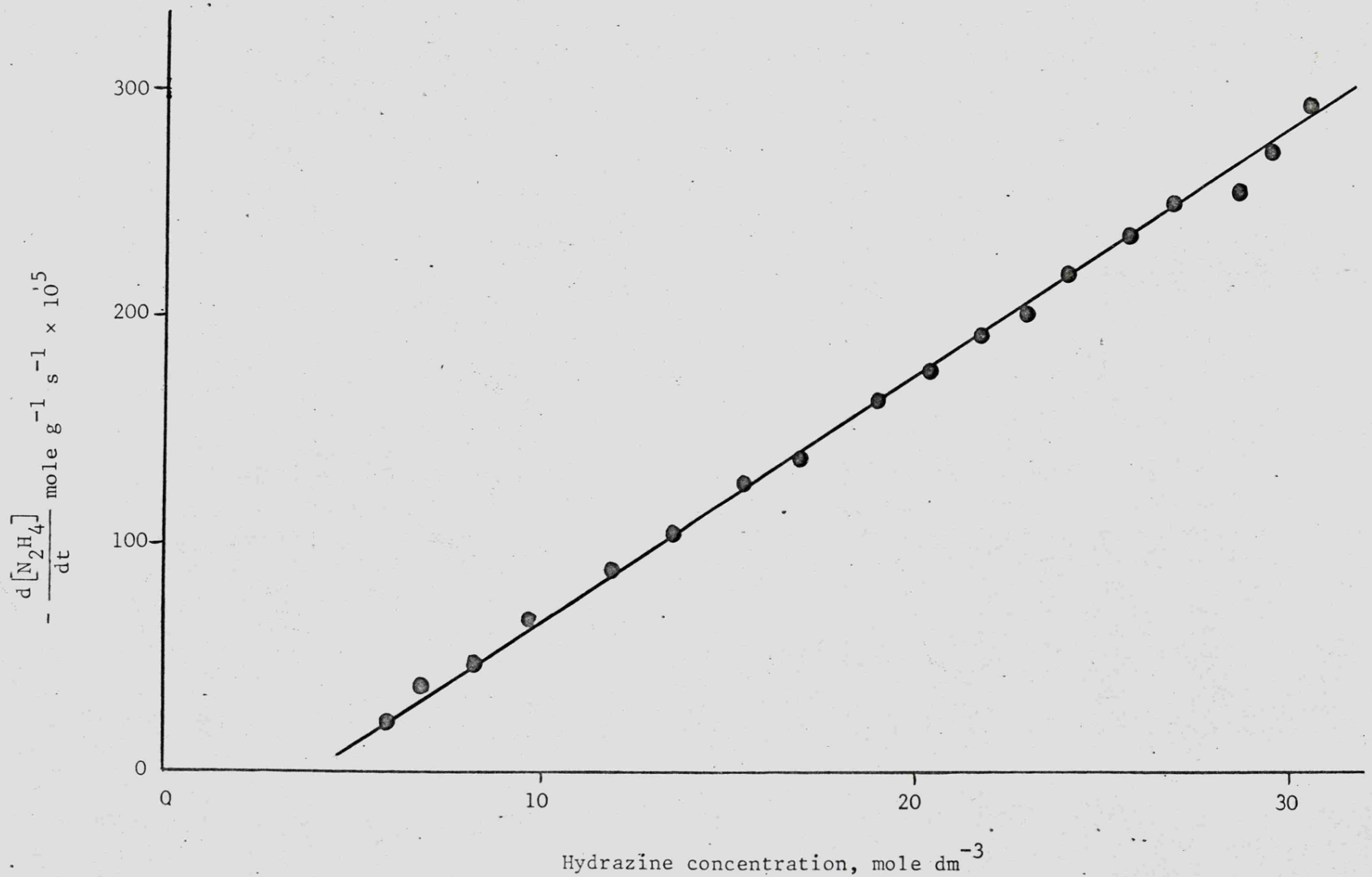

Fig. 6.2 Rate of decomposition of hydrazine on the iridium catalyst

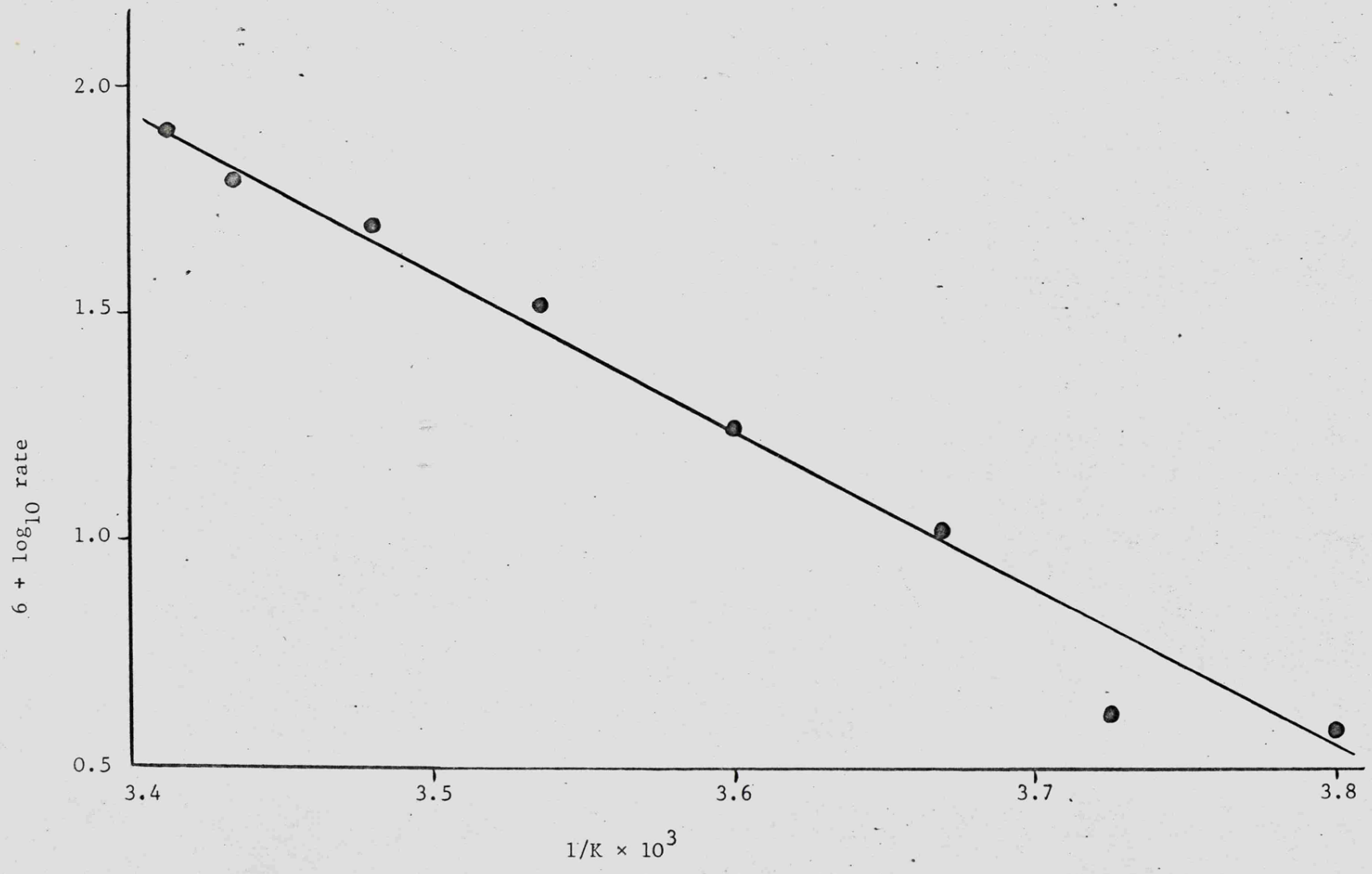

Fig. 6.3 Arrhenius plot for the decomposition of 9.45 mole dm^{-3} hydrazine on the iridium catalyst

TABLE 6.4

Rate of decomposition of hydrazine at 22°C with respect to hydrazine concentration

Hydrazine concentration mole dm^{-3}	Rate of decomposition $-\frac{d[N_2H_4]}{dt}$ mole gm^{-1} sec^{-1} $\times 10^5$
5.0	9.9
6.3	32.5
7.8	42.4
9.8	69.5
11.2	81.8
12.9	96.6
14.7	118.0
16.3	128.0
18.9	163.0
20.6	178.0
22.2	195.0
24.5	216.0
25.6	236.0
27.1	252.0
28.6	260.0
29.5	275.0
31.0	306.0

TABLE 6.5

Temperature dependence of the rate of decomposition of 9.45 mole dm^{-3} hydrazine solution

Temperature °C	Temperature °K	$\frac{1}{K} \times 10^3$	Rate of decomposition $-\frac{d[N_2H_4]}{dt}$ mole gm^{-1} sec^{-1} $\times 10^5$	$k \times 10^5$ dm^3 gm^{-1} sec^{-1}	$6 + \log_{10} k$
19.8	293.0	3.410	74.5	7.9	1.898
19.2	292.5	3.431	56.2	5.95	1.775
15.3	288.5	3.478	46.0	4.87	1.688
10.0	283.2	3.534	30.4	3.20	1.505
5.0	278.2	3.597	16.5	1.75	1.243
0	273.2	3.663	10.2	1.08	1.033
- 5.0	268.2	3.731	6.5	0.39	0.591
-10.0	263.2	3.802	3.7	0.39	0.591

TABLE 6.6

Temperature dependence of the rate of decomposition of 10.1 mole dm^{-3} hydrazine solution

Temperature ^{o}C	Temperature ^{o}K	$\frac{1}{K} \times 10^{3}$	Rate of decomposition $-\frac{d[N_2H_4]}{dt}$ mole gm^{-1} sec^{-1} $\times 10^{5}$	$k \times 10^{5}$ dm^{3} gm^{-1} sec^{-1}	$6 + \log_{10} k$
22.0	295.2	3.390	68.8	6.85	1.836
14.0	287.2	3.484	32.4	3.23	1.509
9.0	282.2	3.546	20.6	2.05	1.312
2.0	275.2	3.636	9.8	0.97	0.987
- 3.0	270.2	3.704	5.9	0.59	0.771
- 8.0	265.2	3.774	3.45	0.34	0.531
-12.0	261.2	3.831	2.26	0.23	0.362
-16.0	257.2	3.891	1.28	0.13	0.114

TABLE 6.7

Temperature dependence of the rate of decomposition of 31.0 mole dm^{-3} hydrazine solution

Temperature ^{o}C	Temperature ^{o}K	$\frac{1}{K} \times 10^{3}$	Rate of decomposition $-\frac{d[N_2H_4]}{dt}$ mole gm^{-1} sec^{-1} $\times 10^{5}$	$k \times 10^{5}$ dm^{3} gm^{-1} sec^{-1}	$6 + \log_{10} k$
22.0	295.2	3.390	306.0	9.90	1.996
15.0	288.2	3.472	157.0	5.08	1.706
10.0	283.2	3.534	98.0	3.17	1.501
5.0	278.2	3.597	59.0	1.90	1.279
0	273.2	3.663	36.5	1.18	1.072

of decomposition of 10.1 mole dm^{-3} hydrazine is shown in Fig. 6.4 and the calculated activation energy is 65.4 ± 0.2 kJ $mole^{-1}$. The results obtained using the 31.0 mole dm^{-3} hydrazine solution are shown in the form of an Arrhenius plot in Fig. 6.5 and the calculated activation energy is 65.4 0.2 kJ $mole^{-1}$. The mean activation energy calculated from the Arrhenius plots for 10.1 and 31.0 mole dm^{-3} hydrazine solutions is 65.4 ± 0.2 kJ $mole^{-1}$.

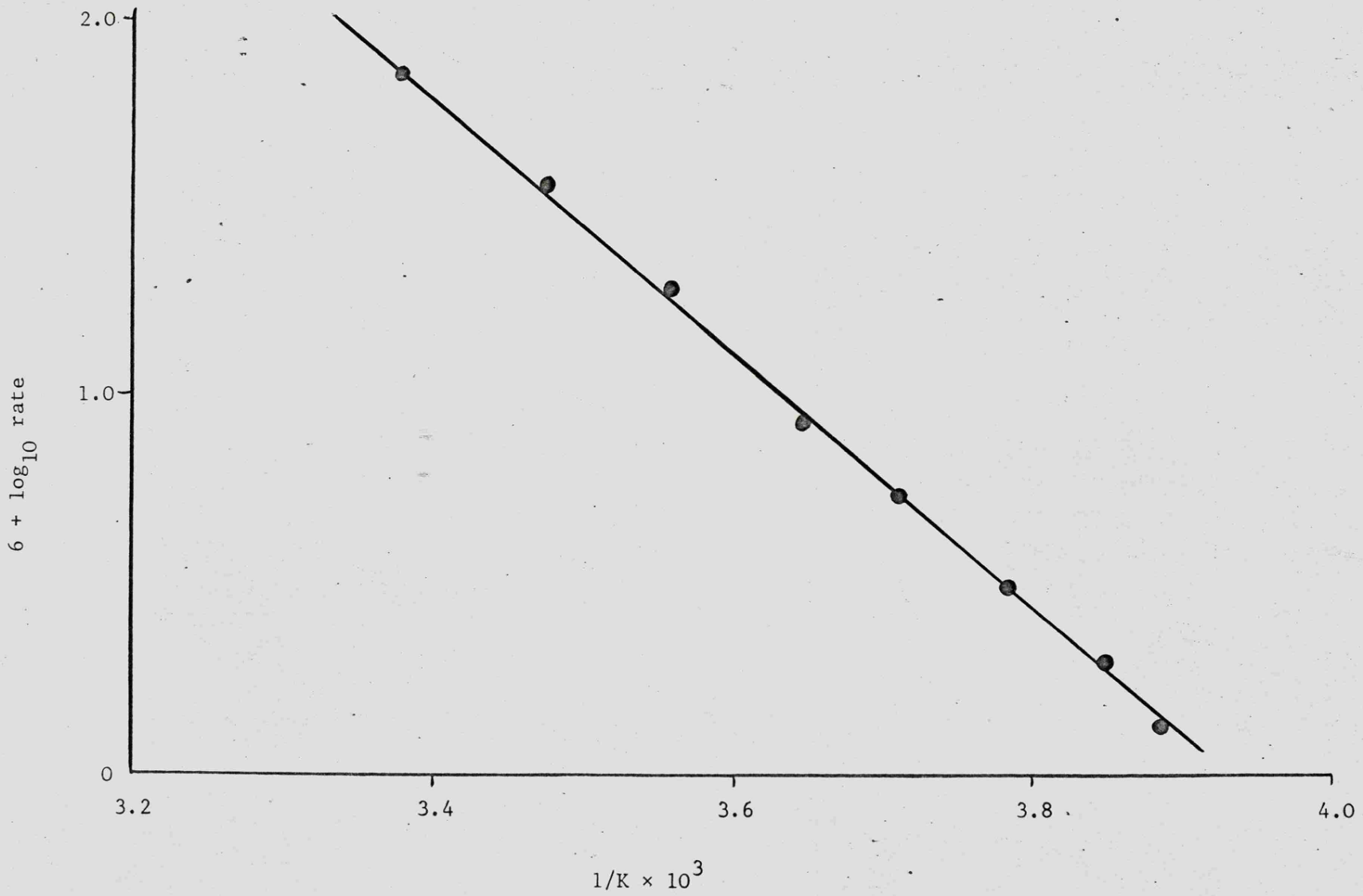

Fig. 6.4 Arrhenius plot for the decomposition of 10.1 mole dm^{-3} hydrazine on the iridium catalyst

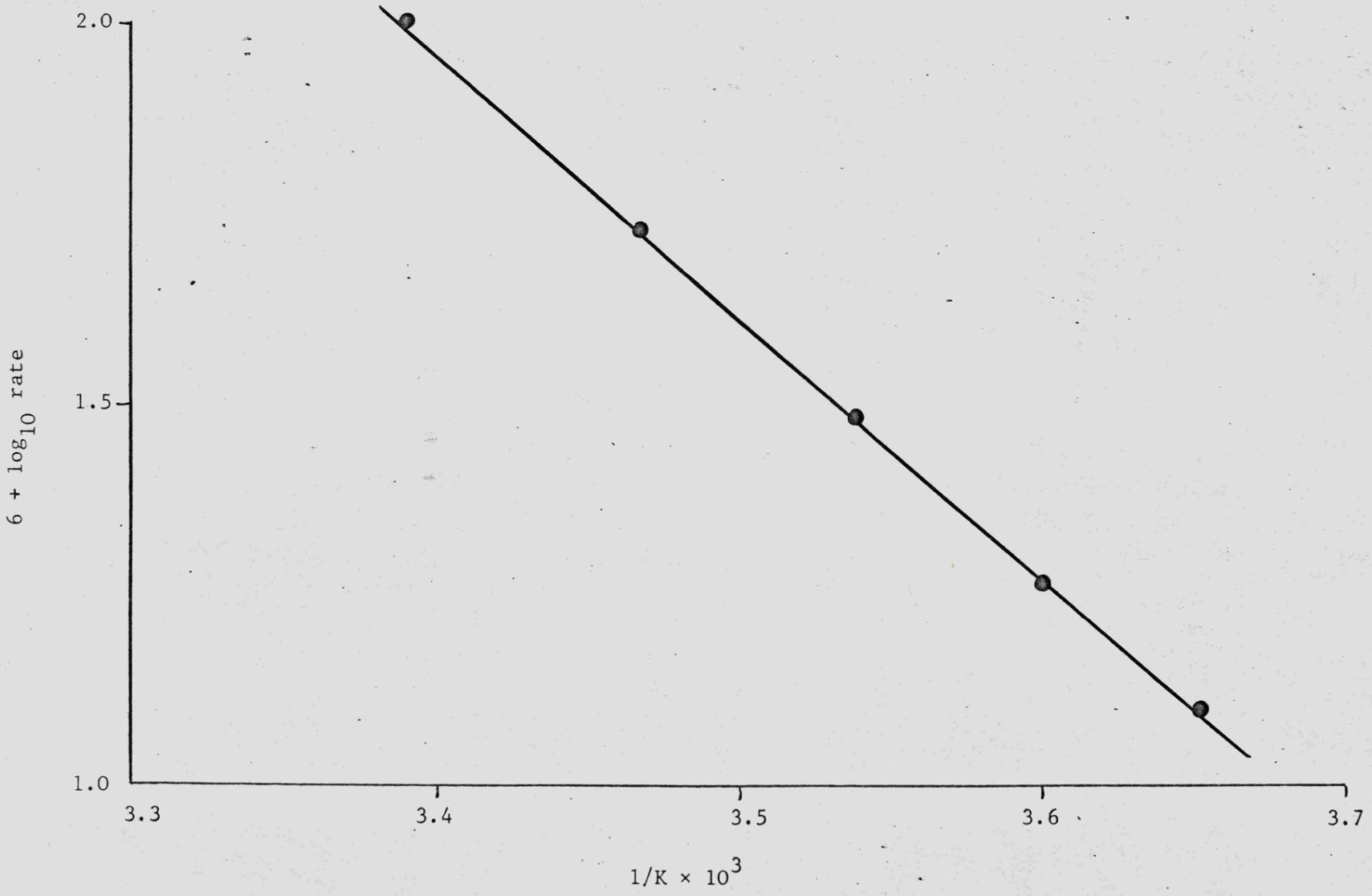

Fig. 6.5 Arrhenius plot for the decomposition of 31.0 mole dm^{-3} hydrazine on the iridium catalyst

The activation energy calculated from the results obtained using the apparatus shown in Fig. 2.7 is higher than that calculated from results obtained using the apparatus shown in Fig. 2.6. In the latter case the pellets were exposed to the laboratory atmosphere while being transferred to the hydrazine solution and during this time some heating of the cooled catalyst will have occurred raising the temperature of the catalyst surface above the required experimental temperature. This has the effect of giving an increased rate of decomposition and as the differential between the experimental and laboratory temperatures increases so the increase in rate will also increase resulting in a reduction in the slope of the Arrhenius plot and hence a lower activation energy. Therefore the activation energy of 65.4 ± 0.2 kJ $mole^{-1}$, determined using the apparatus shown in Fig. 2.7, is considered to be the most accurate.

In addition to the data presented in Tables 6.6 and 6.7 relating to the temperature dependence of the rate of decomposition some additional experiments were carried out and the results are presented in Table 6.8 and are also shown in Fig. 6.6.

TABLE 6.8

The variation of the rate of decomposition with respect to hydrazine concentration at set temperatures

Hydrazine concentration mole dm^{-3} / Rate of decomposition $-\frac{d[N_2H_4]}{dt}$ mole gm^{-1} $sec^{-1} \times 10^5$	0°C	5°C	10°C	15°C	22°C
4.9					10.2
6.2				14.8	29.6
9.9	8.1	14.3	21.8	35.9	68.8
12.6	12.1	20.0	30.2	52.1	97.3
15.8	20.0	26.8	45.2	67.0	128.0
24.9	27.0	50.0	79.7	120.0	236.0
29.1	35.0	57.0	93.0	142.0	275.0
31.0	37.0	59.0	98.0	157.0	306.0

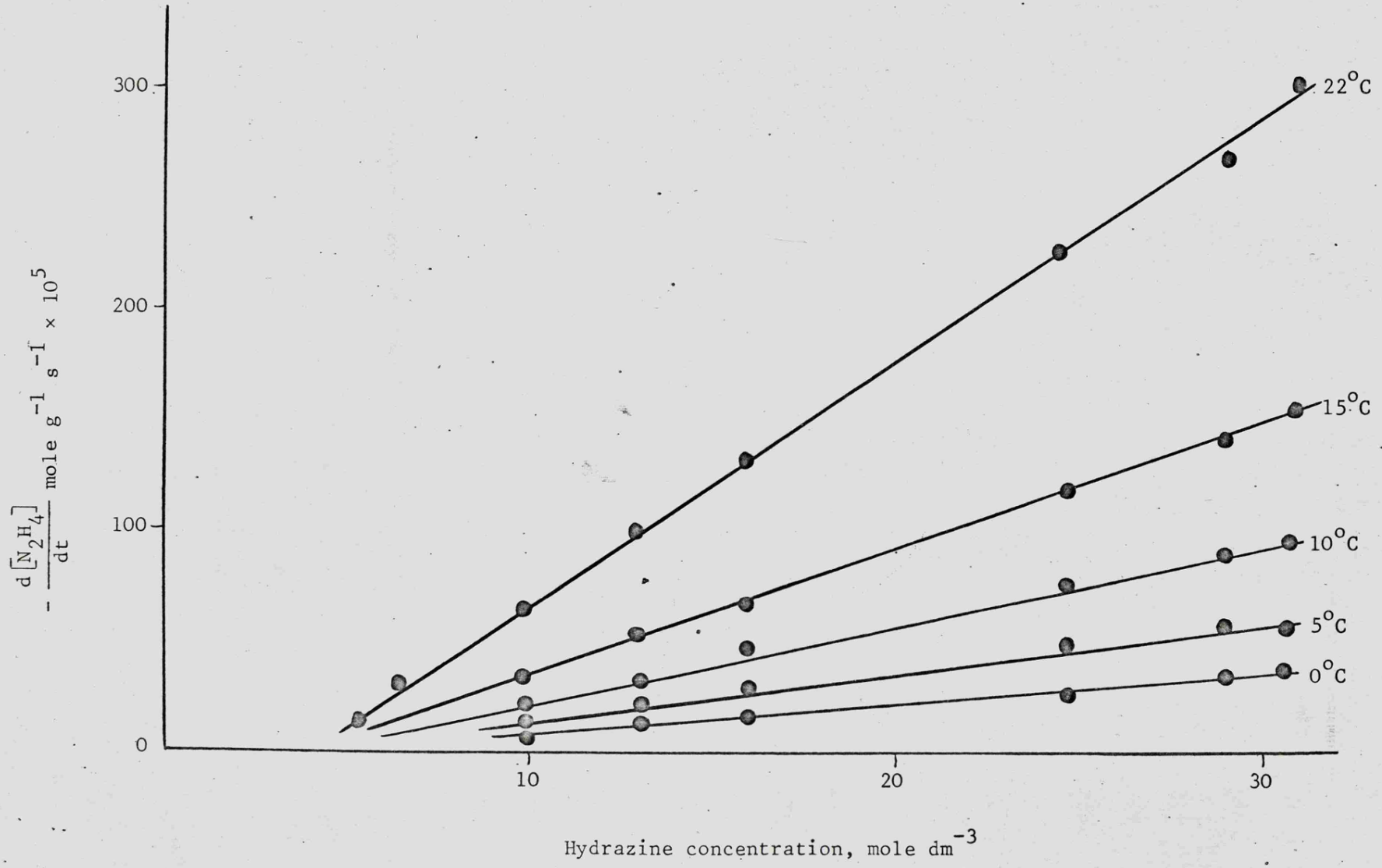

Fig. 6.6 Rate of decomposition of hydrazine on the iridium catalyst at set temperatures

The results show that the rate of decomposition of less than 4.0 mole dm^{-3} hydrazine solution is very low and below the useable range of the flowmeters.

To study the rate of decomposition of low concentrations of hydrazine on the Shell 405 catalyst it was necessary to use gas burettes to measure the rate of evolution of nitrogen. The variation of the rate of decomposition at 20°C with respect to hydrazine concentration is presented in Fig. 6.7 and the results are also given in Table 6.9. The temperature dependence of the rate of decomposition of 1.75 mole dm^{-3} hydrazine was studied and the results are presented in Table 6.10. The data is also shown in the form of an Arrhenius plot in Fig. 6.8 from which an activation energy of 35.1 ± 2.4 kJ $mole^{-1}$ was calculated.

TABLE 6.9

Variation of the rate of decomposition at 20°C with respect to hydrazine concentration up to 3 mole dm^{-3} on the Shell 405 catalyst

Hydrazine concentration mole dm^{-3}	Rate of decomposition $-\frac{d[N_2H_4]}{dt}$ mole gm^{-1} sec^{-1} × 10^5
0.28	0.15
0.61	0.33
0.91	0.58
1.17	0.66
1.51	0.80
1.77	0.98
2.15	1.13
2.37	1.32
2.73	1.50
3.01	1.65
3.33	2.04
3.59	2.77

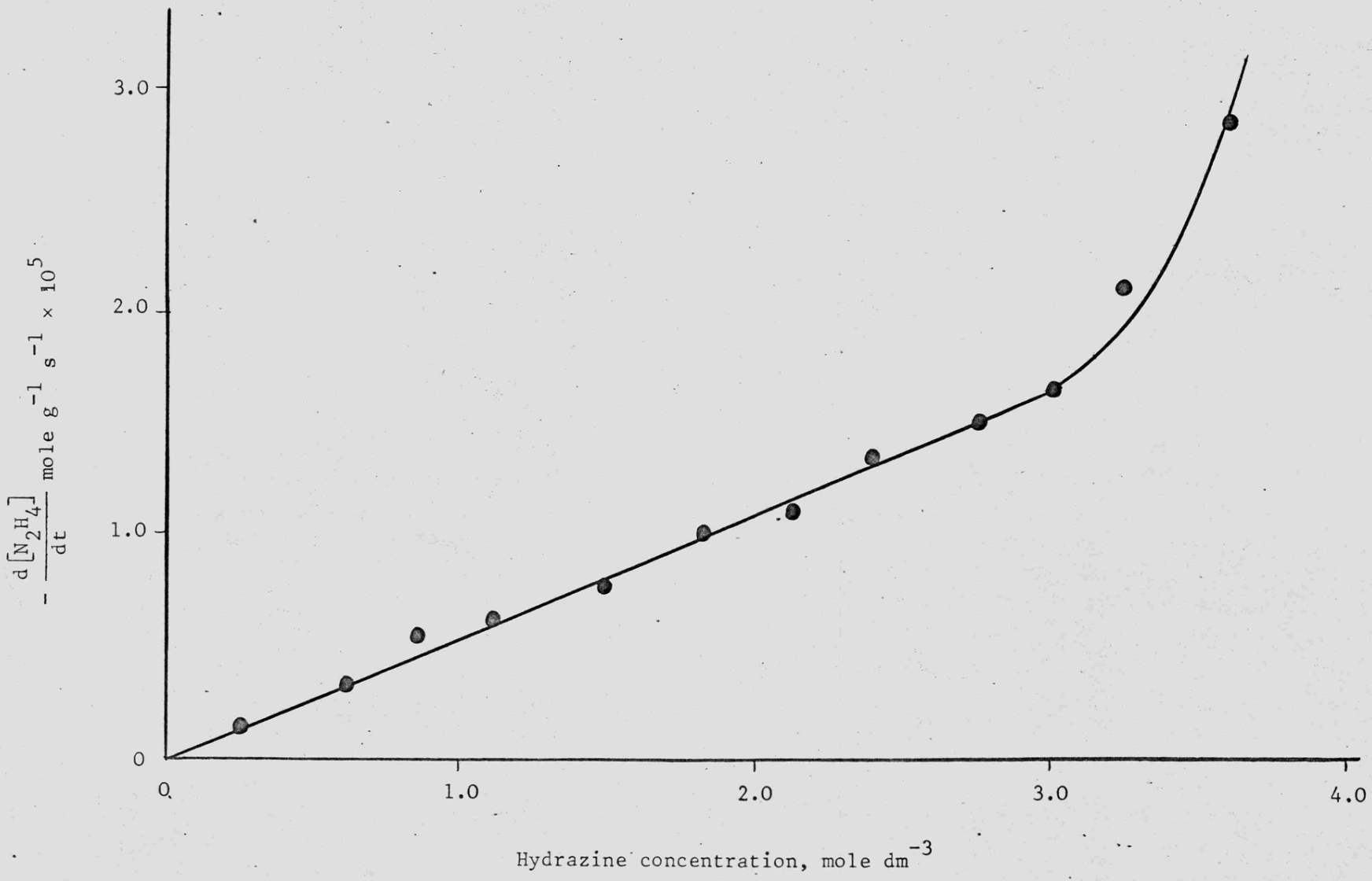

Fig. 6.7 Rate of decomposition of hydrazine at concentrations of up to 4.0 mole dm^{-3}

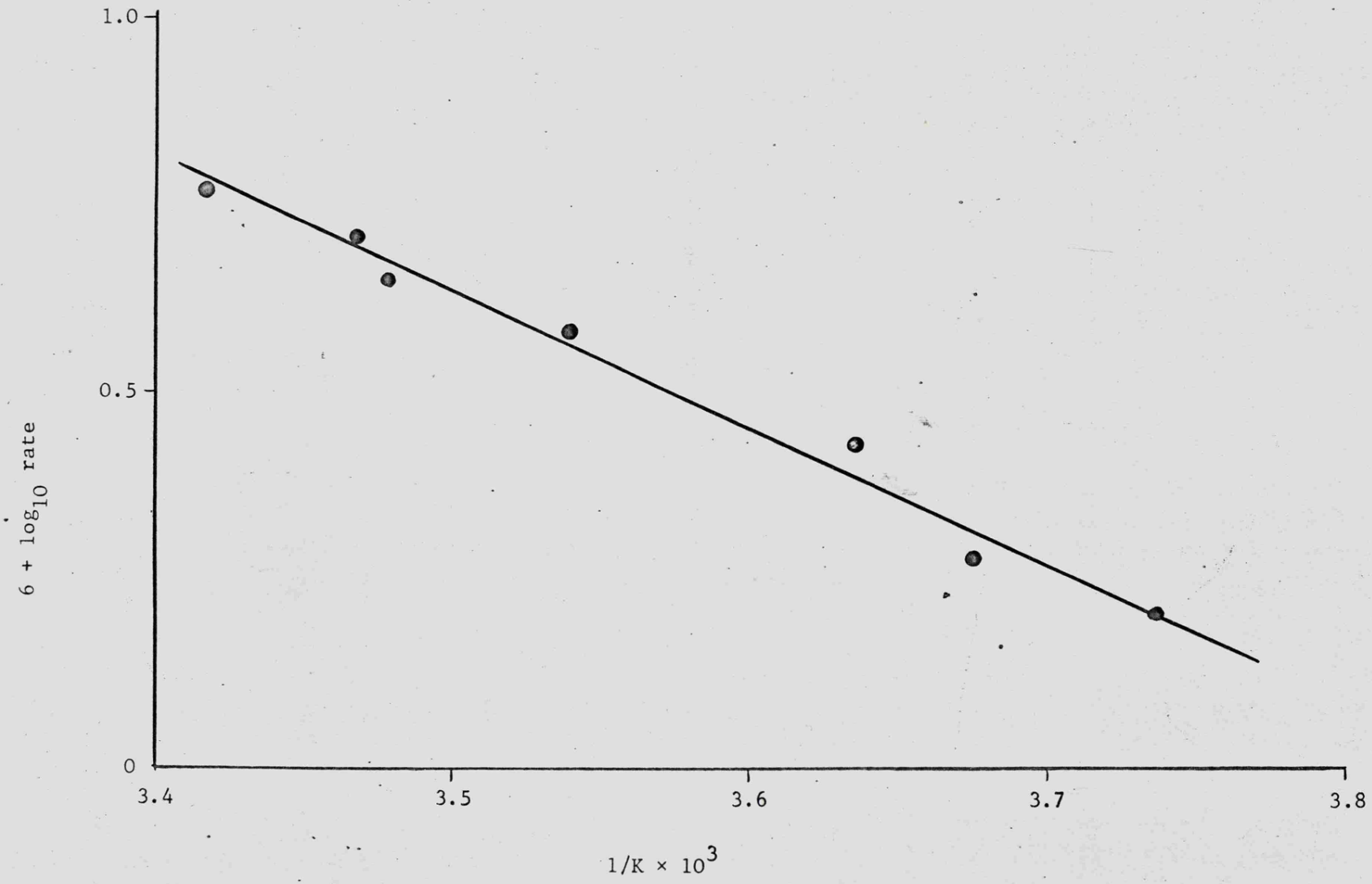

Fig. 6.8 Arrhenius plot for the decomposition of 1.75 mole dm^{-3} hydrazine on the iridium catalyst

TABLE 6.10

Variation of the rate of decomposition of 1.75 mole dm^{-3} hydrazine solution with respect to temperature

Temperature °C	Temperature °K	$\frac{1}{K} \times 10^3$	Rate of decomposition $-\frac{d[N_2H_4]}{dt}$ mole gm^{-1} sec^{-1} $\times 10^6$	$k \times 10^6$ dm^{-3} gm^{-1} sec^{-1}	$6 + \log_{10} k$
20.4	293.6	3.420	10.3	5.86	0.768
16.6	289.8	3.470	8.91	5.09	0.707
13.8	287.0	3.484	7.68	4.39	0.643
9.8	283.0	3.534	6.84	3.91	0.592
3.5	276.8	3.634	4.94	2.82	0.450
0.3	273.5	3.670	3.54	2.02	0.305
-4.7	268.5	3.739	2.77	1.58	0.198

2. The effect of metal content on the rate of decomposition of hydrazine.

A series of supported iridium catalysts prepared by Engelhard Industries were tested to determine the variation of the rate of decomposition of 31.0 mole dm^{-3} hydrazine solution at 15°C with respect to iridium concentration. The results are given in Table 6.11.

TABLE 6.11

Variation of the rate of decomposition of 31.0 mole dm^{-3} hydrazine solution at 15°C with respect to percentage metal loading on the catalyst

Percentage iridium w/w	Rate of decomposition $-\frac{d[N_2H_4]}{dt}$ mole gm^{-1} sec^{-1} $\times 10^5$
5	31.1
10	85.0
15	86.0
20	172.0
25	179.0
25 (Note 1)	201.0
30	191.0
33 (Shell 405)	157.0
35	172.0
40	186.0

Note 1 This batch of catalysts was prepared at the Atomic Energy Research Establishment, Harwell by the co-precipitation of an iridium salt and aluminium hydroxide. The mixture was then dried, pelleted and the iridium salt reduced to the metal. This was the only sample produced by this technique.

3. The effect of the iridium:oxygen atomic ratio on the rate of decomposition of hydrazine.

The variation of the rate of decomposition of hydrazine with respect to iridium:oxygen ratio was studied using samples of Shell 405 catalyst which had been over-oxidised under carefully controlled conditions. To prepare the sample of catalyst with an iridium to oxygen ratio of 1:0.6 the catalyst was heated to 200°C in an atmosphere of 10% oxygen and 90% nitrogen, the 1:0.8 ratio catalyst was prepared by heating to 300°C in 15% oxygen and 85% nitrogen and the 1:1.0 ratio sample was prepared by heating at 500°C in air.

The variation of the rate of decomposition of hydrazine with respect to hydrazine concentration as a function of the iridium to oxygen ratio is shown in Tables 6.12 and 6.13. The data in Table 6.12 was obtained using flow meters to measure the rate of gas evolution while the data in Table 6.13 was obtained using gas burettes to determine the rate of gas production. The results are also shown in Fig. 6.9 and 6.10 respectively.

TABLE 6.12

Variation of the rate of d ecomposition of hydrazine at 15°C with respect to hydrazine concentration as a function of the iridium to oxygen ratio

Hydrazine concentration mole dm^{-3} / Rate of decomposition $-\frac{d[N_2H_4]}{dt}$ mole gm^{-1} $sec^{-1} \times 10^5$	Ir:O 1:0.4	Ir:O 1:0.6	Ir:O 1:0.8	Ir:O 1:1.0
6.3	14.8			
9.9	35.9			
12.6	52.1			
14.1	-	9.5		
15.8	67.0	20.1		
18.8	-	38.1		
21.8	-	53.2		
23.0	-	60.0	8.0	
24.9	120.0	70.2	22.0	
28.1	-	88.5	43.0	
29.1	142.0	-	-	
29.8	-	98.0	52.5	
31.0	157.0	104.0	60.0	9.2

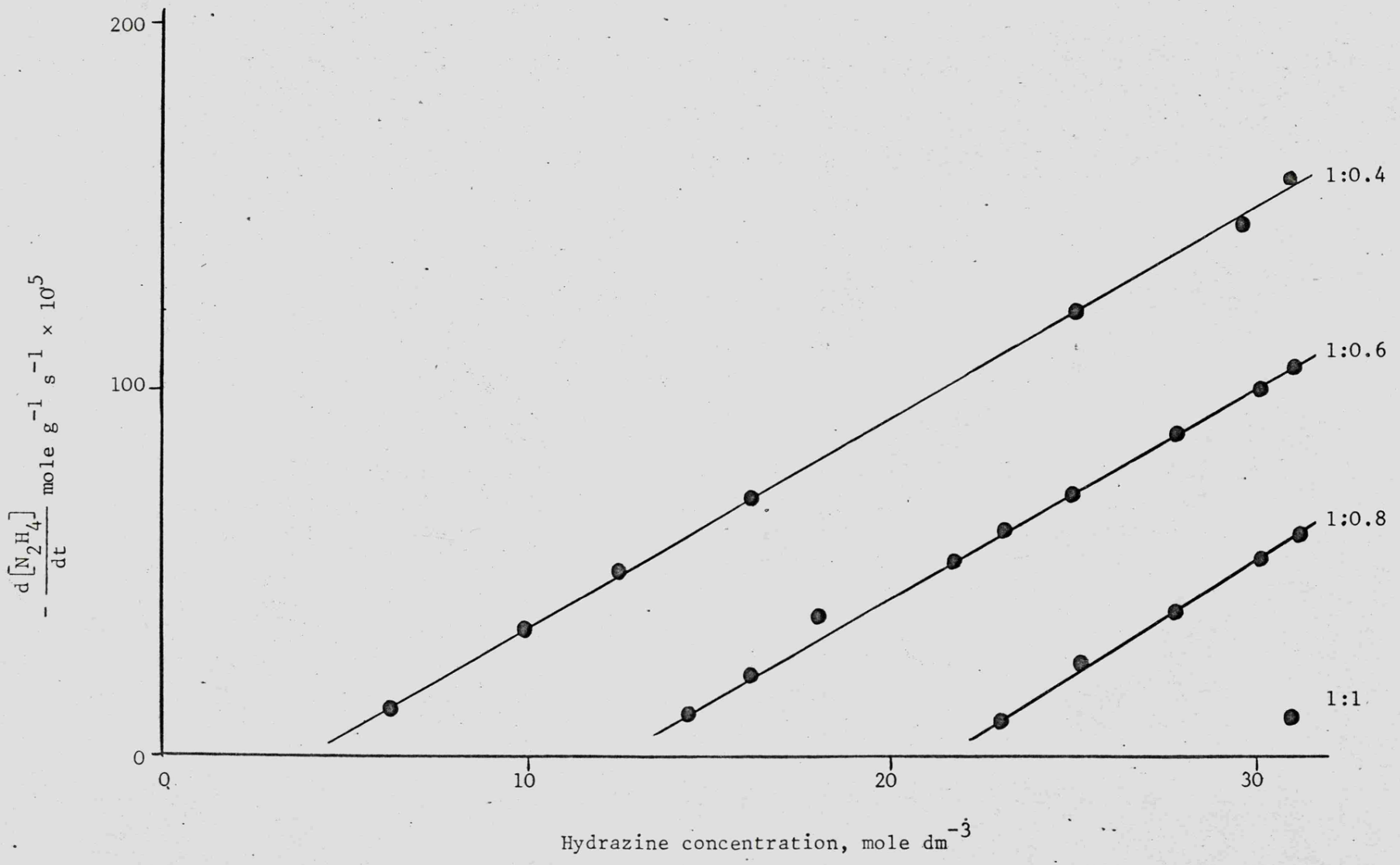

Fig. 6.9 Rate of decomposition of hydrazine as a function of iridium to oxygen ratio

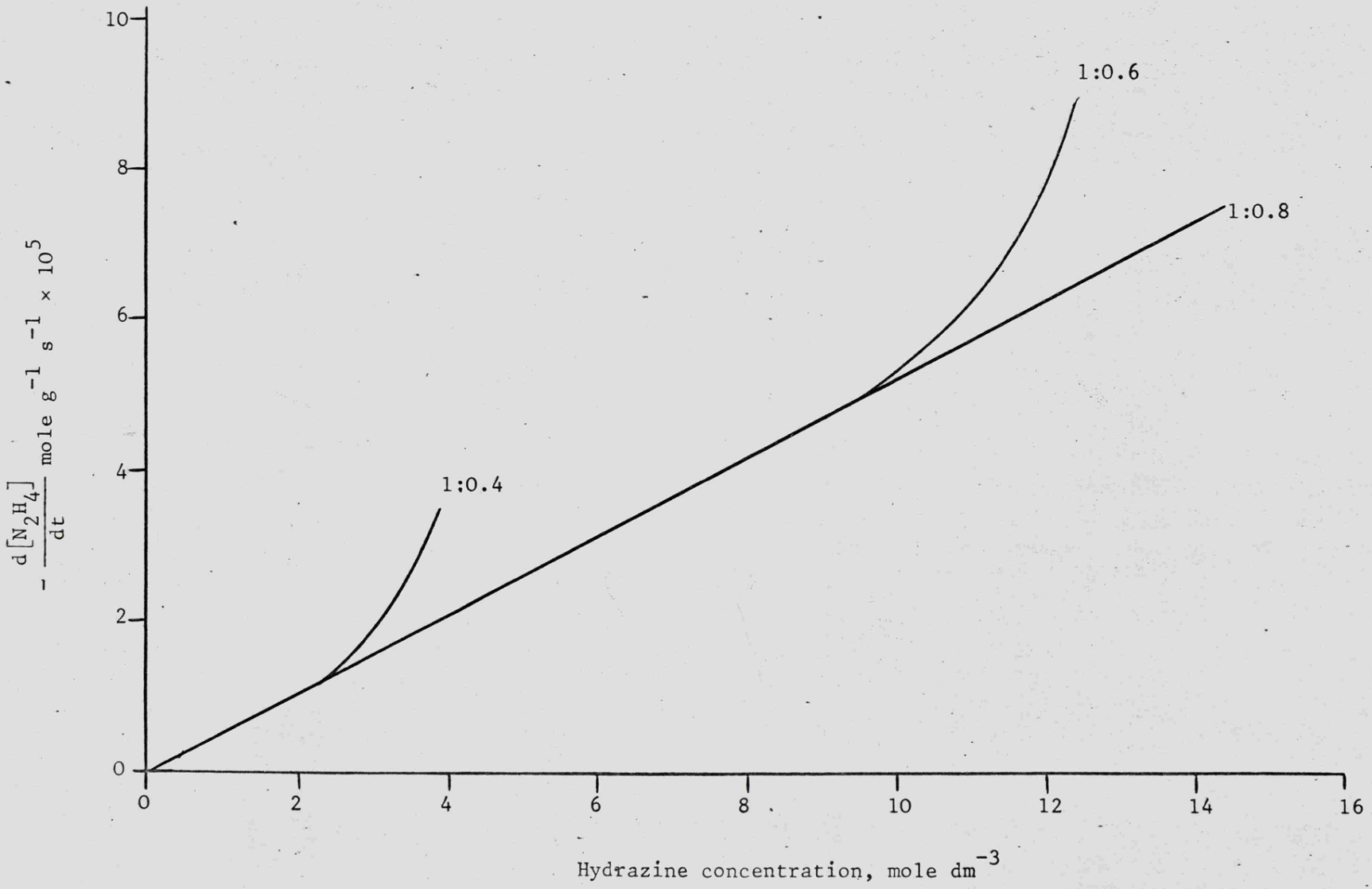

Fig. 6.10 The rate of hydrazine decomposition as a function of iridium to oxygen ratio

TABLE 6.13

Variation of the rate of decomposition of hydrazine with respect to hydrazine concentration as a function of the iridium to oxygen atomic ratio

Hydrazine concentration mole dm^{-3} / Rate of decomposition $-\frac{d[N_2H_4]}{dt}$ mole gm^{-1} $sec^{-1} \times 10^5$	Ir:O 1:0.4	Ir:O 1:0.6	Ir:O 1:0.8	Ir:O 1:1.0
0.63	0.36	0.38	0.33	
1.56	0.86	0.93	0.82	
1.77	0.98	1.00	0.93	
2.28	1.29	1.21	1.14	
3.06	1.89	1.57	1.68	
3.56	2.82	1.86	1.71	
4.38	-	2.00	2.29	
5.38		2.86	2.71	
6.25		3.43	3.36	
7.81		4.07	4.21	
9.38		5.07	5.00	
11.0		6.43	5.71	
12.5		>10	6.57	

Samples of Shell 405 catalyst were also prepared in the fully reduced state but attempts to measure the rate of decomposition of hydrazine on these samples were unsuccessful. When samples of reduced catalyst were kept in a glove box under an inert atmosphere prior to use, the observed rate was identical to that obtained using the standard catalyst under similar conditions. When samples of reduced catalyst were prepared immediately prior to use and maintained under hydrogen then the resulting rate of decomposition was very low, and some pellets appeared to be totally inactive.

4. The effect of solvent composition on the rate of decomposition of hydrazine.

A series of experiments were carried out in which methanol and ethanol were used as diluents in place of water to prepare solutions of hydrazine.

The effect of using these diluents on the rate of decomposition of hydrazine is shown in Fig. 6.11 and the results are also presented in Table 6.14. The results obtained using water as the diluent are also given for comparison.

TABLE 6.14

Variation of the rate of decomposition of hydrazine in alcohol solutions at 15°C with respect to hydrazine concentration

Hydrazine concentration mole dm^{-3} / Rate of decomposition $-\frac{d[N_2H_4]}{dt}$ mole gm^{-1} $sec^{-1} \times 10^5$	Water solvent	Methanol solvent	Ethanol solvent
6.3	15.6	-	5.0
7.8	24.2	5.7	14.3
10.9	42.0	25.7	33.6
12.5	51.1	36.2	43.0
15.0	65.4	52.0	58.5
17.2	78.0	66.3	72.0
19.4	90.3	80.6	85.5
21.6	10.30	95.0	99.0
23.4	114.0	107.0	110.0
25.0	122.0	117.0	120.0
27.8	138.0	136.0	137.0
30.8	156.0	-	-

The effect of solvent composition was also studied using a standard hydrazine concentration of 7.8 mole dm^{-3} and varying the mole fraction composition of the diluent. The results are given in Table 6.15 for the effect of varying the ethanol/water ratio in the solution and the results are also shown in Fig. 6.12.

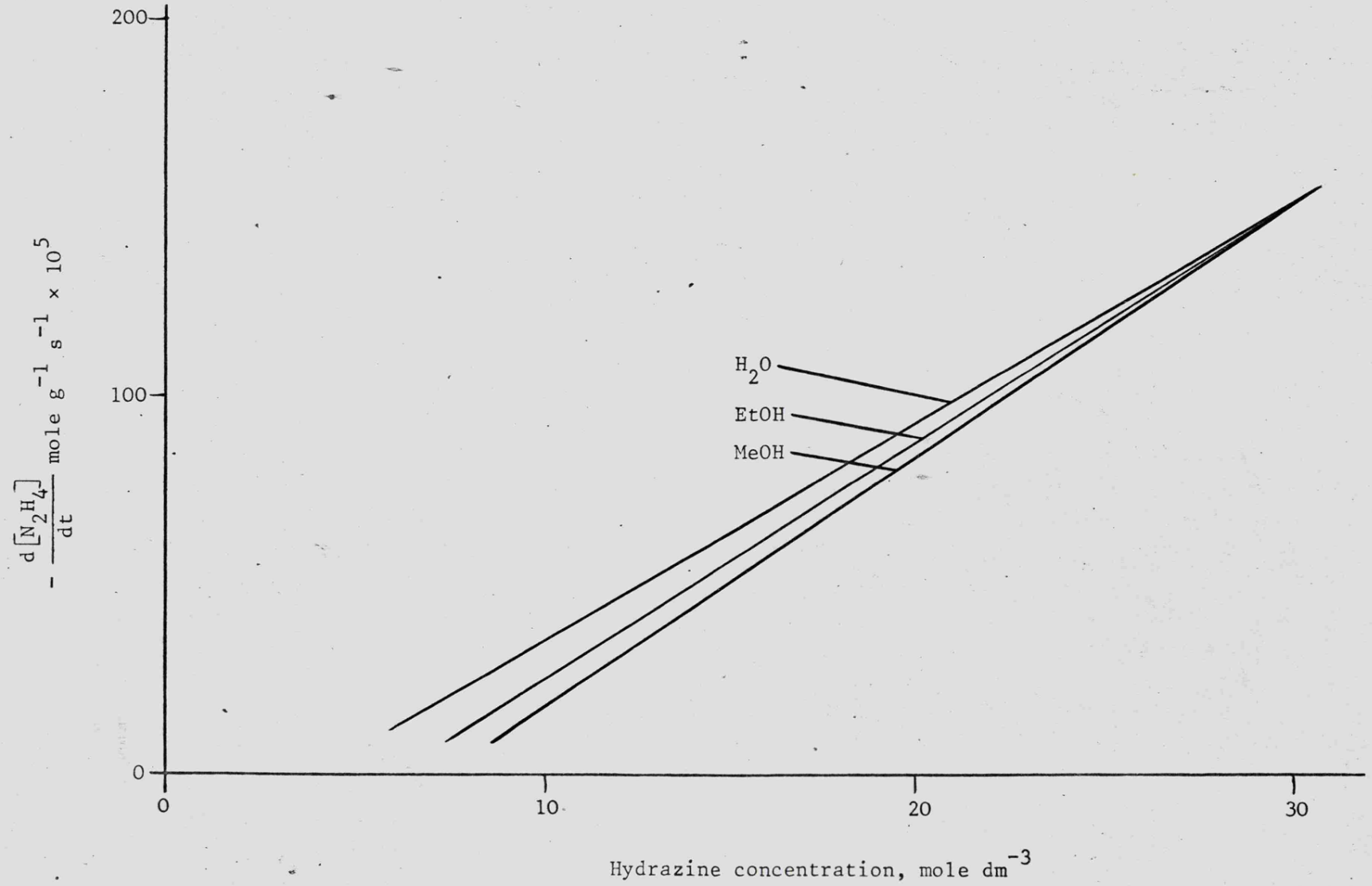

Fig. 6.11 Variation of the rate of decomposition of hydrazine with respect to solvent

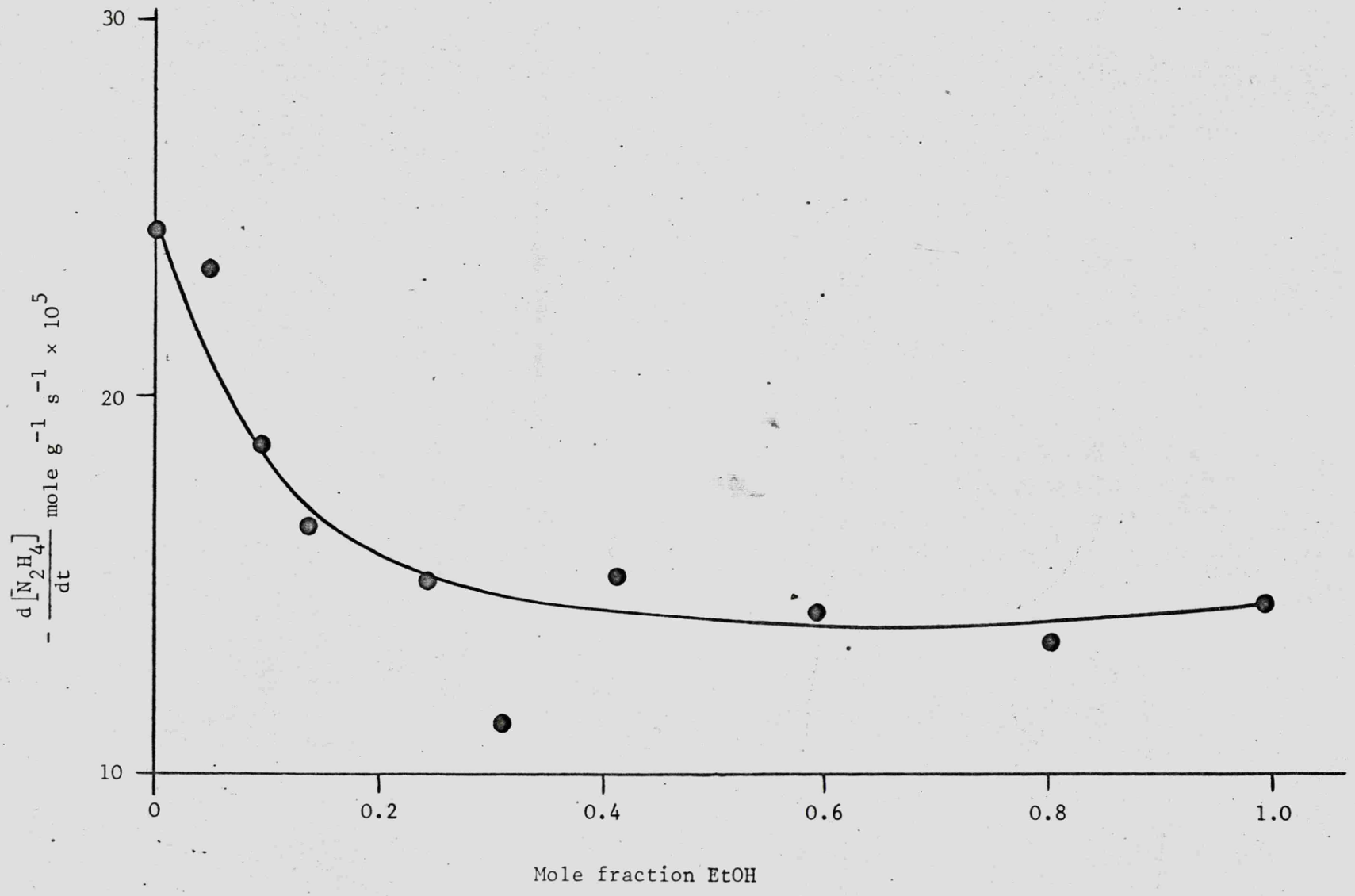

Fig. 6.12 Variation of the rate of decomposition of 7.8 mole dm^{-3} hydrazine with respect to solvent composition

TABLE 6.15

Variation of the rate of decomposition of 7.8 mole dm^{-3} hydrazine solution at 15°C with respect to solvent composition

Composition of ethanol-water solvent		Rate of decomposition $-\frac{d[N_2H_4]}{dt}$ mole gm^{-1} sec^{-1} × 10^5
% w/w ethanol	Mole fraction ethanol	
0	0	24.2
10.5	0.045	23.0
21.7	0.097	19.1
28.4	0.134	17.1
47.1	0.258	15.5
54.3	0.316	11.0
64.8	0.419	15.5
79.3	0.601	14.1
90.9	0.793	13.4
100	1.0	14.3

6.1.4 The induction period of the decomposition of hydrazine on the Shell 405 catalyst

The initial series of tests was to measure the induction period of the decomposition of hydrazine on various samples of Shell 405 catalyst and to study the effect of pre-treatment of the catalyst. The results are presented in Table 6.16. Sample A, which had previously been used in laboratory experiments, gave a longer induction period than either samples B or C. The remainder of the tests were carried out using sample B as sample C was only available at the end of the programme to provide a comparison to the other samples.

The variation of the induction period of the decomposition of 30.8 mole dm^{-3} hydrazine on the Shell 405 catalyst with respect to temperature was studied using sample B and the results are presented in Table 6.17.

TABLE 6.16

The induction period of the decomposition of hydrazine on three samples of the Shell 405 catalyst

Catalyst sample	Previous history and pre-treatment	Induction period milliseconds
A	Previously used in laboratory, no pre-treatment	137 ± 92
A	Pumped at 1 mm Hg at 25°C	411 ± 190
A	Pumped at 1 mm Hg at 160°C	1000 ± 700
A	Pumped at 10^{-4} mm Hg at 580°C	40.7 ± 26.6
B	Uncertain history, no pre-treatment	14.6 ± 4.4
B	Pumped at 10^{-4} mm Hg at 580°C	14.7 ± 3.9
C	New sample, no pre-treatment	14.8 ± 4.1
C	Pumped at 10^{-4} mm Hg at 580°C	15.2 ± 4.2

TABLE 6.17

Variation of the induction period and the rate of decomposition of 30.8 mole dm^{-3} hydrazine solution on the Shell 405 catalyst

Temperature °C	Temperature °K	$\frac{1}{K} \times 10^3$	Induction period milliseconds	Rate of decomposition $-\frac{d[N_2H_4]}{dt}$ mole gm^{-1} sec^{-1} $\times 10^5$	$5 + \log_{10}$ rate
2.0	275.2	3.636	99.6	88	1.944
8.0	281.2	3.559	46.4	89	1.949
15.0	288.2	3.472	21.2	97	1.987
20.0	293.2	3.413	22.9	117	2.068
23.0	296.2	3.378	14.6	119	2.076
30.0	303.2	3.300	13.2	124	2.093
37.0	310.2	3.226	9.5	165	2.217

An Arrhenius plot of the temperature vairation of the rate of decomposition of hydrazine on the Shell 405 catalyst is shown in Fig. 6.13 and an activation energy of 12.66 ± 1.08 kJ $mole^{-1}$ was calculated from the data.

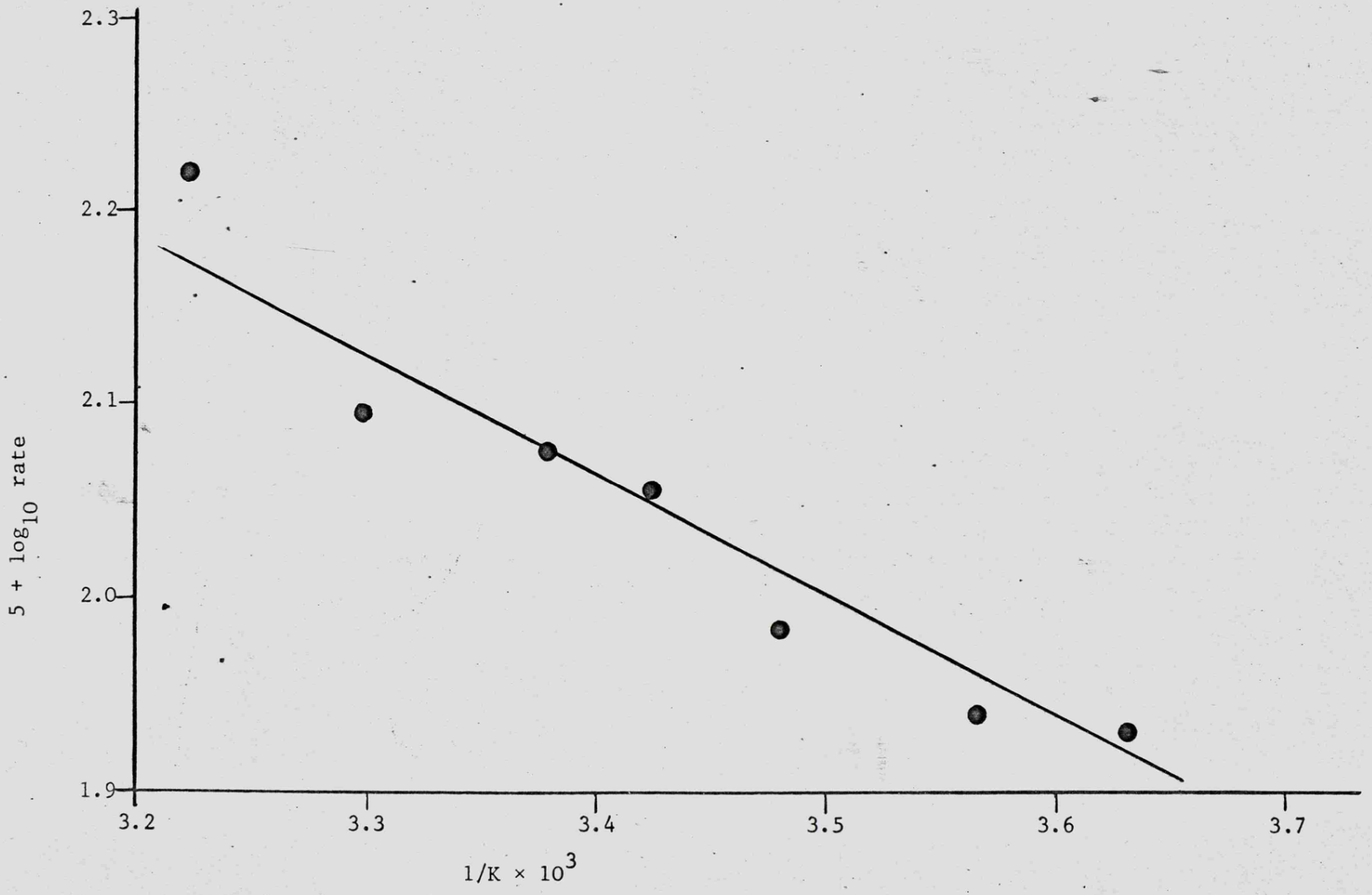

Fig. 6.13 Arrhenius plot for the decomposition of 30.8 mole dm^{-3} hydrazine

6.1.5 Search for free radicals in solution

The electron spin resonance spectrometer was used to scan the hydrazine solution immediately after contact with a sample of Shell 405 catalyst in a flow system to detect and identify any radicals present in the solution. Comparing the spectrum obtained from the flow system to the blank spectrum obtained from the same cell filled with hydrazine showed no difference between the two systems. Therefore either no free radicals are produced as intermediates in the decomposition reaction or if radicals are produced and liberated into solution, the life-times of the radicals were too short to allow detection in the scanned cell of the esr spectrometer. Under the conditions of the experiments the flow rate of hydrazine was such that the time interval between passing the catalyst and actually reaching the scanned part of the cell was of the order of 10 milliseconds.

The results of the thin layer chromatography analysis was that no cyclohexane-1,2-dicarboxylic acid could be detected, only the starting material 4-cyclohexene-1,2-dicarboxylic acid was found. This result indicates that no diimide, which hydrogenates the unsaturated to the saturated acid, was present in the hydrazine solution during the reaction sequence.

Both these results indicate the absence of radicals in the hydrazine solution but do not rule out the possibility of radicals being formed and remaining on the catalyst surface.

6.2 Discussion

6.2.1 Reaction stoichiometry

Throughout the hydrazine concentration range of 1 to 31 mole dm^{-3} and under all the experimental conditions which were studied the permanent gas was observed to consist of at least 99% nitrogen and for each mole of hydrazine decomposed 1.33 mole of ammonia were formed. The consistency of these results show that the decomposition of hydrazine on the supported iridium catalyst follows reaction (2):

$$3N_2H_4 \rightarrow N_2 + 4NH_3 \qquad (2)$$

The use of ^{15}N as a tracer has shown that the nitrogen molecule is formed from the two nitrogen atoms of one hydrazine molecule without N-N bond fission.

6.2.2 Kinetics and mechanism

The variation of the rate of decomposition of hydrazine on the supported iridium catalyst with respect to hydrazine concentration may be divided into "low rate" and "high rate" regions. The low rate reaction is characterised by an activation energy of 35.1 ± 2.4 kJ $mole^{-1}$ and obeys first order kinetics over a limited range of hydrazine concentration. The limit of the first order kinetics is dependent upon the atomic ratio of iridium to oxygen for the catalyst (see Fig. 6.9 and 6.10) such that an increase in oxygen content results in the observation of first order kinetics over a wider range of hydrazine concentration.

Above a certain hydrazine concentration there is a marked increase in the rate of decomposition of hydrazine into a high rate region. This high rate reaction has an activation energy of 65.4 ± 0.2 kJ $mole^{-1}$ and the rate of decomposition is some linear function of hydrazine concentration. The high rate reaction cannot be classified as true first order as the rate is not directly proportional to the hydrazine concentration in the bulk solution i.e. doubling the hydrazine concentration does not double the rate of decomposition. A first order reaction may be expressed in the form of a rate equation

$$R = k\,c$$

where R is the rate of reaction, k the rate constant and c is the concentration. In Fig. 6.6 it may be seen that the rate/concentration graph extrapolates to zero rate at a definite concentration which is independent of temperature. Modifying the first order rate equation to take account of this observation results in the expression:

$$R = k (c_b - c_o)$$

where c_b is the bulk concentration of hydrazine and c_o is that concentration, obtained by extrapolation, for which the value of R is zero.

The value of c_o is dependent on the atomic ratio of iridium to oxygen on the catalyst such that increasing the oxygen content results in an increase in the value of c_o. It would appear that the low rate reaction is occurring on sites of high oxidation state, say type 1, and these are also of low activation energy and hence preferrentially covered. As the hydrazine concentration increases so the fraction of the sites of type 1 covered by adsorbed species increases until at c_o all these sites are covered. Further increase in the hydrazine concentration results in the adsorption of hydrazine on sites of low oxidation state, type 2, and the occurrence of the high rate reaction with its high activation energy. It is only when the type 1 sites of low energy have been saturated that adsorption occurs on the high energy sites of type 2 and the kinetics indicate that the concentration of reacting species for the high rate reaction is proportional to the bulk concentration less the concentration required to saturate the type 1 sites. However one additional observation which also requires explanation is that the rate of decomposition in the low rate reaction region is uneffected by an increase in oxygen content for a given hydrazine concentration (see Fig. 6.10).

Characterisation of the Shell 405 catalyst has shown that the normal catalyst, which has an iridium to oxygen atomic ratio of 1:0.4, has an excess of oxygen atoms over that number required to give a monolayer coverage of the surface iridium atoms. The excess oxygen atoms may be associated with the surface iridium atoms or with the bulk metal. Carlson et al[62] suggest that temperatures in excess of 300°C are required before the bulk iridium atoms are oxidised, however the temperature of the catalyst surface during the re-oxidation stage is unknown and as the process is strongly exothermic there

remains the possibility of oxidation of the bulk metal. In the case of the catalyst sample of iridium to oxygen ratio of 1:0.8 prepared at 500°C then oxidation of the bulk metal has almost certainly occurred.

No firm conclusion may be arrived at concerning the occurrence of the low and high rate reactions but taking into account the experimental observations and the results of the characterisation of the catalyst, the following is tentatively proposed as an explanation. The low rate reaction 1 occurs on the oxide sites of type 1 which may be formed by the adsorption of one oxygen atom on each exposed iridium atom. The adsorption of hydrazine on these sites occurs preferrentially due to the low activation energy and only when these sites are saturated does adsorption occur on the sites of type 2. Adsorption of hydrazine on these sites is accompanied by a high activation energy hence the adsorption process is energetically less favourable. Increasing the oxygen content does not effect the surface oxide layer but results in the oxidation of the iridium atoms in the layers below the surface. The adsorption of hydrazine on these sites is energetically less favoured than on the surface oxide sites and consequently reaction only occurs on these sites after the readily available sites have been saturated and hence the rate of reaction 1 for a given hydrazine concentration appears to be independent of oxygen content. However these additional oxide sites are energetically favoured compared to sites of type 2 and therefore the onset of reaction on type 2 sites occurs at increasing hydrazine concentrations as more hydrazine is required to saturate the increased number of type 1 sites.

This tentative proposal has only been put forward in an effort to account for the observed kinetics. Any mechanism put forward to account for the two reactions must explain the following observations:-

(1) The reaction stoichiometry, for both regions, is:-

$$3N_2H_4 \longrightarrow N_2 + 4NH_3 \quad .$$

(2) In each case the nitrogen molecule is formed from the two nitrogen atoms of one hydrazine molecule without N-N bond fission.

(3) The low rate reaction is first order chemically controlled; the high rate reaction is also chemically controlled but the rate is proportional to the bulk concentration less some concentration of hydrazine which is a function of the iridium to oxygen atomic ratio of the catalyst. It is postulated that in both regions the same mechanism applies and the differences in rate of reaction and activation energy arise from the nature of the site on which the reaction occurs. The overall reaction mechanism consists of the associative adsorption of hydrazine molecules to form an activated complex which then breaksdown to yield nitrogen and ammonia. It is not considered feasible to define the rate controlling step which may be an adsorption step or reaction between adsorbed molecules and a single molecule from solution.

6.2.3 The effect of metal loading on the catalytic activity

The results of the variation of the rate of decomposition of 31.0 mole dm^{-3} hydrazine solution at 15°C with respect to metal loading on the catalyst are shown in Table 6.11. The results show the usual trend of increasing catalytic activity with respect to metal loading as the available metal surface area increases. As progressively more metal is loaded on the support the available metal surface area levels out and becomes invariant with respect to metal loading and the same trend is noted for the catalytic activity. Compared to the samples of catalyst containing 30% to 35% iridium prepared at Engelhard Industries the activity of the Shell 405 catalyst is considerably lower. Surface area determinations at Warren Spring Laboratory have shown that the metal surface area of the Shell 405 catalyst is approximately double the metal surface area of the sampler prepared at Engelhard Industries, actual values of 19.6 and 9.4 $m^2 g^{-1}$ respectively. Therefore for this particular reaction, which is an extremely vigorous liquid phase reaction, the nature of the support and the ease with which the liquid can contact the

metal are as important, or more so, than the metal surface area as determined by hydrogen chemisorption.

6.2.4 The induction period of the decomposition of hydrazine on the Shell 405 catalyst

The induction period may be defined as the period of time between the hydrazine contacting the catalyst surface and the appearance of the gaseous products. During this period several physical and chemical processes occur, these are:-

(1) Diffusion of the reactant to the metal site.

(2) Adsorption of hydrazine.

(3) Reaction.

(4) Desorption of the products.

(5) Diffusion of the products away from the metal surface.

All these processes are temperature dependent such that the rate of the process increases with increasing temperature. Therefore the time taken for each step to occur, and hence the induction period, will decrease with increasing temperature. The experimental tests showed that the induction period decreased from 100 milliseconds at $2^{o}C$ to 10 milliseconds at $37^{o}C$.

The variation of the rate of decomposition of hydrazine on the Shell 405 catalyst with respect to temperature was also studied and this produced a value of 12.66 ± 1.08 kJ $mole^{-1}$ for the activation energy of the reaction. An activation energy of this order indicates that the reaction is diffusion controlled whereas under the well-stirred isothermal conditions used to study the kinetics the reaction was chemically controlled with an activation energy of 65.4 ± 0.2 kJ $mole^{-1}$.

CHAPTER SEVEN

THE USE OF A SUPPORTED PLATINUM CATALYST

7.1 Results

7.1.1 Product analysis

The gas chromatograph was used to determine the composition of the permanent gas formed by the decomposition of aqueous hydrazine solutions on the supported platinum catalyst. The variation of the composition of the evolved permanent gas with respect to hydrazine concentration at 25°C is presented in Table 7.1.

TABLE 7.1

Variation of the permanent gas composition with respect to hydrazine concentration

Hydrazine concentration mole dm^{-3}	Permanent gas composition	
	% H_2	% N_2
0.62	8.0	92.0
1.2	16.5	83.5
3.1	31.0	69.0
4.7	39.0	61.0
6.3	44.5	55.5
9.4	50.0	50.0
12.5	51.2	48.8
15.6	50.5	49.5
19.4	48.5	51.5
21.8	50.7	49.3
25.6	49.2	50.8
28.1	48.3	51.7
30.8	51.1	48.9

The percentage of hydrogen in the evolved permanent gas increases with increasing hydrazine concentration.

The effect of temperature on the permanent gas composition was studied using 30.8 mole dm^{-3} hydrazine solution and the results are presented in Table 7.2.

TABLE 7.2

Effect of temperature on the evolved permanent gas composition

Temperature, °C	Permanent gas composition	
	% H_2	% N_2
15.0	48.2	51.8
20.0	50.6	49.4
25.0	51.1	48.9
29.8	50.7	49.3
34.2	49.9	50.1
40.0	51.1	48.9
45.8	53.0	47.0
53.5	49.1	50.9
58.8	47.9	52.1

The relative proportions of hydrogen and nitrogen in the evolved permanent gas are independent of temperature for the decomposition of 30.8 mole dm^{-3} hydrazine solution on the platinum catalyst.

The effect of the pre-adsorption of products of the reaction on the surface of the catalyst on the composition of the permanent gas was also studied. The effect of the pre-adsorption of hydrogen at various hydrazine concentrations and temperatures is given in Table 7.3 and similar data for the effect of the pre-adsorption of ammonia is given in Table 7.4.

TABLE 7.3

The effect of the pre-adsorption of hydrogen on the permanent gas composition

Hydrogen pre-adsorbed	Hydrazine concentration mole dm^{-3}	Temperature, °C	Permanent gas composition	
			% H_2	% N_2
No	1.2	10	11.3	88.7
Yes	1.2	10	48.2	51.8
No	1.2	25	16.5	83.5
Yes	1.2	25	50.7	49.3
No	1.2	40	17.0	83.0
Yes	1.2	40	50.1	49.9
No	4.7	25	39.0	61.0
Yes	4.7	25	49.1	50.9
No	25.6	25	49.2	50.8
Yes	25.6	25	51.3	48.7

TABLE 7.4

The effect of the pre-adsorption of ammonia on the permanent gas composition

Ammonia pre-adsorbed	Hydrazine concentration mole dm^{-3}	Temperature, ^{o}C	Permanent gas composition	
			% H_2	% N_2
No	1.2	10	11.3	88.7
Yes	1.2	10	51.3	48.7
No	1.2	25	16.5	83.5
Yes	1.2	25	52.4	47.6
No	1.2	40	17.0	83.0
Yes	1.2	40	47.1	52.9
No	4.7	25	39.0	61.0
Yes	4.7	25	47.9	52.1
No	25.6	25	49.2	50.8
Yes	25.6	25	49.1	50.9

These results show that compared to the standard catalyst the effect of the pre-adsorption of both ammonia and hydrogen is to increase the percentage of hydrogen in the permanent gas to a limiting value of approximately 50%.

It was also observed that the composition of the evolved permanent gas changed with respect to time of reaction. For all the concentrations of hydrazine the limiting composition of the permanent gas was approximately equimolar quantities of nitrogen and hydrogen.

Titrimetric analysis was used to determine the ratio of the number of moles of ammonia formed by the decomposition of one mole of hydrazine. The results for the analysis carried out for the decomposition of 9.4 mole dm^{-3} hydrazine solution on the supported platinum catalyst are presented in Table 7.5.

TABLE 7.5

Determination of the conversion of hydrazine to ammonia

Moles of hydrazine			Total moles of alkali[4]	Moles of ammonia formed[5]	N_2H_4:NH_3 ratio
Start[1]	Finish[2]	Decomposed[3]			
0.0347	0.0217	0.0130	0.0345	0.0128	0.97
0.0347	0.0061	0.0286	0.0347	0.0286	1.00
0.0347	0.0113	0.0234	0.0343	0.0230	0.98
0.0347	0.0101	0.0246	0.0332	0.0231	0.94

Notes

1. Starting number of moles of hydrazine determined by Andrews titration.
2. Final number of moles of hydrazine determined by Andrews titration.
3. Given by (1-2).
4. Total alkali (ammonia + hydrazine) after reaction determined by acid titration.
5. Given by (4-2).

These results show that the decomposition of one mole of hydrazine is accompanied by the formation of 0.97 mole of ammonia.

7.1.2 Results of the kinetic experiments

The variation of the overall rate of decomposition of hydrazine at 25°C on the supported platinum catalyst with respect to hydrazine concentration is presented in Table 7.6. The results are also presented in Fig. 7.1 where it can be seen that the overall rate of decomposition is a curved function of the hydrazine concentration.

The variation of the overall rate of decomposition of 30.8 mole dm^{-3} hydrazine solution on the supported platinum catalyst with respect to temperature is given in Table 7.8. The results are also presented in Fig. 7.2 in the form of an Arrhenius plot.

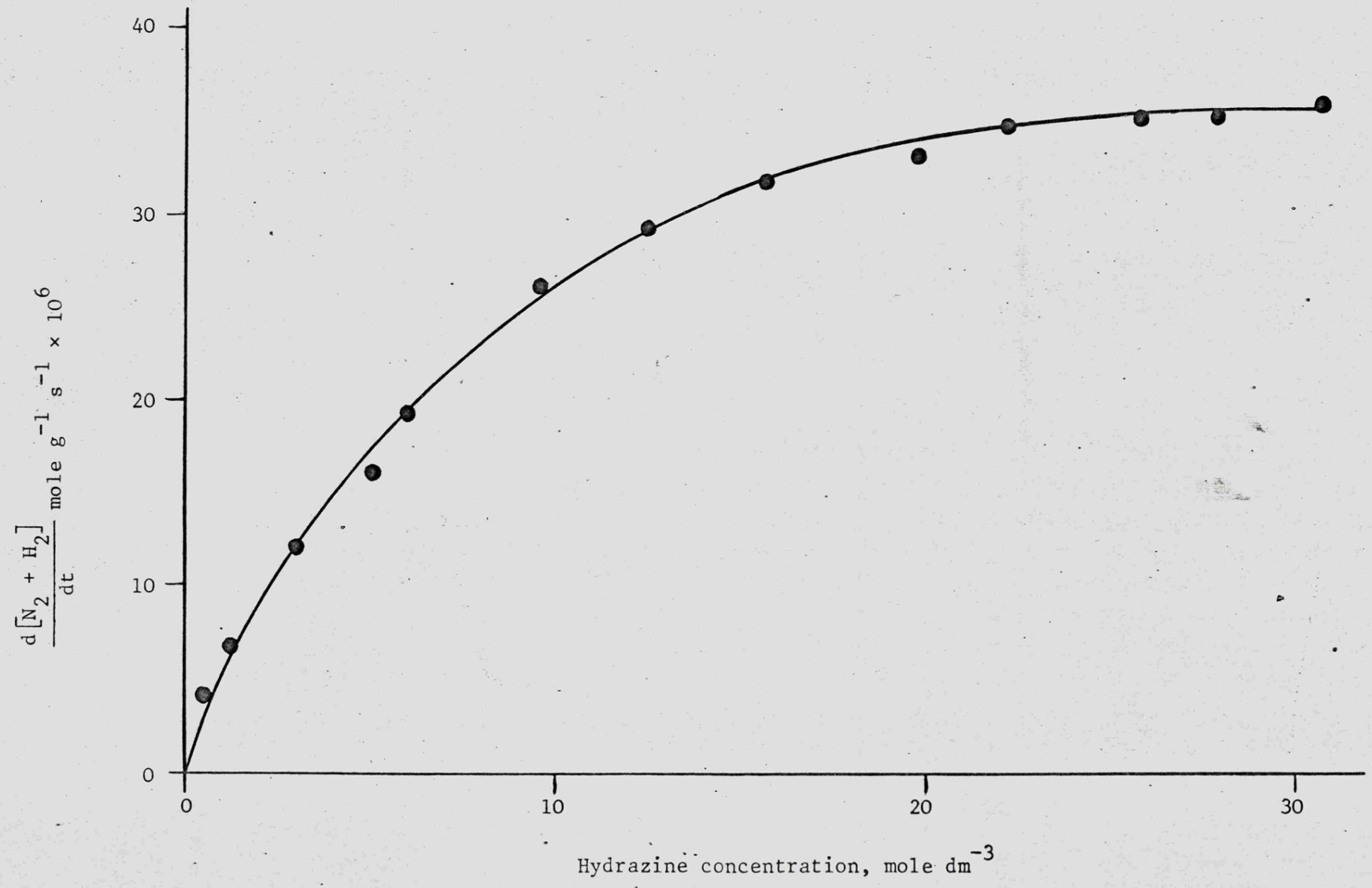

Fig. 7.1 Overall rate of decomposition of hydrazine on the platinum catalyst

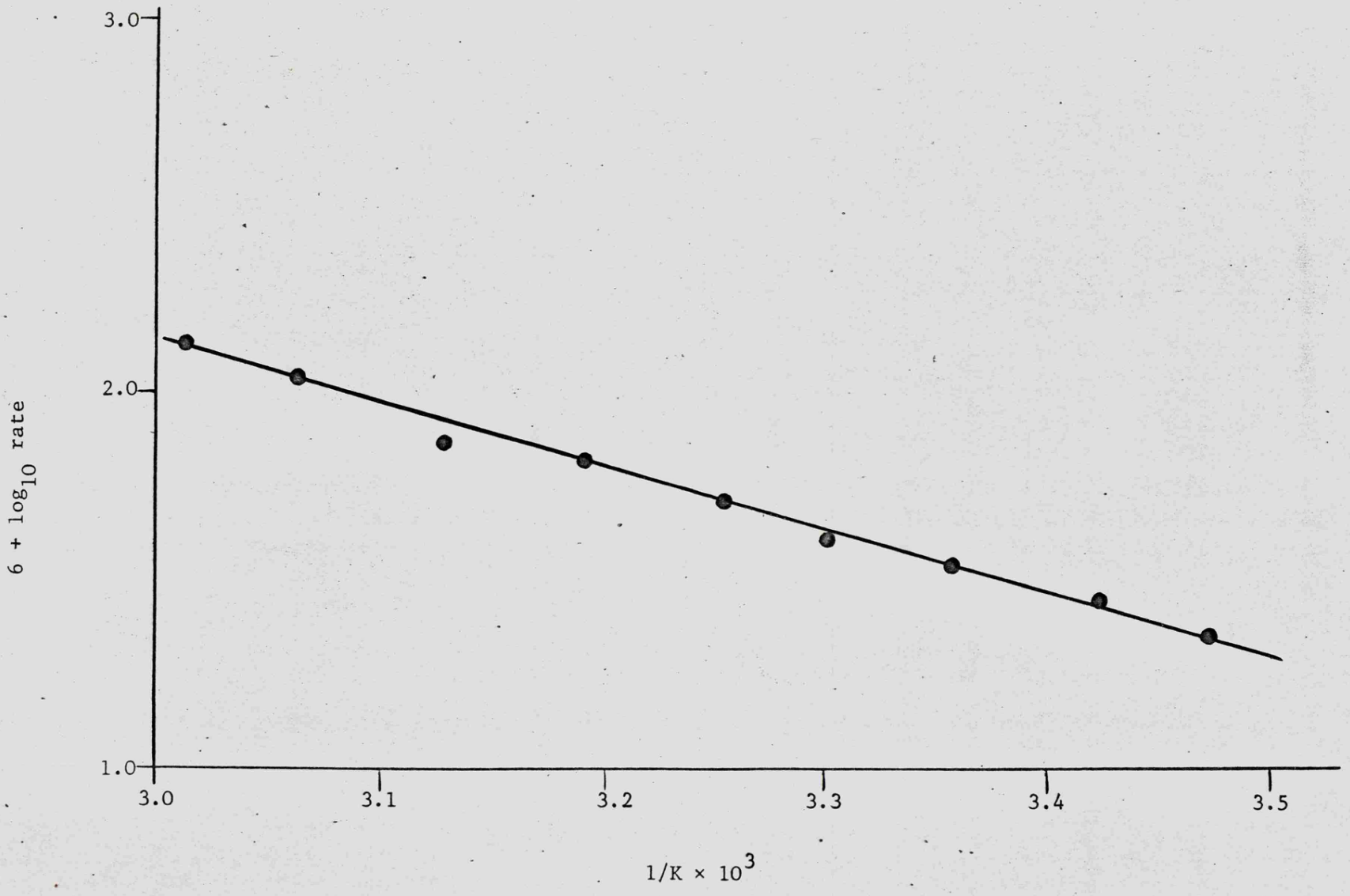

Fig. 7.2 Arrhenius plot for the decomposition of 30.8 mole dm^{-3} hydrazine on the platinum catalyst

TABLE 7.6

Variation of the overall rate of decomposition of hydrazine at 25°C on the supported platinum catalyst with respect to hydrazine concentration

Hydrazine concentration mole dm^{-3}	Overall rate of decomposition $\frac{d[N_2 + H_2]}{dt}$ mole $gm^{-1}\ sec^{-1} \times 10^6$
0.62	4.38
1.2	6.59
3.1	11.9
4.7	16.1
6.3	19.3
9.4	26.0
12.5	29.7
15.6	31.3
19.4	33.0
21.8	34.5
25.6	35.0
28.1	34.8
30.8	36.4

TABLE 7.7

Variation of the overall rate of decomposition of 30.8 mole dm^{-3} hydrazine solution on the supported platinum catalyst with respect to temperature

Temperature, °C	Temperature, °K	$\frac{1}{K} \times 10^3$	Overall rate of decomposition $\frac{d[N_2 + H_2]}{dt}$ mole $gm^{-1}\ sec^{-1} \times 10^6$	$6 + \log_{10}$ rate
15.0	288.2	3.470	23.0	1.362
20.0	293.2	3.411	29.0	1.462
25.0	298.2	3.353	35.5	1.550
29.8	303.0	3.300	41.5	1.618
34.2	307.4	3.253	54.0	1.732
40.0	313.2	3.193	63.1	1.800
45.8	319.0	3.135	79.5	1.900
53.5	326.7	3.061	110.0	2.041
58.8	332.0	3.012	132.0	2.121

The effects of pre-adsorbing the products of the reaction on the catalyst on the rate of decomposition were also studied but the results were not reproducible and only qualitative results could be obtained. The effect of the pre-adosrption of hydrogen on the catalyst was to reduce the rate of decomposition to less than 30% of the decomposition rate observed using the standard catalyst. The effect of the pre-adsorption of ammonia on the catalyst was to strongly, and in some cases totally, inhibit the decomposition of hydrazine. However this was only a temporary effect as after a short time interval the rate of reaction began to increase and ultimately the rate of decomposition of hydrazine on the ammonia pre-treated catalyst was similar to the limiting rate observed with the standard catalyst under identical conditions.

7.2 Discussion

In the discussion of the decomposition of hydrazine on a supported palladium catalyst it was postulated that variation of the permanent gas composition was a result of some of the hydrogen formed by the reaction being adsorbed on the catalyst. The results were analysed in terms of the occurrence of reaction (6) and the kinetics were found to be one half order. On this basis a reaction mechanism was postulated in which the initial, slow step was the dissociative chemisorption of hydrazine.

The results of the permanent gas analysis of the products of the decomposition of hydrazine on the supported platinum catalyst are qualitatively similar to those obtained using the palladium catalyst. Therefore it is suggested that the decomposition of hydrazine on the supported platinum catalyst also follows reaction (6) and the non stoichiometric composition of the evolved permanent gas is due to the adsorption on the catalyst of some of the hydrogen produced by the reaction. Pre-adsorbing hydrogen or ammonia on the catalyst covers the catalyst surface with adsorbed species resulting in a decrease in the rate of decomposition of hydrazine and the

evolved permanent gas has the true reaction stoichiometry as there are no sites available for the adsorption of hydrogen. The limiting composition of the permanent gas under all experimental conditions is approximately equimolar quantities of hydrogen and nitrogen which is consistent with the occurrence of reaction (6). The conversion of hydrazine to ammonia is on the basis of one to one which also agrees with the occurrence of reaction (6).

The kinetics of the decomposition of hydrazine on the supported platinum catalyst will now be considered. The rate of reaction (6) may be calculated on the basis that it is twice that proportion of the overall rate of decomposition which is due to nitrogen evolution. The calculation of the rate of reaction (6) is presented in Table 7.8 and the results are also shown in Figs. 7.3 and 7.4. In Fig. 7.3 it may be seen that the rate of reaction is a curved function of the hydrazine concentration at low concentrations becoming independent of hydrazine at high concentrations. Plotting the results in log-log form in Fig. 7.4 shows that at low concentrations the order of reaction is one half decreasing to zero order at high concentrations of hydrazine. This change in the kinetics is the same as observed for the decomposition of hydrazine on the supported rhodium catalyst and the rate equations may be derived on the same basis, ie the use of the Langmuir adsorption isotherm assuming the dissociative chemisorption of hydrazine is occurring to give two NH_2 radicals each of which covers one site. On this basis the relevant rate equation is:-

$$R = \frac{k_2 K^{\frac{1}{2}} c^{\frac{1}{2}}}{(1 + K^{\frac{1}{2}} c^{\frac{1}{2}})} .$$

At low concentrations of hydrazine c is small and $K^{\frac{1}{2}} c^{\frac{1}{2}} < 1$ so:-

$$R \approx k_2 K^{\frac{1}{2}} c^{\frac{1}{2}}$$

and the reaction obeys one half order kinetics. At high concentrations of hydrazine c is large and $K^{\frac{1}{2}} c^{\frac{1}{2}} > 1$ so:-

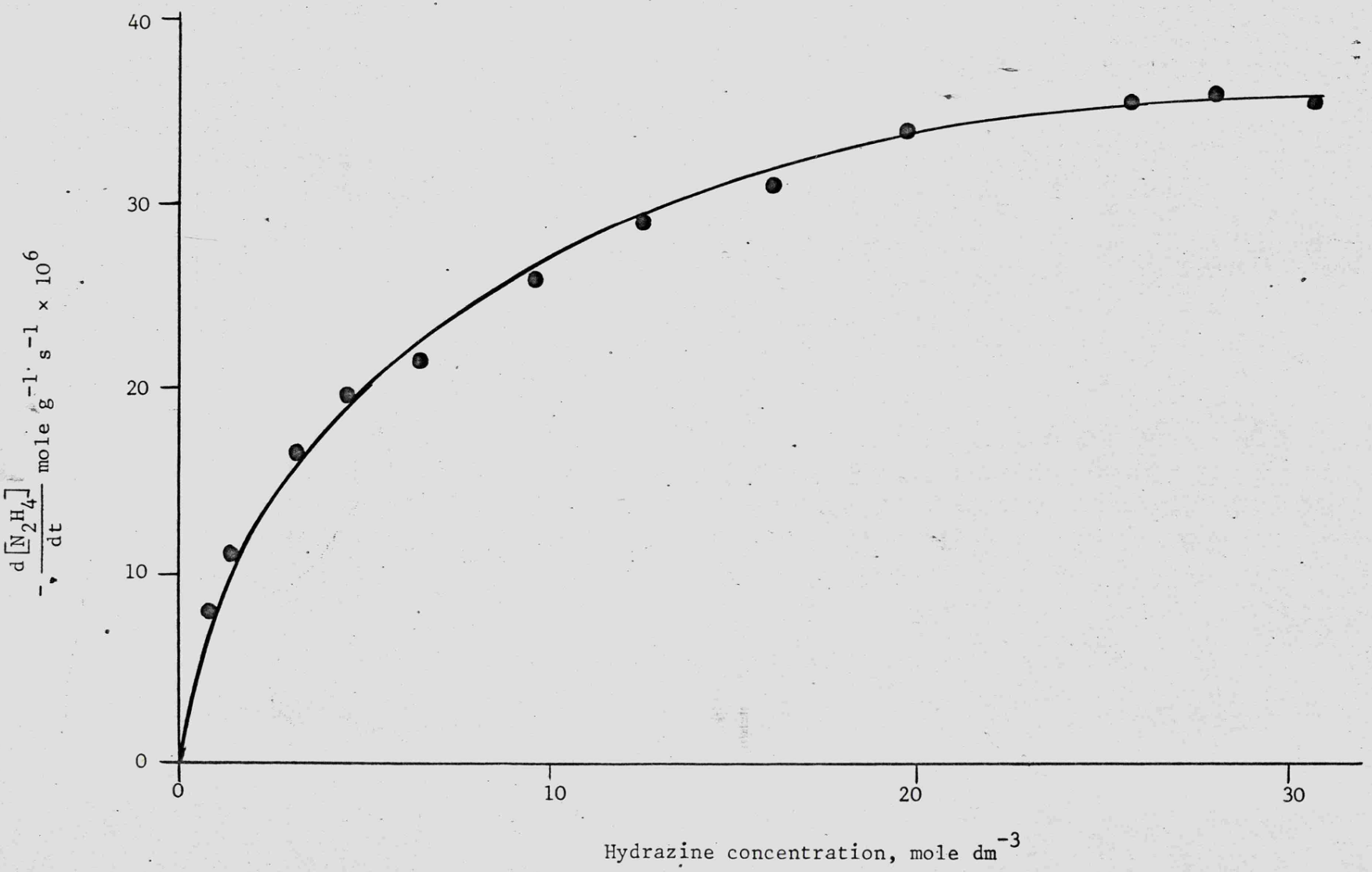

Fig. 7.3 Rate of reaction (6) on the platinum catalyst

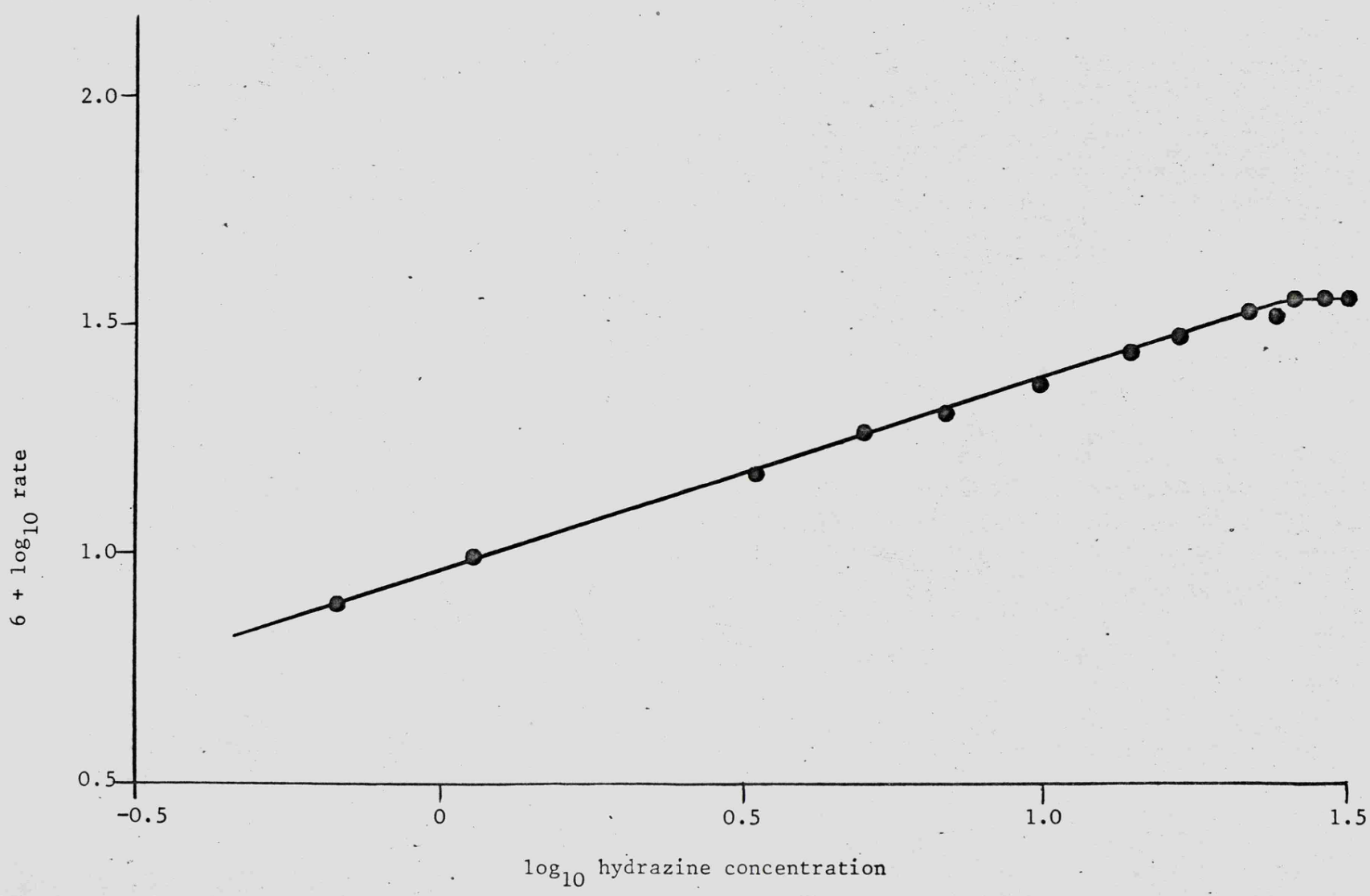

Fig. 7.4 Plot of $\log_{10}$ rate with respect to $\log_{10}$ hydrazine concentration for reaction (6) on the platinum catalyst

TABLE 7.8

Calculation of the rate of reaction (6) for the decomposition of hydrazine on the supported platinum catalyst

Hydrazine concentration mole dm^{-3}	Overall rate of reaction $\frac{d[N_2 + H_4]}{dt}$ mole gm^{-1} sec^{-1} $\times 10^6$	% nitrogen in permanent gas	Rate of nitrogen formation $\frac{d[N_2]}{dt}$ mole gm^{-1} sec^{-1} $\times 10^6$	Rate of reaction (6) $-\frac{d[N_2H_4]}{dt}$ mole gm^{-1} sec^{-1} $\times 10^6$	$\log_{10}$ hydrazine concentration	$\log_{10}$ rate of reaction (6)
0.62	4.38	92.0	4.0	8.1	-0.208	0.906
1.2	6.59	83.5	5.5	11.0	0.079	1.042
3.1	11.9	69.0	8.2	16.4	0.491	1.215
4.7	16.1	61.0	9.8	19.6	0.672	1.293
6.3	19.3	55.5	10.7	21.4	0.799	1.331
9.4	26.0	50.0	13.0	26.0	0.973	1.415
12.5	29.7	48.8	14.5	29.0	1.097	1.462
15.6	31.3	49.5	15.5	31.0	1.193	1.491
19.4	33.0	51.5	17.0	34.0	1.288	1.531
21.8	34.5	49.3	17.0	34.0	1.338	1.531
25.6	35.0	50.8	17.8	35.6	1.408	1.551
28.1	34.8	51.7	18.0	36.0	1.449	1.556
30.8	36.4	48.9	17.8	35.6	1.489	1.551

$$R \approx k_2$$

and the reaction obeys zero order kinetics.

As both k_2 and K are temperature dependent it is necessary to determine the variation of the rate of reaction with respect to temperature using a concentration of hydrazine in the zero order range in order to be able to calculate the activation energy of the reaction. Otherwise there will be a contribution from the temperature variation of K. Fig. 7.2 shows an Arrhenius plot for the decomposition of 30.8 mole dm^{-3} hydrazine solution with respect to temperature and the calculated activation energy is 32.2 ± 0.4 kJ $mole^{-1}$.

The same reaction mechanism may be postulated to account for the decomposition of hydrazine on the supported platinum catalyst as was suggested to account for the occurrence of reaction (6) on the other supported metal catalysts. The initial step is the dissociative chemisorption of hydrazine in the form of two NH_2 radicals each of which covers one site. Then a Langmuir-Rideal reaction occurs between adsorbed radicals, either NH_2 or NH, and an hydrazine molecule from solution to form the products of the reaction. This is also consistent with the dual plane theory of Cosser and Tompkins on the basis that reaction only occurs on those planes which are active for the dissociative chemisorption of hydrazine.

C H A P T E R E I G H T

CONCLUSIONS

The study of the heterogeneous decomposition of hydrazine on the supported platinum group metal catalysts has shown the supported iridium catalyst to be the most active (see Table 8.1). The remaining four catalysts have activities which are only of the order of 1 to 3% of that of the supported iridium catalyst. For hydrazine thruster applications, for which a catalyst having a high activity with respect to the decomposition of hydrazine is required, the supported iridium catalyst is the only candidate.

TABLE 8.1

The rate of decomposition of 31.0 mole dm^{-3} hydrazine at 23 ± 2°C

Catalyst	Rate of decomposition $-\frac{d[N_2H_4]}{dt}$ mole g^{-1} s^{-1} × 10^5
Iridium	306
Ruthenium	9.0
Platinum	3.6
Rhodium	3.2
Palladium	2.2

The first objective of the study was to find an alternative to the iridium catalyst and the second objective, if no alternative was available, was to explain the unique activity of the iridium catalyst. The most obvious difference between iridium and the other catalysts is the overall reaction stoichiometry. On the iridium catalyst the decomposition follows the reaction:-

$$3N_2H_4 \rightarrow N_2 + 4NH_3 \qquad (2)$$

while on the rhodium palladium and platinum catalysts the reaction may be represented by:-

$$2N_2H_4 \rightarrow N_2 + H_2 + 2NH_3 \qquad (6)$$

and the activity of these catalysts is only 1% of that of the iridium catalyst. The decomposition of hydrazine on the ruthenium catalyst was observed to be complex and was explained on the basis of the simultaneous occurrence of both reactions.

However the most important difference between iridium and the other catalysts would appear to be the complex nature of the kinetics of the decomposition of hydrazine on the iridium catalyst. The kinetics exhibit a change from a low rate reaction at low concentrations of hydrazine to a high rate reaction for hydrazine concentrations in excess of some value, this value being dependent upon the iridium to oxygen ratio of the catalyst. By extrapolation the low rate reaction would result in a rate of decomposition of 31.0 mole dm^{-3} hydrazine at 22°C of 9.0×10^{-5} mole g^{-1} s^{-1} but the high rate reaction gives rise to the greatly increased rate of 306×10^{-5} mole g^{-1} s^{-1}. The reason for the change in kinetics is not understood but it is postulated to arise from a two site mechanism in which the low rate reaction occurs preferentially on oxide sites. When these sites are saturated reaction then occurs on sites of a lower oxidation state and this is the high rate reaction.

On the rhodium palladium and platinum catalysts the decomposition of hydrazine is postulated to occur via the dissociative chemisorption of hydrazine. The overall mechanism is considered to be consistent with the dual plane theory of Cosser and Tompkins on the assumption that reaction only occurs on those planes active for the dissociative chemisorption of hydrazine. On the ruthenium catalyst some planes are active for the dissociative chemisorption of hydrazine and reaction on these planes follows reaction (6). Some planes are not active for the dissociative chemisorption of hydrazine and on these planes reaction (2) occurs following associative adsorption of hydrazine molecules.

ACKNOWLEDGEMENTS

Copyright, Controller HMSO. The author wishes to thank Dr. D. Sutton of RPE Westcott and Dr. K.M.C. Davis of the University of Leicester for their comments and discussion while the work was carried out. The author also wishes to thank Mr. J.R. McLean who set up the gas chromatograph, Mr. A. I'Anson who carried out the mass spectrometric analysis and Dr. J.A. Brivati of Leicester University who carried out the e.s.r. experiments. Thanks are also due to Mr. D.A.R. Herrick who constructed all the glass apparatus.

Finally the author wishes to acknowledge the assistance of the Management of the Rocket Propulsion Establishment and of the Procurement Executive, Ministry of Defence without whose kind permission the programme of work could not have been submitted for the degree of Ph.D.

REFERENCES

1. Monopropellant Hydrazine Design Data published by the Rocket Research Corporation, Seattle, Washington.
2. F.S. Forbes and D.D. Huxtable, Monopropellant catalyst evaluation, presented at the Third International Conference of Space Technology 3-8 May 1971, Rome, Italy.
3. H. Greer, Vacuum startup of reactions for catalytic decomposition of hydrazine, J. Spacecraft 1970, 7, 522-528.
4. S. Tanatar, Z. Physik Chem 1902, 40, 475.
5. S. Tanatar, Z. Physik Chem 1902, 41A, 37.
6. A. Purgotti and L. Zanichelli, Gazz Chim Ital. 1904, 34, 1, 57.
7. A. Gutbier and K. Neundlinger, Z. Physik Chem 1913, 8, 4, 203.
8. G.V. Vitvitskaya and G.B. Grabovskaya, Zh. Prikl Fhim (Leningrad) 1969, 42, 2091-2095.
9. L.F. Audrieth and N.L. Jolly, J. Phys Colloid Chem 1951, 55, 524.
10. L. Irrera, Soc. Ital Progresso Sci, 1939, 5, 353.
11. L.P. Kuhn, Paper presented at 117th Meeting of American Chemical Society, Detroit (1950).
12. E. Santacesaria, L. Giuffre and D. Gelosa, Riv Combust 1970, 24(3), 101-118.
13. D.A. Ramsay, Phys Chem 1953, 57, 415.
14. G. Wettermark, Arkiv for Kemi 1961, B18 N1 Stockholm.
15. P. Gray and M. Spencer, Combustion and Flame 1962, 6, 337.
16. F. Kamenetsky, Acta Phys Chim 1939, 10, 365.
17. A.R. Hall and M.G. Wolfhard, Trans Faraday Soc 1956, 52, 1520.
18. G.K. Adams and G.W. Stocks, 4th Symposium (International) on Combustion, New York 1956.
19. P. Gray, J.C. Lee, H.A. Leach and D.C. Taylor, 6th Symposium on Combustion 1956.

20. M. Gilbert, Combustion and Flame 1958, 2, 137.

21. A. van Tiggelen and S. De. Jaegere, Rev. de l'Inst Francais du Petrole 1958, 13, 4.

22. M. Gilbert and D. Altman, Jet Propulsion Lab 1955.

23. M. Gilbert, Jet Propulsion Lab Prog. Rep. 1957, 20, 318.

24. G.K. Adams and G.B. Cook, Combustion and Flame 1960, 4, 9.

25. P. Gray and J.C. Lee, 7th Symposium (International) on Combustion 1959.

26. G. Pannetier, M. Guenebaut and R. De Hartoulary, Rev. de l'Inst Francais du Petrole 1958, 13, 457.

27. G. Gerstein and A. Melvin, ARS Journal 1959, 29, 7, 514.

28. A. van Tiggelen and J. Deckers, 6th Symposium on Combustion 1956.

29. W. Jost, Aeron Research Lab Report ARL 62-330, 1962.

30. K.W. Kichel and H.G.G. Wagner, 10th Symposium (International) on Combustion 1965.

31. W.H. Moberly, J. Phys Chem 1962, 66, 366.

32. R. Diesen, J. Chem Phys 1963, 39, 2121.

33. E.T. McHale, B.E. Knox and H.B. Palmer, 10th Symposium (International) on Combustion 1965.

34. E.F. Greene and D.F. Horning, J. Chem Phys 1958, 21, 617.

35. A. Kantrowitz, J. Chem Phys 1959, 14, 16.

36. M. Lucien, J. Chem Eng Data 1961, 6, 4, 584.

37. M. Szwarc, Proc. Roy Soc A 1949, 198, 267.

38. T.J. Hanratty, J.N. Pattinson, J.W. Clegg and A.W. Lemmon, Ind and Eng Chem 1951, 43, 1113.

39. M. Gilbert, Jet Propulsion Lab Prog Rep 1957, 20, 336.

40. H.F. Cordes, J. Phys Chem 1961, 6, 4, 1473.

41. I. Glassman and I.J. Eberstein, 10th Symposium (International) on Combustion 1965.

42. J.C. Elgin and W. Taylor, J. Amer Chem Soc 1929, 51, 2059.

43. P.J. Askey, J. Amer Chem Soc 1930, 52, 970.

44. E.A.B. Birse and H.W. Melville, Proc Royal Soc 1940, A175, 164.

45. A. Kant and W.J. McMahon, J. Inorg Nucl Chem 1960, 15, 305.

46. A.J.B. Robertson and E.M.A. Willhoft, Paper on "Mass spectrometric and other techniques for the investigation of the catalytic decomposition of hydrazine on platinum at low pressures", Gas Council Basic Research Group, Fulham.

47. G. Rienacker and J. Volter, Z. Anorg Chem 1959, 302, 292.

48. V.J. Volter and W. Kuhn, Z. Anorg Chem 1965, 340, 216.

49. G. Schulz-Ekloff and P. Jiru, Collect, Czech Chem Commun 1970, 35(12) 3765.

50. J. Volter and G. Lietz, Z. Anorg Allgem Chem 1969, 366, 191.

51. K-1 Aika, T. Ohhata and A. Ozaki, Journal of Catalysis 1970, 19, 140.

52. R.C. Cosser and F.C. Tompkins, Trans Faraday Soc 1971, 67, 526.

53. R.C.A. Contaminard and F.C. Tompkins, Trans Faraday Soc 1971, 67, 545.

54. E. Santacesaria, L. Guiffre and D. Gelosa, Riv Combust 1971, 23(2), 62.

55. A.S. Kesten, J.D. Rockenfeller and J.J. Sangiovanni, "Unpublished work".

56. G. Pannetier and J.P. Contour, Bull Soc Chim fr. 1970, 12, 4260.

57. W.C.E. Higginson and D. Sutton, J. Chem Soc 1953, 287, 1402.

58. L.J. Stief, J. Chem Phys 1970, 52, 4841.

59. A.L. Vaughan, J.H. Williams and J.T. Tate, Phys Review 1934, 46, 327.

60. C.S. Brooks, J. Colloid and Interface Science 1970, 34(3), 419.

61. S. Hunig, H.R. Muller and W. Thier, Angewandte Chemie 1965, 4, 271.

62. R.A. Carlson, J.L. Blumenthal and R.J. Grassi, "Unpublished work".

APPENDIX A

The solubility of ammonia in hydrazine

The solubility of ammonia at pressures of up to 780 mm Hg in hydrazine over the temperature range $0^{o}C$ to $30^{o}C$ has been studied as no data was available at the time.

After the laboratory work had been completed a report was received which covered similar ranges (E.T. Chang, N.A. Gokcen and T.M. Poston, unpublished work). This showed that the solubility of ammonia in hydrazine obeys Henry's Law and reported that the molar heat of solution is 21.77 kJ and the entropy of solution is 94.5 J $mole^{-1}$ K^{o}.

Experimental

Hydrazine of at least 98.4% w/w purity, obtained from Olin Mathieson Corporation, USA, was used throughout the experiments. Ammonia gas was obtained from cylinders of liquid ammonia.

The all glass apparatus consisted of two carefully calibrated bulbs, one large gas storage bulb, a sample tube and a mercury manometer. The volumes of the volumes of the sample tube and the manifold were calculated from Boyle's Law by expanding gas at a known pressure from the calibrated bulbs into the required volume which had been evacuated, and re-measuring the pressure. As a mercury manometer was used to measure the pressure it was necessary to allow for the change in volume with respect to pressure caused by the movement of the mercury column.

For each experiment 10 ml hydrazine was placed in the sample tube and degassed by repeated freeze-pump-thaw cycles. The large storage bulb was filled with ammonia gas at 800 mm Hg pressure and the remainder of the apparatus evacuated. Ammonia gas was then admitted to the manifold and to the calibrated bulbs as required by the experimental conditions. The amount of ammonia, N_1 , in moles was obtained by measurement of the pressure, P_1 ,

and the absolute temperature, T_1 , in a known volume, V_1 , and by the use of $P_1V_1 = RT_1N_1$ where R is the gas constant. The ammonia was admitted to the sample tube and the hydrazine agitated until a minimum pressure was maintained. The amount of ammonia, N_2 , remaining in the gas phase was calculated from P_2 , T_2 and V_2 . The amount of ammonia dissolved was $(N_1 - N_2)$ moles at a pressure of (P_2 - vapour pressure of hydrazine) mm Hg. This procedure was repeated, summing the number of moles of ammonia dissolved at each stage until the pressure of ammonia reached 760 mm Hg.

Results

The solubility of ammonia in 98.4% w/w hydrazine is shown in Fig. 1 as plots of the mole fraction of dissolved ammonia with respect to pressure of ammonia above the solution. The plots are straight lines showing that Henry's Law is obeyed. The variation of the solubility of ammonia in hydrazine with respect to temperature is shown in Fig. 2, in the form of a plot of $\log_{10} K$, where K is the slope of the relevant plot in Fig. 1, against $1/T$.

Discussion

The slope of each plot in Fig. 1 is the equilibrium constant, K , for the system of ammonia gas at a pressure of P atmospheres in equilibrium with dissolved ammonia at a concentration of M mole fraction:-

$$K = M/P \quad .$$

The change in Gibbs free energy may be expressed in two ways:-

$$\Delta G^{o} = - RT \ln K$$

and

$$\Delta G^{o} = \Delta H^{o} - T\Delta S^{o}$$

Therefore:-

$$- RT \ln K = \Delta H^{o} - T\Delta S^{o}$$

which may be written as:-

$$\log_{10} K = - \frac{\Delta H^{o}}{2.303\ RT} + \frac{\Delta S^{o}}{2.303\ R} \quad .$$

A plot of $\log_{10} K$ against $1/T$ gives a straight line and ΔH^{o} may be calculated from the slope and ΔS^{o} from the intercept. From the plot in Fig. 2 the value of ΔH^{o}, the heat of solution, is 21.8 kJ mole^{-1} and that of ΔS^{o}, the entropy of solution, is 93.3 J mole^{-1} K^{o}. These results are in excellent agreement with the results of Chang et al.

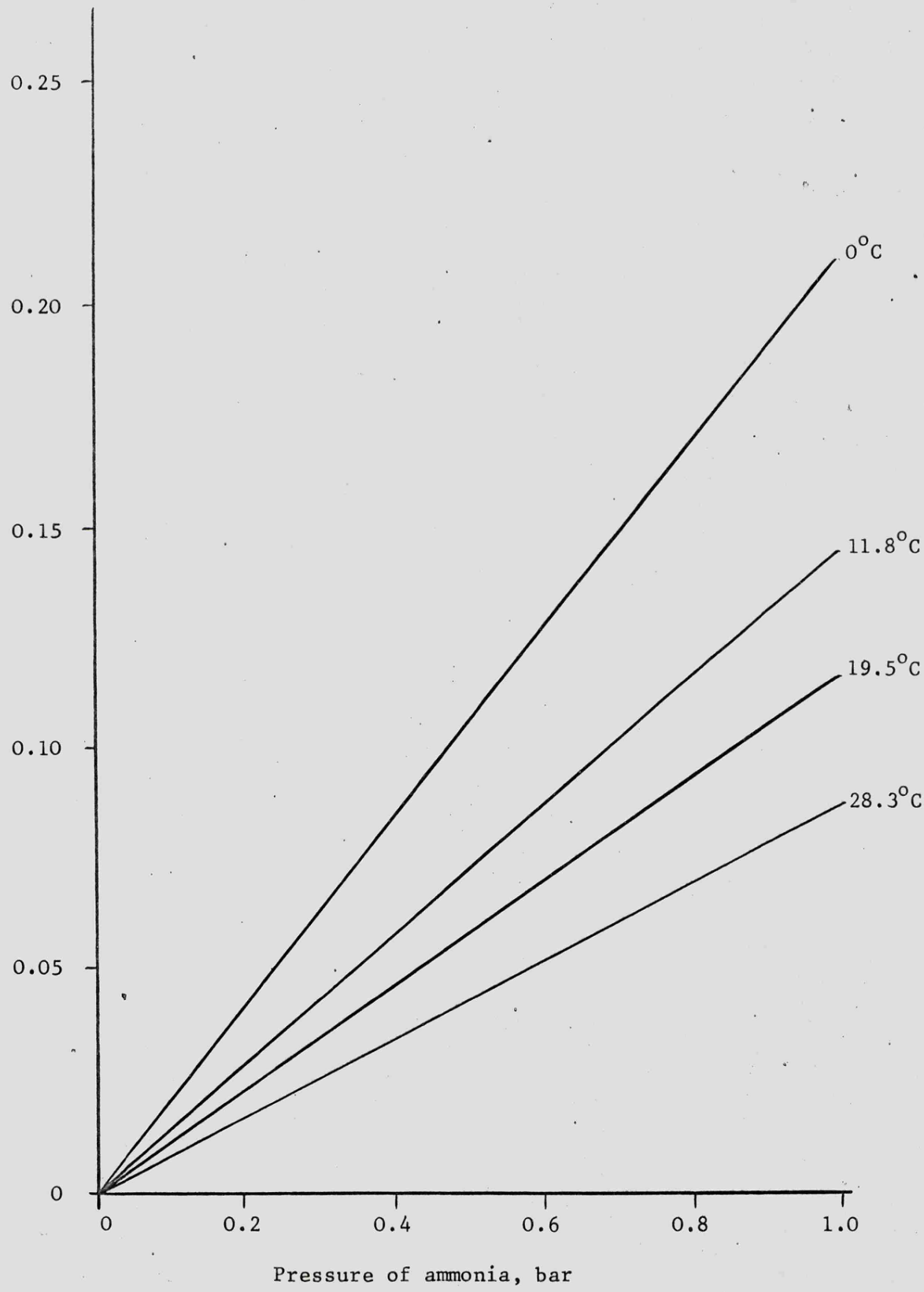

Fig. 1 Mole fraction of ammonia dissolved in 98.4% hydrazine with respect to ammonia pressure

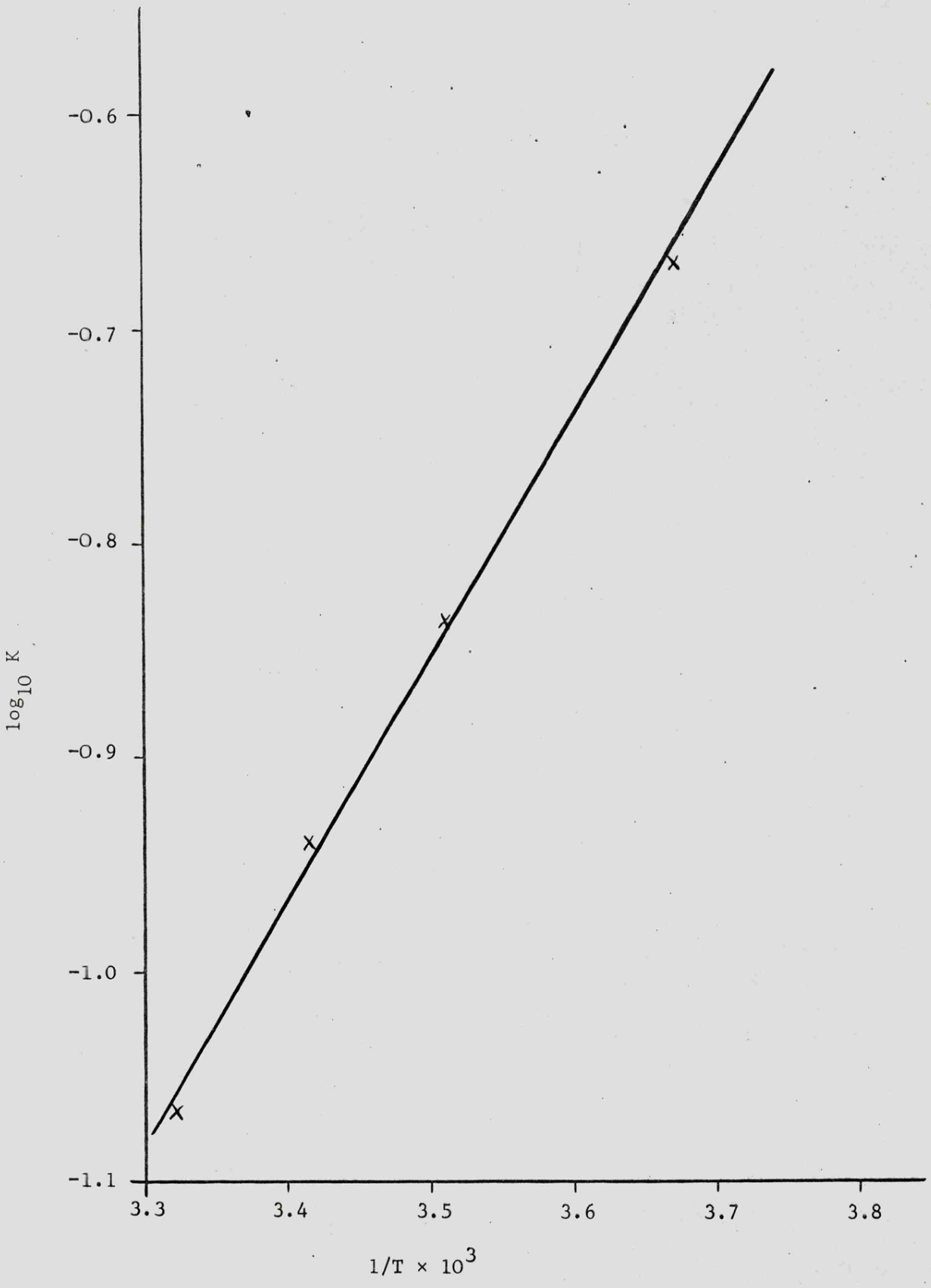

Fig. 2 Plot of $\log_{10} K$ against $1/T$

ABSTRACT

The heterogeneous decomposition of liquid hydrazine on supported platinum group metal catalysts has been found to follow one, or both of the reactions:-

$$3N_2H_4 \rightarrow N_2 + 4NH_3 \quad (1)$$

$$2N_2H_4 \rightarrow N_2 + H_2 + 2NH_3 \quad (2)$$

On rhodium, palladium and platinum catalysts reaction (2) occurs while on the ruthenium catalyst both reactions occur. Reaction (2) occurs following the dissociative chemisorption of hydrazine molecules in the form of amide radicals followed by a Langmuir-Rideal reaction between adsorbed radicals and a solution phase hydrazine molecule to form the products. Reaction (1) occurs following the associative adsorption of hydrazine molecules to form an activated complex which then breaks down to yield the products. These mechanisms are consistent with the dual plane theory postulated by Cosser and Tompkins to explain the decomposition of hydrazine on tungsten films.

The decomposition of hydrazine on the supported iridium catalyst was observed to follow reaction (1) but the kinetics were found to be complex. For concentrations of hydrazine up to 3 mole dm^{-3} the reaction was observed to be first order with an activation energy of 35 kJ $mole^{-1}$. Increasing the concentration of hydrazine results in a change in kinetics to a reaction having an activation energy of 65 kJ $mole^{-1}$ and although the rate is a linear function of hydrazine concentration the reaction is not true first order. The hydrazine concentration at which the change in kinetics occurred was found to increase with increasing oxide content of the catalyst. It has been postulated that at low concentrations of hydrazine the associative adsorption of hydrazine molecules occurs on the sites of higher oxidation state as these are energetically favoured. Only when these sites have been saturated does adsorption and decomposition of hydrazine occur on the sites of lower oxidation state.